



NTNU – Trondheim
Norwegian University of
Science and Technology

Strategies for Smart Charging of Electric Vehicles

Line Fiskum Hexeberg

Master of Energy and Environmental Engineering

Submission date: June 2014

Supervisor: Olav B Fosso, ELKRAFT

Norwegian University of Science and Technology
Department of Electric Power Engineering

TASK DESCRIPTION

This project will focus on smart strategies for charging of electric vehicles (EVs). To demonstrate the principles, algorithms will be developed for smart charging procedures of EVs, where the storage capability of the batteries will be used to provide network services such as active and reactive power under a given set of rules. The smart charging will follow an optimization routine with a dynamic time horizon.

To show the concept, the designed algorithms will be applied to a number of electrical vehicles in a large residential area. The algorithm success will be rated according to its capability to avoid low voltages on some feeders during the charging process, by using charging control and coordination as active and reactive power services.

PREFACE

This thesis is submitted in fulfilment of the requirements for the degree of Master of Science (MSc) at the Norwegian University of Science and Technology.

The focus in this thesis is smart charging of electric vehicles. To demonstrate the principles, algorithms have been developed and implemented into MATLAB, and simulations have been run to investigate the voltages at the demand nodes of a distribution test feeder.

For the purpose of the simulations, MATPOWER was chosen as simulation tool. As the test cases in MATPOWER all are models of transmission networks, it was decided to model a new test case in MATPOWER based on the data from the IEEE 13 node test feeder.

With approval from my supervisor, I decided to focus on two smart charging scenarios. The first scenario is the *profit maximization scenario* where the vehicle owners' profit is to be maximized by charging at low electricity prices and discharging back to the grid at high electricity prices. This charging scenario is actually an extension of my specialization project during the fall semester of 2013. The results from this project are presented in appendix B. The other smart charging scenario is the *power factor control scenario*, where low voltages in the grid are to be avoided by instructing EVs to inject reactive power while charging.

In addition to these two smart charging scenarios, a *dumb charging scenario*, where there is no smart control of the vehicle charging, is also presented in this thesis. This scenario is included in the thesis to serve as a reference case when investigating the effectiveness of the algorithms for the smart charging scenarios.

The plan was originally to make the algorithms for all the scenarios with a dynamic time horizon, as stated in the task description. For the *profit maximization scenario*, it is however decided that the battery should be charged to a certain level at 6:00 in the morning each day, as it is assumed that this would be a demand from the vehicle owners. Therefore it was natural to make the charging schedule last for 24-hours. By minor adjustments, the algorithm presented in this thesis for this scenario can be altered to make it suitable for a dynamic time horizon. When presenting the profit maximization scenario in this thesis, it is included a short description of how I would suggest this alteration to be made.

ACKNOWLEDGEMENTS

I would like to express my sincere gratitude to my supervisor Olav Bjarte Fosso. You have been a source of motivation throughout the process, both during the work of my specialization project and the master thesis. Whenever I have needed your guidance, even when you have been travelling, you have been available for me.

Besides my supervisor, I would like to thank the other professors teaching the courses I have taken during my years at the university. You have really opened my eyes for the very interesting and important field of electric power engineering.

I would also like to express my gratitude to my parents, Unni and Gustav, for supporting me throughout my whole education. You have given me every opportunity to do whatever I wanted in life. A thanks also goes to my father for proof-reading my thesis and for giving me useful feedback during the finalizing of this thesis.

I would also like to thank my lovely daughter, Amalie. You brighten up even the darkest days.

Finally, the most special thank you goes to my husband, Magnus. So many days, so many nights. It has been a struggle combining studies and family life. The significance of your loving support, encouragement and understanding cannot be put into words.

Line Fiskum Hexeberg,

Frogner, June 2014.

ABSTRACT

The electrification of the transport sector is put on the agenda as an important means to reduce the greenhouse gas emissions in Norway, EU and other parts of the world. Chargeable vehicles have the potential to reduce the greenhouse gas emissions both because they are four to five times more energy effective than today's petrol-powered vehicles, and because the electricity they use can come from renewable production. Questions regarding sufficient access of conventional oil and increasing challenges with local emissions will also contribute in the electrification of the transport sector [1].

The electrification of the transport sector brings with it some challenges. The charging of the electric vehicles leads to an increase in demand. If no sort of smart control of the charging is put in place, it could be safe to assume that many vehicle owners would plug-in their vehicles when they come home from their last journey of the day, leading to an increase in power demand at the time when there already might be a peak in demand. This charging regime is often referred to as "dumb charging".

This thesis focuses on "smart strategies" for charging of electric vehicles and presents two "smart strategies" for charging of the electric vehicles, the *profit maximization scenario* and the *power factor control scenario*. In these scenarios it is assumed that a control system is put in place so that specific chargers can be instructed to change the power factor and to begin and stop charging. The technical specifications of this control system has not been studied, it is simply assumed that such a control system is put in place.

In the profit maximization scenario, it is assumed that technology facilitating the electric vehicles to discharge energy back to the grid is put in place. The electric vehicles are then instructed to charge when the electricity prices are low and discharge back to the grid when the electricity prices are high. Since the demand and electricity price pattern follows a similar pattern (high prices when the demand is high, and low prices when the demand is low), this procedure should have a smoothing effect on the demand pattern with the right choice of parameters.

In the power factor control scenario, all electric vehicles are assumed to be plugged-in and start charging as soon as they return from the last journey of the day. When there are voltages in the grid below a certain value, electric vehicles charging at that time is instructed to reduce the charging power factor. By reducing the power factor, reactive power can be injected into the grid.

To demonstrate the principles, algorithms have been developed and implemented in MATLAB for both the dumb charging scenario and the two smart charging scenarios. A model of the IEEE 13 node test feeder has been modelled in MATPOWER, and power flow simulations of the three charging scenarios have been run, assuming a vehicle adoption of 50%. The algorithms' success has then been rated according to their capability to avoid low

voltages on the demand nodes in this test case. For the purpose of this thesis it is assumed that the designed model is a distribution network in Norway. Therefore the base demand pattern used in the simulations follows the actual base demand pattern for a chosen 24-hour period in Norway.

The results from the simulations showed that when all vehicles were charged as soon as they return from their last journey of the day, it resulted in a major peak in demand, and thus a reduction of the voltage between 18:00 and 21:00.

Both smart strategies presented in this thesis improved the voltage profile. While the lowest node voltage in the simulations of the dumb charging scenario was 0.915 pu, the lowest node voltage in the profit maximization scenario was 0.932, and the lowest voltage in the power factor control scenario was 0.934 pu.

In the profit maximization scenario, the demand profile, and thus the voltage profile, did however not smooth out as much as expected. Since the electricity prices change when there is a change in demand, the algorithm is designed to find the charging schedule for one vehicle at the time, changing the electricity prices in between. A further study on this scenario should focus on finding a better relationship between changes in demand and electricity prices.

In the power factor control scenario, the minimum voltage allowed was not avoided at all nodes in the designed test case. The simulations showed that one of the nodes experienced a voltage violation. This scenario did however only assume that the vehicles were only available for grid services the first eight hours after the return of the last journey of the day. If the vehicles were available at other times too, this voltage violation could however be avoided.

SAMMENDRAG

Elektrifiseringen av transportsektoren er satt på agendaen som et virkemiddel for å redusere klimagass utslippene i Norge, EU og andre deler av verden.

Elektrifiseringen av transportsektoren bringer med seg noen utfordringer. Dersom ingen «smarte» ladestrategier tas i bruk, kan det være naturlig å anta at mange elbiler vil bli ladet rett etter dagens siste kjøretur. Dette er noe som kan føre til en økning i lasten på et tidspunkt hvor det allerede er høy last i nettet. Denne ladestrategien kalles ofte «dum lading».

Denne oppgaven har fokus på “smarte ladestrategier” for elbiler, og presenterer to ulike smarte strategier for lading av elbiler. I den første smarte ladestrategien, er det antatt at teknologi som gjør det mulig for elbilene å “selge kraft” tilbake til nettet er på plass, såkalt «Vehicle-to-Grid» teknologi. Ideen er at elbilene skal lade når strømprisen er lav, og selge kraft tilbake til nettet når strømprisen er høyere. Siden lasten i nettet og strømprisen følger liknende mønster (høye strømpriser når lasten er høy og lave strømpriser når lasten er lav), vil dette i teorien ha en utflatende effekt på last mønsteret.

I den andre smarte ladestrategien, antas det i utgangspunktet at alle elbilene lader så snart de kommer hjem fra dagens siste kjøretur, slik som i den dumme ladestrategien. Når spenningene ved utvalgte noder i nettet faller under et visst nivå, vil elbiler bli kommandert til å redusere effektfaktoren. Ved å redusere effektfaktoren, vil det være mulig å tilføre reaktiv effekt inn på nettet samtidig som bilen lader.

For å demonstrere prinsippet, har algoritmer blitt implementert i MATLAB for både den dumme ladestrategien og de to smarte ladestrategiene, og simuleringer er utført på en modell av et lavspenningsnett basert på *IEEE 13 node test feeder* i MATPOWER. I simuleringene er det antatt en elbilandel på 50%. Effekten av å innføre de smarte ladestrategiene har deretter blitt vurdert etter algoritmenes evne til å unngå lave spenninger ved last nodene.

Resultatene fra simuleringen viste at når elbilene fulgte en dum ladestrategi, resulterte det til en stor topp i lasten mellom kl. 18:00 og 21:00. Laveste spenning var da på 0.915 pu. Begge de smarte ladestrategiene som er presentert i denne oppgaven førte til en økning i den laveste spenningen. Scenarioet der elektrisitetsprisene satte føringer for når elbilene skulle lade, hadde 0.932 pu som laveste spenning. Simuleringer av scenarioet der effektfaktoren ble endret, hadde 0.934 som laveste spenning.

I scenarioet der strømprisen satte føringer for når elbilene skulle lade, flatet imidlertid ikke last- og spenningsprofilen seg ut i like stor grad som forventet. En videre studie av denne ladestrategien burde ha fokus på å finne et bedre forhold mellom endring av elektrisitetsprisene ved lastendringer.

CONTENTS

- 1 Introduction..... 1
 - 1.1 Motivation 1
 - 1.2 Method..... 1
 - 1.3 Charging Scenarios..... 2
 - 1.4 Thesis Organization..... 3
- 2 Power System..... 4
 - 2.1 Electricity Grid Infrastructure 4
 - 2.2 Balance between Generation and Demand..... 4
 - 2.3 Node Voltages in the Distribution System 4
 - 2.4 The Electricity Price in Norway 5
- 3 Electric Vehicles 7
 - 1.1 Different Types of Electric Vehicles 7
 - 3.1 The Electric Vehicle Battery 7
 - 3.1.1 Battery capacity - Peukert’s formula..... 8
 - 3.1.2 State of Charge 9
 - 3.1.3 Charge efficiency 9
 - 3.2 Electric Vehicle Charging Schemes 9
 - 3.2.1 Active power charging control..... 9
 - 3.2.2 Power factor control..... 10
 - 3.2.3 Objectives for smart charging control..... 11
- 4 Simulation model..... 12
 - 4.1 Network Description..... 12
 - 4.1.1 The original IEEE 13 node test feeder 12
 - 4.1.2 The designed 11 node test feeder 12
- 5 Power Flow Analysis 16
 - 5.1 Power Flow Analysis..... 16
 - 5.2 Power Flow Analysis in MATPOWER..... 16
 - 5.2.1 Power flow solvers in MATPOWER..... 16
- 6 Case Study 18
 - 6.1 Base Demand Pattern..... 18

6.2	Driving Behavior and Availability of EVs for Grid Services	20
6.2.1	Data sources	20
6.2.2	Driving distance	21
6.2.3	Return of the last journey of the day	21
6.2.4	Availability of electric vehicles for grid services (parking time).....	21
6.3	Daily Power Demand from Charging of the Electric Vehicles	22
6.4	Dumb Charging – A Reference Scenario	24
6.5	Profit Maximization Scenario.....	24
6.5.1	Procedure for finding the total demand profile in the profit maximization scenario 24	
6.5.2	Algorithm for finding optimal charging for <i>one</i> EV based on electricity prices 25	
6.5.3	The change in electricity prices due to change in demand.....	27
6.5.4	Profit maximization scenario with a dynamic time horizon	30
6.6	Power Factor Regulation Scenario	32
6.6.1	Power factor control mode	32
6.6.2	Procedure for finding the demand in the power factor control scenario	34
6.7	Summary of Assumptions	36
7	Results.....	38
7.1	Impact of Dumb Charging Scenario	38
7.1.1	Demand pattern in the dumb charging scenario.....	38
7.1.2	Voltage pattern in the dumb charging scenario.....	39
7.2	Impact of Profit Maximization Scenario	40
7.2.1	Charging schedule for electric vehicles in the profit maximization scenario	40
7.2.2	Demand pattern in the profit maximization scenario	42
7.2.3	Voltage pattern in the profit maximization scenario	44
7.3	Impact of Reactive Power Regulation Scenario	45
7.3.1	Demand pattern in the power factor control scenario	45
7.3.2	Voltage pattern in the power factor control scenario	47
7.4	Summary of Results.....	47
8	Discussion.....	50
8.1	Simulation Model	50
8.2	Electric Vehicle Availability for Grid Services.....	50
8.3	Simplifications Made for the Electric Vehicle Battery	51
8.4	Profit Maximization Scenario.....	52

8.5	Power Factor Control Scenario.....	52
8.6	Combination of Different Charging Scenarios.....	53
9	Conclusion and Further Work.....	54
9.1	Conclusion.....	54
9.2	Further work.....	55
	References.....	57

APPENDICES

Appendix A: Calculation of Line Phase Impedances and Total Line Charging Susceptance for the 11 Node Test Feeder.

Appendix B: Matlab scripts.

Appendix C: “*Optimal Charging of Electric Vehicles Including Service Provision to the Distribution Network*” (2013) by Hexeberg, Fosso and Molinas.

LIST OF FIGURES

Figure 3.1: Battery capacity at different discharge rates.....	8
Figure 4.1: One line diagram of the IEEE 13 node test feeder [25].....	12
Figure 4.2: One line diagram of the 11 node test feeder.....	13
Figure 6.1: Actual demand in Norway November 5th 6:00 PM to November 6th 6:00 PM. ..	19
Figure 6.2: Percentage of the German vehicle fleet returning from their last journey at different times during the day	21
Figure 6.3: Electric vehicle availability for grid services.. ..	22
Figure 6.4: Relationship between power demand and electricity prices.....	28
Figure 6.5: Flow chart for finding the final demand at node 671 when the objective is profit maximization of the EV fleet	31
Figure 6.6 PQ circle.	33
Figure 6.7: Flow chart for finding the voltage and demand pattern for all demand nodes in the reactive power charging control scheme	35
Figure 7.1: Effect of dumb charging scenario on the demand at node 652.....	39
Figure 7.2: Effect of dumb charging scenario on the voltages at node 652.....	39
Figure 7.3: Schedule for charging and discharging of the calculated in the profit maximization scenario. This schedule is the first schedule calculated.	41
Figure 7.4: Schedule for charging and discharging of the calculated in the profit maximization scenario. This schedule is the last schedule calculated.	41
Figure 7.5: Active power demand at node 651 with 50 % EV adoption and all EVs charging according to the profit maximization scenario	43
Figure 7.6: Active power demand in Norway with 50% EV adoption and all EVs charging according to the profit maximization scenario	43
Figure 7.7: Active power demand in Norway with 50 % EV adoption and all EVs charging according to the profit maximization scenario. Price of discharge is set to 0.01 EUR/MWh below the price for charging.....	44
Figure 7.8: Voltages at node 652 with a 50% EV adoption charged in the profit maximization scenario.....	45
Figure 7.9: Active power demand pattern in the reactive power regulation scenario with 50 % EV adoption.....	46
Figure 7.10: Reactive power demand pattern in the reactive power regulation scenario with 50% EV adoption	46
Figure 7.11: Voltage at node 652 in the power factor control scenario	47
Figure 7.12: Voltage pattern at node 652 at 50% EV adaption.....	48

LIST OF TABLES

Table 4-1: Base values 13

Table 4-2: Calculated line impedances for the 11 node test feeder 14

Table 4-3: Shunt capacitors in the IEEE 13 node test feeder [25] 14

Table 4-4 Average base demand at the 11 node test feeder 15

Table 6-1 Number of houses and EVs served by each node in the 11 node test case..... 23

Table 6-2: Assumptions 36

Table 6-3: Parameters related to choice of vehicle model 37

Table 7-1: Results from simulations of a 50% EV demand at 11 node test feeder..... 48

1 INTRODUCTION

1.1 Motivation

Norway has what are probably the world's best incentives for chargeable electric vehicles. Norway also has the highest number of electric vehicles (EVs) per capita by a wide margin, and the percentage of the vehicle fleet consisting of electric vehicles are still increasing [2]. More than four times as many electric vehicles were registered during the five first months of 2014 compared to the same period the year before [3] and by the end of May 2014 there were more than 30 000 registered chargeable EVs in Norway [4].

It is not only in Norway there is a focus on electrification of the vehicle fleet. Questions regarding sufficient access of conventional oil and increasing challenges with local emissions will contribute in the electrification of the transport sector in both EU and the rest of the world [1].

However, the electric vehicle (EV) charging will place a substantial pressure on the grid, and in particularly at the medium and low voltage levels [5]. If there are no "smart charging control" of the electric vehicles, most owners would probably plug-in their vehicles and charge when they come home from their last journey of the day. This would probably cause a peak in demand somewhere in the afternoon, when there might already be a peak in the base demand.

1.2 Method

The purpose of this thesis is to investigate how different charging philosophies would impact the distribution grid when there is a large scale adoption of electric vehicles. To do this, different charging scenarios are presented and charging algorithms are designed for these charging scenarios. The designed algorithms are then implemented in MATLAB to calculate the resulting demand pattern.

It was a wish to rate the algorithms' success by investigating the voltages at some specific nodes in a distribution network. MATPOWER, which works in the workspace of MATLAB, is chosen as simulation tool. Since all built-in cases in MATPOWER are models of different transmission networks, a model of a distribution network based on the IEEE 13 node test feeder is designed in MATPOWER for the purpose of this thesis.

The effectiveness of the designed algorithms is then investigated by running simulations on this designed model in MATPOWER. For the simulations in this thesis, it is chosen to simulate a vehicle adoption of 50%. For the purpose of this thesis, it is assumed that the designed model is a model of a distribution network in Norway. The base demand pattern for the simulations therefore follows the actual demand profile in Norway for a chosen 24-hour period.

Traffic patterns are an important input when studying the influence of EVs on the grid as they will dictate the total energy requirements for charging the vehicles and define the period in which users must recharge them. When studying smart charging strategies of the EV fleet, the driving pattern also dictates the availability of the EVs for grid services. With this in mind, it is strived in this thesis to take the main features of the traffic pattern into consideration when designing the different charging scenarios.

1.3 Charging Scenarios

There are three different charging scenarios presented in this thesis, the *dumb charging scenario*, the *profit maximization scenario* and the *power factor control scenario*.

The most straight-forward charging scenario studied in this thesis is the *dumb charging scenario*, where the vehicle owner plug-in and charge at unity power factor as soon as they come home from their last journey of the day. This is likely to result in a peak in demand sometime in the afternoon, when there already might be a peak in base demand.

In the *profit maximization scenario*, the vehicles are to be charged when the electricity price is low and discharge back to the grid at high prices. Both charging and discharging back to the grid is assumed to be with a unity power factor. The idea with this scenario is that since the price pattern often follows a similar pattern as the demand pattern, this procedure will smooth out the demand pattern, and thus in turn also the voltage pattern at the demand nodes. The *profit maximization scenario* was studied by the writer of this thesis as a project at NTNU during the fall of 2013. A paper by Hexeberg (the writer of this thesis), Fosso and Molinas presents the results from this study [6]. The article is unpublished, and therefore attached in the appendices. In this article, the change in electricity prices due to change in demand is not taken into consideration. This led to an unrealistic demand pattern with a high peak when the electricity prices were low, and the demand became unrealistically low when the electricity prices were high. In this thesis the algorithm in the paper is further developed, and the change in electricity prices due to changes in demand when the EV demand is added to the base demand is taken into consideration.

In the *power factor control scenario*, the idea is that when the voltages are above a certain level, the vehicles charges as in the *dumb charging scenario*. However, if voltages below the minimum allowable value are detected at any of the demand nodes, the power factor for the charging of electric vehicles charging at that time is reduced. By reducing the power factor, reactive power is allowed to be injected into the grid. The idea is that by injecting reactive power, the voltage violation will be avoided.

The *profit maximization scenario* and the *power factor control scenario* assumes that a control system can be put in place that can instruct chargers to begin and stop charging/discharging and change the power factor when charging. The methods of operation of this system are not considered in this thesis; it is simply assumed that this type of smart control is implemented.

1.4 Thesis Organization

In chapter 2, some main features of the power system are given. This is not meant as a complete introduction to the power system, only the features considered most relevant for the understanding of the case study are presented here.

Chapter 3 focuses on EV theory. Here different types of EVs and charging schemes are presented. In this thesis, simplifications are made concerning the electric vehicle battery. Nevertheless, some important factors concerning the battery are also included in this chapter to give a better understanding of the simplifications made.

The designed simulation model is presented in chapter 4, and chapter 5 serves as a brief introduction to power flow analysis.

The case study is presented in chapter 6. The first three subchapters in chapter 6 focus on the choices made concerning the driving pattern, base load and daily energy consumption of the electric vehicles. The second half of chapter 6 presents the charging scenarios and describes the accompanying designed algorithms in detail.

Chapter 7 presents the main results from the simulations of a 50% EV adoption in the three different charging scenarios.

Chapter 8 evaluates the results and discusses the limitations of the study. Chapter 9 concludes the study and gives recommendations for further work.

2 POWER SYSTEM

2.1 Electricity Grid Infrastructure

The electricity infrastructure consists of three major elements; generation, transmission and distribution. The generation covers the production of electricity from various resources such as fossil fuels, nuclear, hydro, wind and solar. In Norway most of the power production comes from hydroelectric power plants. The transmission covers the transportation of electricity along high voltage lines in the transmission grid, from the generator to the distributor. The distribution covers the transportation of lower voltage electricity, in the distribution grid, to the consumer [7].

2.2 Balance between Generation and Demand

One of the great challenges in power system engineering is making sure that the amount of power supplied to the loads is in line with expectations. Since the active power have to be consumed at the exact time as it is produced, the amount of active power consumed plus losses should always equal the active power produced and/or supplied from energy storage within the system. If more power would be produced than consumed the frequency, which is the same in the whole system, would rise and vice versa.

As mentioned by Freris et al [8], there are several reasons why it is desirable to keep the frequency in a power system within narrow bounds. One of the reasons is that it ensures that electric motors operate at a virtually constant speed, which is required in many consumer applications. Another reason is that transformers are sensitive to frequency variations and may be overloaded if the frequency deviates substantially from the nominal value [8].

2.3 Node Voltages in the Distribution System

Another great challenge of power system engineering is keeping the voltages in line with expectations. The manufacturers of electrical appliances design their products to operate with a certain nominal voltage in order to achieve effective performance and comply with safety standards. As mentioned in [9], electric drives and motors are affected by voltages below and above the nameplate voltages.

- Power is proportional to the product of current and voltage. Therefore, if electric motors are subjected to voltages below the nameplate rating, current must increase to provide the same amount of power, which increases the build-up of heat within the motor. Furthermore, the mechanical torque is inversely proportional to the square of the voltage. Thus a 10% reduction from the nameplate voltage would reduce the torque by a factor 0.9^2 which mean that the resulting torque would be only 81% of the original value [9].
- A higher than nominal voltage can also lead to over-currents. High voltages to a motor tend to push the magnetic portion of the motor into saturation. This causes the motor

to draw excessive current in an effort to magnetize the iron beyond the point to which it can easily be magnetized [9].

Voltage, unlike the frequency, is not the same at all nodes in the system. The voltage drop between the two nodes A and B in a transmission or distribution line can be estimated using the equation below;

$$\Delta U_{AB} \approx \frac{P \cdot R_L + Q \cdot X_L}{U_A} \quad (1)$$

R_L is the line resistance and X_L is the line reactance. P and Q are the active and reactive power carried by the line and U_A is the voltage at node A. Note that this is only an estimation. The detailed derivation and assumptions made to come to this estimation can be found in “Renewable Energy in Power Systems” by Freris et al. (2008), p. 158. [8].

According to equation (1), both active and reactive power flows over distribution and transmission lines will affect the voltage profiles of the different nodes in the network. Whether it is the active or reactive power flow who affects the voltage stability more strongly depends upon whether the corresponding lines are predominantly resistive ($R_L > X_L$) or reactive ($R_L < X_L$). In the case were the line is predominantly resistive, the term $P \cdot R_L$ will generally be more important in the relation than $Q \cdot X_L$. Transmission lines are predominantly reactive ($X_L \gg R_L$). The voltages are consequently mainly affected by the reactive power and the influence from the active power can be ignored. For the distribution grid, the influence from the active power can no longer be ignored, as the distribution lines are predominantly resistive [9].

One way of increasing the voltage at a node is by injecting reactive power. Reactive power transmitted from the energy source to the consumer through the transmission and distribution system causes increased energy losses and decreases the system efficiency [10]. This is an argument for injecting the needed reactive power locally.

2.4 The Electricity Price in Norway

The main features of the electricity price in Norway are given in section II in the article by Hexeberg et al. given in the appendices. For the sake of completeness it is chosen to include this section here, with only minor changes.

The Nordic countries deregulated their power markets in the early 1990s, and their individual markets were brought into a common Nordic market. Estonia and Lithuania deregulated their power markets in the late 2000s, integrating the Nordic and Baltic power markets. The market place, which is called Nord Pool Spot, is own by the Nordic and Baltic transmission system operators and runs the leading power market in Europe.

In the deregulated power market, the electricity price is mainly determined by the balance between generation and demand of electric power [11]. The higher the demand gets, more expensive units have to produce power, and the higher the price gets. Due to transmission

restrictions, the prices in different areas are however somewhat different. The Norwegian electricity market is for instance divided into five price areas.

The hourly electricity prices for the different Nordic and Baltic countries can be found at Nord Pool Spot's webpages [11]. It is clear that there is a smaller variation in the electricity prices in Norway compared to the other Nordic and Baltic countries. This is due to the fact that most of the Norwegian power production comes from hydroelectric power plants, which has excellent regulation ability compared to most other types of power plants. Norway's potential for wind power is however excellent and wind power is predicted to constitute a significant part of the Norwegian electricity supply in the future [12]. Wind power is known to have large variations in production, which in turn will give more variation in the electricity prices. There is also a transition from reliance on fossil fuels towards utilizing renewable-based energy with more fluctuations in production in other countries in the northern part of Europe. This is also likely to influence the Norwegian energy prices since the national energy markets are integrated.

Currently most Norwegian consumers do not face any incentive to respond to price changes as their meters account for accumulated consumption only and the hourly prices remain invisible due to lack of enabling technology and respective pricing methods [13]. Norwegian Government has however decided that the implementation of advanced metering system should be completed before January 1, 2019 [14]. The smart meters will make it possible to give a more accurate billing, and thereby making it more attractive to shift some of the load from periods of the day when the price is at its highest, to periods when the electricity price is lower.

3 ELECTRIC VEHICLES

1.1 Different Types of Electric Vehicles

There are four main types of electric vehicles [15]:

1. Hybrid electric vehicles (HEVs)
The HEV uses a small electric battery to supplement a standard internal combustion engine. The battery is recharged by the gasoline engine and regenerative braking.
2. Plug-in Hybrid Electric Vehicles (PHEVs)
The PHEV is also a dual-fuel car in which both the electric motor and the internal combustion engine can propel the car. Compared to the HEV, it has however a larger battery-pack and it can be charged directly from the power grid.
3. Extended-Range Electric Vehicles (ER-EVs)
The ER-EV uses an internal combustion engine to power an electric generator that charges the battery system in a linear process. Unlike HEVs and PHEVs, only the electric motor powers the wheels of the ER-EV. The internal combustion engine only charges the batteries.
4. Battery Electric Vehicles (BEVs)
The BEV is all electric - it has no internal combustion engine and must be plugged into the electric power grid for recharging. This type of EV requires larger batteries than the combined electric-petroleum vehicles.

In this thesis the term electric vehicle (EV) will be used for BEVs when not mentioned otherwise.

3.1 The Electric Vehicle Battery

In all EVs, the battery is a key component. In the classical EV, the battery is the only energy source, and the component with the highest cost, weight and volume [16].

An electric battery is a combination of two or more electric cells connected together. The cells consist of positive and negative electrodes in an electrolyte. The chemical reaction between the electrodes and the electrolyte generates DC electricity. In the case of rechargeable batteries the chemical reaction can be reversed by reversing the current which will make the battery return to a charged state [16].

The traditional rechargeable battery type used in EVs is the lead-acid battery, but there are others that are becoming more popular in modern EVs. Currently most EVs, including the Nissan Leaf, the Mitsubishi MiEV, the Chevrolet Volt, the Tesla Roadster and the Tesla model S uses lithium-ion batteries.

Although a basic understanding of the chemistry is important, from the EV designer's point of view, the battery can be treated as a 'black-box' that has a range of performance criteria [16]. Some of these criteria will be presented below.

3.1.1 Battery capacity - Peukert's formula

The purpose of the battery is to store energy, and the amount of stored energy in the battery is clearly a crucial parameter. Often the capacity of the EV battery is given in kWh. The capacity can however also be presented in amp-hours, Ah ($kWh = 1000 \cdot V \cdot Ah$). The capacity of a battery might be '10 amp-hours', which means that it can provide for example 1A for 10 hours or 2A for 5 hours [16].

Peukert's formula gives the capacity of a battery in terms of the rate at which it is discharged. The higher discharge rate you use, the less energy you can recover from the battery [16]. The Peukert's formula is given in equation (2).

$$T = \frac{C}{I^n} \quad (2)$$

Where C is the theoretical capacity in amp-hours, I is the current, T is the time (in hours), and n is the Peukert number of the battery. The Peukert number is determined empirically, by testing the battery at different rates [16].

Figure 3.1 shows the capacity at different discharge rates for different Peukert numbers. As seen in the figure, the actual amount of energy that can be retrieved from the battery decreases as the discharge rate increases.

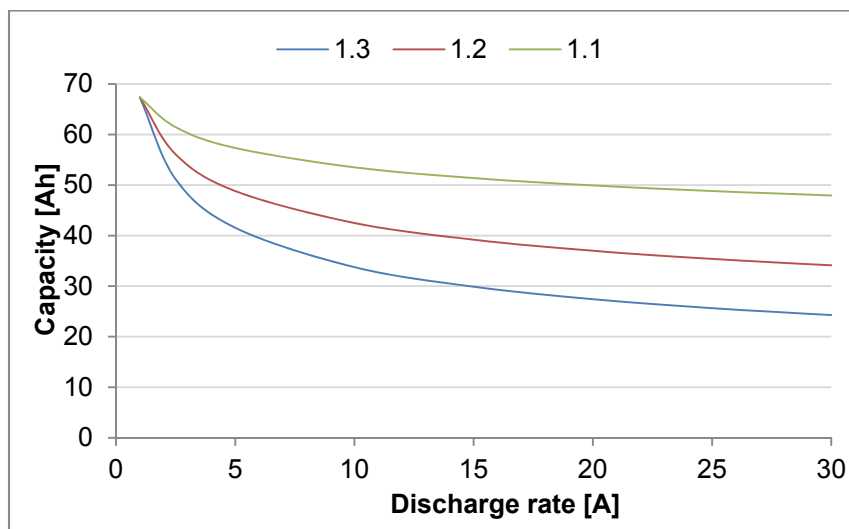


Figure 3.1: Battery capacity at different discharge rates. Calculated by using the Peukert's formula for batteries with Peukert number 1.3, 1.2 and 1.1.

As illustrated in the figure, a battery with a Peukert's number of 1.3 has *half* the capacity of a battery with a Peukert's number of 1.1 at a discharge rate of 25 amps, even though they both have the same theoretical capacity.

The Peukert's formula has however some limitations. Dorfell et al [17] examined the Peukert phenomenon for different lead-acid batteries, and concluded that the Peukert relationship is only valid if the discharge current is constant and the temperature increase inside the battery is limited.

It should also be noted that with modern lithium batteries, like the one in Nissan Leaf, the impact is much less than in lead-acid batteries, but the impact is still nonzero.

3.1.2 State of Charge

The state of charge of the battery (SOC) is defined as the remaining capacity of the battery [18].

$$SOC = \frac{\text{Remaining Capacity}}{\text{Rated Capacity}} \quad (3)$$

For lithium ion batteries the charging power should be reduced when the SOC exceeds a certain percentage. It is recommended in the user's manual [19] to avoid charging above 80 % too often.

For EV analysis purposes, it is important to be aware that when the SOC exceeds a certain percentage the charging will go slower [5].

3.1.3 Charge efficiency

The precise value of the charge efficiency varies with different types of battery, temperature and rate of charge. It is also generally understood that the battery charge efficiency is high at low states of charge and that this efficiency drops off near full charge [16].

Ricardo analysis based on existing charger technology performed by [20] imply that a charger efficiency of 90% is a good estimation.

3.2 Electric Vehicle Charging Schemes

The impact the EVs will have on the power grid will depend on the number of EVs in the vehicle fleet and the charging scheme used. Four different schemes for charging of active power are presented below.

3.2.1 Active power charging control

1. Dumb Charging

The most conventional charging scheme is to plug in the vehicle and get it charged like any other regular load. This is often referred to as *dumb charging* [18]. When using dumb charging, obviously no active power charging control is used; it is only included in this list for completeness.

2. Smart charging

Smart charging is when the vehicle is charged when the grid allows or needs it to. To make this charging scheme possible, there have to be communications between the grid and the vehicle. The smart grid concept with advanced metering infrastructure facilitates this application [18].

3. Vehicle-to-Grid (V2G)

V2G is the most complicated charging scheme and can be considered as an extension of smart charging. In addition to the functions for the smart charging, it also allows the energy stored in the EV batteries to be delivered back to the grid for grid support [18]. *V2G* can be accomplished by discharging energy through bidirectional power flow, or through charge rate modulation with unidirectional power flow [21].

4. Vehicle-to-building (V2B)

V2B is similar to *V2G*, but instead of communicating with the grid, the vehicle communicates with the building [18]. There will not be any focus on *V2B* in this thesis.

3.2.2 Power factor control

In addition to controlling the active power charging, it is possible to use the EV battery for reactive power regulation. As mentioned in 2.3, reactive power transmitted through the transmission and distribution system causes increased energy losses and decreases the system efficiency. With on-site injection of reactive power from the EV battery, the amount of reactive power needed to be transmitted from the generation side is reduced [10].

The amount of reactive power that the charger can supply during charging mode is limited by the apparent power limit of the charger and the amount of active power drawn from the grid. If the amount of active power drawn from the grid is equal to the apparent power capability, the charger is not capable of producing reactive power. However, if the apparent power capability of a charger exceed the active power drawn from the grid by the battery, the range of allowable reactive power injected is given by equation (4) [22].

$$Q = \sqrt{S^2 - P^2} \quad (4)$$

Here S is the apparent power, P is the active power drawn from the grid, and Q is the reactive power injected in the grid.

If reactive power control is to be used, the charger can be rated at 10% - 20% higher power than the maximum real power drawn during charging. This would make the charger capable of injecting reactive power to the system during all operating conditions [23].

3.2.3 Objectives for smart charging control

Many studies with focus on smart charging control of the EVs have been carried out. When going through the literature on this field, it becomes clear that there are many different philosophies when introducing a smart charging control and the smart charging control can be introduced with different objectives. Here some different charging scenarios are listed. This should not be viewed as a *complete* list of possible scenarios, more as an overview of *some* of the different possibilities.

- Smart charging of EVs could be implemented to avoid distribution level grid congestion. EVs could be instructed to avoid charging if there is congestion in the grid. If V2G technology is assumed implemented, the vehicles could also discharge energy back to the grid at the time of congestion.
- Smart charging of EVs could be implemented to facilitate for integration of renewable energy. In [24], an optimal EV charging scheme for facilitating the integration of wind power is presented. The EVs is used for short times to reduce the imbalances associated with the hourly bidding blocks. The EV demand is a combination of sustained charging during the hours with low day-ahead prices and the more pulse-like charging that is used to “fill-up the corners” between the actual wind power production and the hourly bids. In this way, imbalance costs are reduced by EVs that otherwise would have been charged against day-ahead prices.
- Smart charging could be implemented to avoid peaks in demand. If the demand is above a certain value, the EVs could be instructed to stop charging, or to start discharging to the grid if V2G technology is available.
- Smart charging could be implemented to avoid voltages below a certain value by active power control. EVs could be instructed to stop charging or inject power to the grid when the voltages in the grid fall below a certain value.
- Smart charging could be implemented to avoid low voltages by reactive power injection. This could for example be done by reducing the power factor for vehicles charging at that time.
- The EVs could also be used as reserves in case of suddenly unexpected fall in power production.

4 SIMULATION MODEL

4.1 Network Description

It was a wish to use a simulation model that others easily could reproduce and get the same results. It was also wanted to use a simulation model that was not too big and comprehensive. With those two factors in mind, the IEEE 13 node test feeder described in [25] was considered. Due to limitations in MATPOWER, there has however been made alterations of the IEEE 13 node test feeder for the purpose of this thesis. In this section, the original IEEE 13 node feeder will be briefly described, and then the adapted model used in the simulations in this thesis is presented.

4.1.1 The original IEEE 13 node test feeder

The original IEEE 13 node test feeder is presented in Figure 4.1.

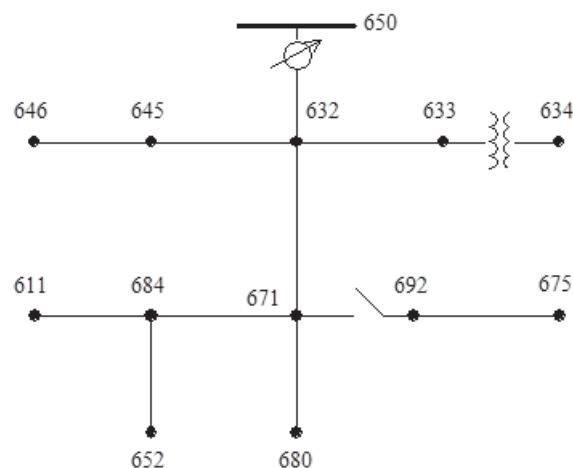


Figure 4.1: One line diagram of the IEEE 13 node test feeder [25]

The IEEE 13 node test feeder operates at a nominal voltage of 4.16 V. The feeder has one substation voltage regulator, two shunt capacitor banks, one in-line transformer and several unbalanced spot loads and one distributed load. There are both overhead and underground lines, which has a variety of phasing. There is also one switch, but this is however closed in the normal operating situation. The complete data of this system can be downloaded from:

<http://ewh.ieee.org/soc/pes/dsacom/testfeeders/index.html>

4.1.2 The designed 11 node test feeder

The test case used in this thesis is constructed from the data describing the IEEE 13 node test feeder, but the regulator, capacitor, switch and distribution lines with zero length have been neglected. After doing these alterations, the one line diagram of the network is as presented in Figure 4.2. This feeder is from now on called *the 11 node test feeder*.

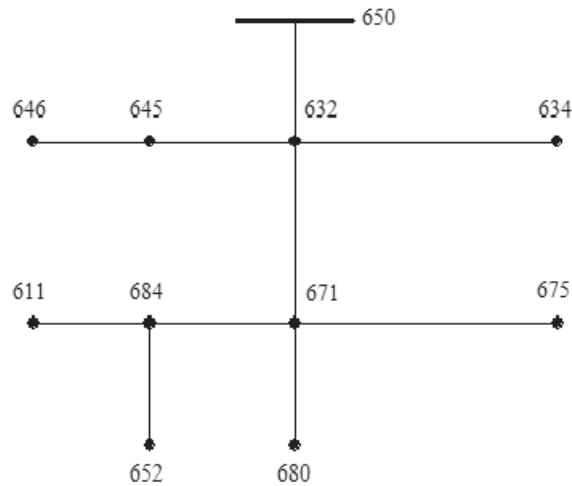


Figure 4.2: One line diagram of the 11 node test feeder. This model is adapted from the data describing the IEEE 13 node test feeder [25]

4.1.2.1 Distribution lines

MATPOWER only considers three phased balanced systems in which the line impedances are equal in all the three phases. MATPOWER therefore uses a single phase representation of the lines.

MATPOWER uses the standard pi one-line equivalent of a three phase transmission line, where all lines are modeled with a series impedance $z_s = r_s + jx_s$ and a total line charging susceptance b . For more details of how the lines are modeled, it is referred to the MATPOWER 4.1 user's manual [26].

A common procedure for representing three phased lines in single line diagrams is to find the positive sequence impedance. The original IEEE 13 node test feeder has however unbalanced line impedances. There is also a combination of tree phase, two phase and single phase lines. It has therefore been necessary to do some simplifications regarding the line impedances when modelling this test case as a single line diagram in MATPOWER. The procedure for finding both the line impedances and susceptances is given in appendix A.

The calculated series impedances are given in Table 4-2. Prior to calculating the series impedances in pu, the base values has to be set. The base values chosen for the purpose of this thesis are presented in Table 4-1.

Table 4-1: Base values

Unit	Base
P_{base}	100 MW
V_{base}	4.16 kV
Z_{base}	0.173 Ω
B_{base}	$\frac{1}{0.173}$ S

Table 4-2: Calculated line impedances for the 11 node test feeder

Node A	Node B	R (Ω)	X (Ω)	R(pu)	X(pu)
632	645	0.1061	0.0798	0.6131	0.4614
632	634	0.0561	0.0720	0.3241	0.4161
645	646	0.0636	0.0479	0.3678	0.2768
650	632	0.0704	0.2260	0.4072	1.3066
684	652	0.2034	0.0776	1.1758	0.4488
632	671	0.0704	0.2260	0.4072	1.3066
671	684	0.0636	0.0507	0.3678	0.2933
671	680	0.0352	0.1130	0.2036	0.6533
684	611	0.0755	0.0766	0.4366	0.4426
671	675	0.0462	0.0393	0.2668	0.2272

4.1.2.2 Shunt elements

In MATPOWER, a shunt connected element such as a capacitor or inductor is modeled as fixed impedance to ground at a node. The admittance of the shunt element at node i is given as

$$y_{sh}^i = g_{sh}^i + jb_{sh}^i \quad (5)$$

In MATPOWER, the parameters g_{sh}^i and b_{sh}^i are specified as equivalent MW (consumed) and MVar (injected) at nominal voltage magnitude of 1.0 pu and angle of zero.

The data describing the IEEE 13 node test feeder, gives two shunt capacitor banks, one at node 675, and one at node 611. The amount of reactive power injected at these buses is given in Table 4-3.

Table 4-3: Shunt capacitors in the IEEE 13 node test feeder [25]

Node	Phase A (kVAr)	Phase B (kVAr)	Phase C (kVAr)
675	200	200	200
611			100
Total	200	200	300

In the 11 node test feeder, it is with that added an injection of 600 kVAr at node 675 ($b_{sh}^{675} = 600$) and 100 kVAr at node 611 ($b_{sh}^{611} = 100$).

4.1.2.3 Load modelling

All loads are modelled as constant power spot loads. The demand at a node is

$$s_d = p_d + jq_d \quad (6)$$

Here p_d is the total demand of active power at and q_d is the total demand of reactive power.

The loads in the IEEE 13 node test feeder have a very unbalanced nature. Due to limitations in MATPOWER, this unbalanced nature has to be ignored, and the power at each node is simply found by summing up the load in each phase. In the IEEE 13 node test feeder, there is a distributed load between node 632 and 671. Due to lack of possibility of modelling distributed loads in MATPOWER, this load is modelled as spot load, where the distributed load is evenly divided by node 632 and node 671. The resulting demands are presented in Table 4-4.

The base demand in this study varies during the studied time period according to a given pattern. The average of the base demand at each of the nodes in the 11 node test feeder is chosen to be equal the demand given in Table 4-4.

Table 4-4 Average base demand at the 11 node test feeder

Node i	p_d (kW)	q_d (kVAr)	Power factor
646	230	132	0.87
645	170	125	0.81
632	100	58	0.87
634	400	290	0.81
611	170	80	0.90
671	1255	718	0.87
675	843	462	0.88
652	128	86	0.83

5 POWER FLOW ANALYSIS

5.1 Power Flow Analysis

AC power flow analysis is basically a steady-state analysis of the AC transmission and distribution grid. The steady state values of node voltages and line power flows are calculated from the knowledge of electric loads and generations at different nodes of the studied system. There are several different solution methodologies, and the methods preferred to solve the power flow in transmission grids differs somewhat from the solution methodology of distribution grids.

The charging scenario used when charging the EVs will alter the demand profiles, and since the voltages in the distribution grid is influenced by the power flow, the voltages changes. Running power flow simulations on a test case is therefore one way of investigating the effectiveness of different EV charging algorithms.

An extension of the power flow analysis is *optimal power flow analysis*. The optimal power flow analysis is in fact done by running a series of power flow analysis to find the optimal power flow.

The 11 node test feeder presented in chapter 4 has only one generator and no dispatchable loads, and thus there is only one valid power flow solution. With only one valid solution a regular power flow gives the same results as optimal power flow, so in this thesis it is only done a regular power flow.

5.2 Power Flow Analysis in MATPOWER

In this thesis MATPOWER is used as power flow simulation tool. MATPOWER is a package of MATLAB files for solving power flow and optimal power flow problems.

The optimal charging schedules for the EVs in this thesis are found by using MATLAB. The fact that MATPOWER works in the workspace of MATLAB is therefore a big advantage. The calculated charging schedule can be used with few intermediate steps to find the resulting voltages. Using MATPOWER as simulation tool also opens up the possibility of using the results from the power flow simulations inside the charging algorithms. Another advantage of MATPOWER is that it is an open source program, which makes it easy to modify [27].

The drawback with MATPOWER is however that MATPOWER is constructed for high voltage transmission networks, and has some limitations when it comes to distribution systems. Since the transmission system usually is balanced, MATPOWER only looks at one line. Distribution systems have on the other hand a much more unbalanced nature.

5.2.1 Power flow solvers in MATPOWER

The default solver in MATPOWER is based on the standard Newton's method. This method is described in detail in many textbooks. There are also included solvers based on variations

of the fast-decoupled method, specifically, the XB and BX methods described in [28]. An advantage with these solvers is that they greatly reduce the amount of computation per iteration, by updating the voltage magnitudes and angles separately based on constant approximate Jacobian which are factored only once at the beginning of the solution process. These per-iteration savings, however, come at the cost of more iterations. There is also a fourth algorithm available in MATPOWER, which is the standard Gauss-Seidel method [26].

The Newton method had problems converging for simulations done on the 11 node test feeder, so one of the other available solvers had to be used. The fast-decoupled method had significantly less iterations than the Gauss-Seidel method. For the purpose of this study, the fast-decoupled method (XB version) is therefore used when doing the simulations.

6 CASE STUDY

In this case study three different scenarios are investigated. In all three scenarios the EV adoption is 50 % of the total vehicle fleet, but in the different charging scenarios, the vehicles charge in different manner.

In the *dumb charging scenario*, the vehicles charge with no concern for grid services or electricity prices. This scenario is presented in 6.4. In 6.5 the *profit maximization scenario* where the EVs charge according to the electricity prices is presented. In this scenario, the vehicles have the possibility to discharge back to the grid (V2G). In 6.6 the *power factor control scenario* is presented. In this smart charging scenario the objective is to avoid voltages below a certain level by adjusting the power factor when charging the EVs.

The different charging algorithms is to be rated according to their effectiveness to avoid low voltages at the nodes in the 11 node test feeder. Therefore, in addition to presenting the scenarios in 6.4 to 6.6, the procedure for finding the resulting demand pattern at the demand nodes at the 11 node test feeder is also presented in these sub chapters.

Before presenting the different charging scenarios, the base demand pattern used in the simulations is presented in 6.1. Then the basic data describing the traffic pattern and the EV availability for regulation services is presented in 6.2. In 6.3 the additional demand at each demand node due to charging of the EVs is presented.

Finally, in 6.7, it is given a table with a summary of the main assumptions made in this chapter.

The resulting demand and voltage profile is calculated by use of MATLAB. The MATLAB code is given in its completeness in the appendices. With the aim of making the code easy to follow, the designed scripts and functions are published by using the MATLAB publish function.

6.1 Base Demand Pattern

For the purpose of this thesis, the power demand at each node is divided into *base demand* and *demand due to charging of the EVs*. The term *base demand* can mean different things in different settings, but in this thesis, when talking about the *base demand* it is always meant the total power demand minus the extra demand due to charging of the EVs.

The total demand at a node during hour i is

$$s_d^i = p_{bd}^i + jq_{bd}^i + p_{EVd}^i + jq_{EVd}^i \quad (7)$$

Here p_{pd}^i and q_{pd}^i is active and reactive base power demand at hour i . This hourly demand is equal in all scenarios. p_{EVd}^i and q_{EVd}^i are the active and reactive power demand from charging the EVs. This demand varies according to which charging scheme is used.

As basis for the simulations it is decided to look at the actual power demand in Norway from 6:00 AM November 5th to 6:00 AM November 6th, 2013. The chosen data gives a typical demand pattern in Norway with two demand peaks; one in the morning and one in the afternoon. The mean demand this period is 15 785 MW. The demand pattern is illustrated in Figure 6.1.

It is assumed that the base demand at all demand nodes in the 11 node test feeder follows the demand pattern in Figure 6.1. It is also assumed that the average base demand during the studied time period is equal the nodal demand presented in Table 4-4, and that the power factor for the base demand is constant and equal the power factor given in Table 4-4.

The base demand pattern at each of the demand nodes is with that found by using equation (8)

$$p_{bd}^i = p_{Nd}^i \cdot \frac{\sum_{i=1}^{24}(p_{bd}^i)}{\sum_{i=1}^{24}(p_{Nd}^i)} \quad (8)$$

Here p_{Nd}^i is the actual power demand in Norway at hour i and p_{bd}^i is the base demand at the studied node at hour i .

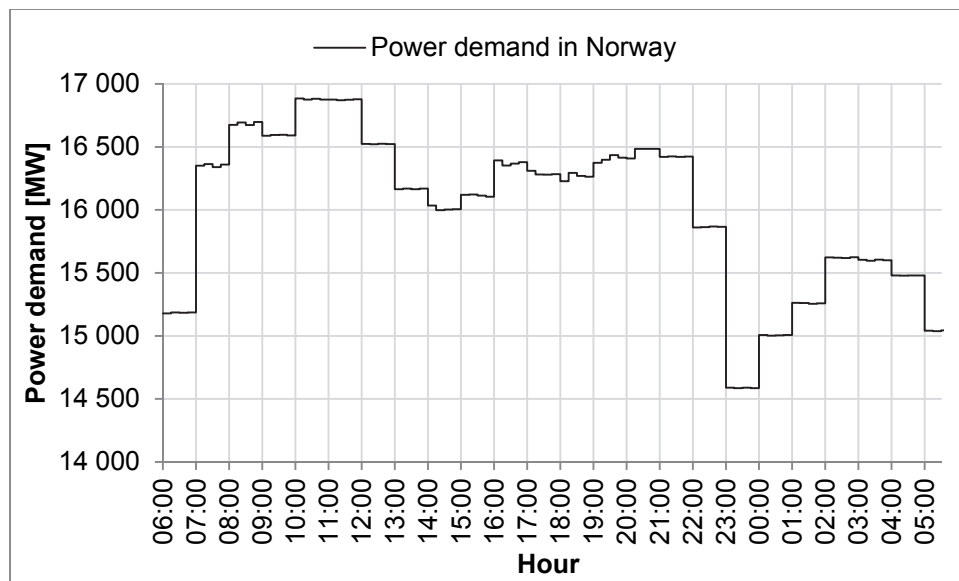


Figure 6.1: Actual demand in Norway November 5th 6:00 PM to November 6th 6:00 PM.

6.2 Driving Behavior and Availability of EVs for Grid Services

6.2.1 Data sources

Reliable data of EV driving behavior is hard to come by. Some studies have been conducted but most of them are geographic and demographically biased. Due to lack of complete information of the driving pattern in Norway, some of the data used in this thesis are actually describing the driving pattern of the neighboring countries. All data used in this thesis describes the driving pattern for conventional vehicles, but it is assumed here that the driving pattern would be similar for the EVs.

The sources of information about the driving pattern used in this thesis are:

- *The Danish National Travel Survey (TU)*
The Danish National Travel Survey is an interview survey which serves to document the travel behavior of the Danish population. The complete dataset from this survey is not open for the public, but in [29] these data are analyzed. Some of the results from this analysis are used in this thesis, with permission from the authors. Data from this survey used in this thesis includes information of when the vehicles are parked.
- *The Norwegian National Travel Survey 2009.*
The Norwegian National Travel Survey is an interview survey which serves to document the travel behavior of the Norwegian population. In the Norwegian National Travel Survey about 29 000 people have been interviewed [30]. Data from this survey used in this thesis includes the average number of vehicles per household.
- *The Mobile Energy Resources in Grids of Electricity (MERGE)*
The MERGE project is a major EU-financed project. The MERGE rapport examines the traffic patterns and human behaviors of drivers across Europe, to provide a benchmark of vehicle usage patterns, against which to compare proposed future developments in electric and plug-in hybrid electric vehicle technology. The data analyzed was collected using a targeted online questionnaire that was filled in by a total of 1 621 people from a number of countries in Europe, from a range of different backgrounds [20]. Data used in this thesis from the MERGE project includes data for return of the last journey of the day.
- *Statistics Norway (SSB).*
Statistics Norway offers statistics about the Norwegian society. Statistics Norway has the overall responsibility for official statistics in Norway, and carries out extensive research and analysis activities. Data used here from Statistics Norway includes the average household consumption, average driving distance and number of registered vehicles [31-33].

6.2.2 Driving distance

According to Statistics Norway, the average driving distance in Norway in 2013 was 36 km [31].

6.2.3 Return of the last journey of the day

Figure 6.2 presents the percentage of the German vehicle fleet returning from their last journey of the day at the different half-hours of the day. The data in the figure are based on data in the MERGE rapport. The MERGE rapport states that there is a regular pattern to the time the drivers return from the last journey of the day, which varies little between the studied countries. For the purpose of this thesis, the pattern described in Figure 6.2 is therefore assumed to be representative for the Norwegian vehicle fleet.

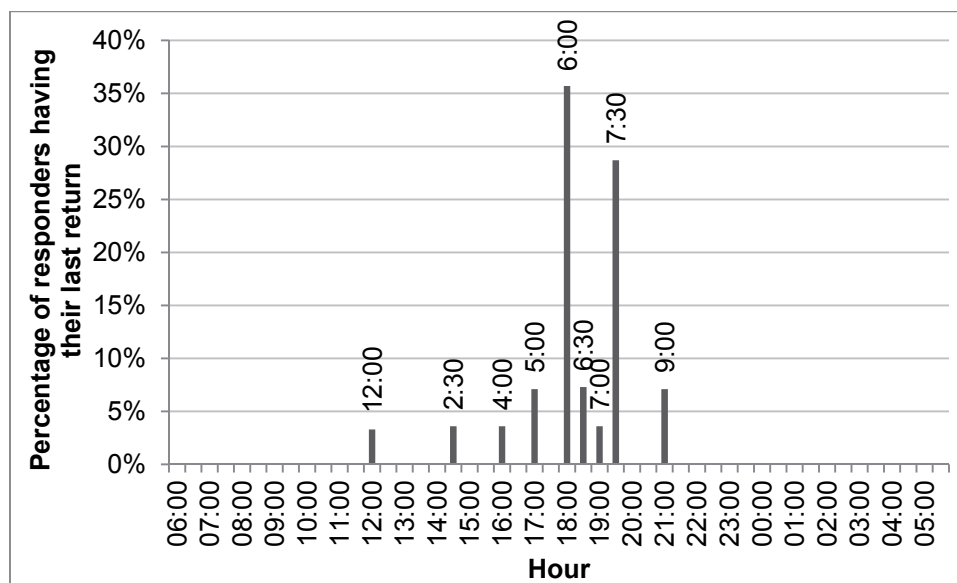


Figure 6.2: Percentage of the German vehicle fleet returning from their last journey at different times during the day

6.2.4 Availability of electric vehicles for grid services (parking time)

Figure 6.3 shows the percentage of the vehicle fleet parked at the different hours of the day. The figure is based on an analysis of the MERGE data performed by [29].

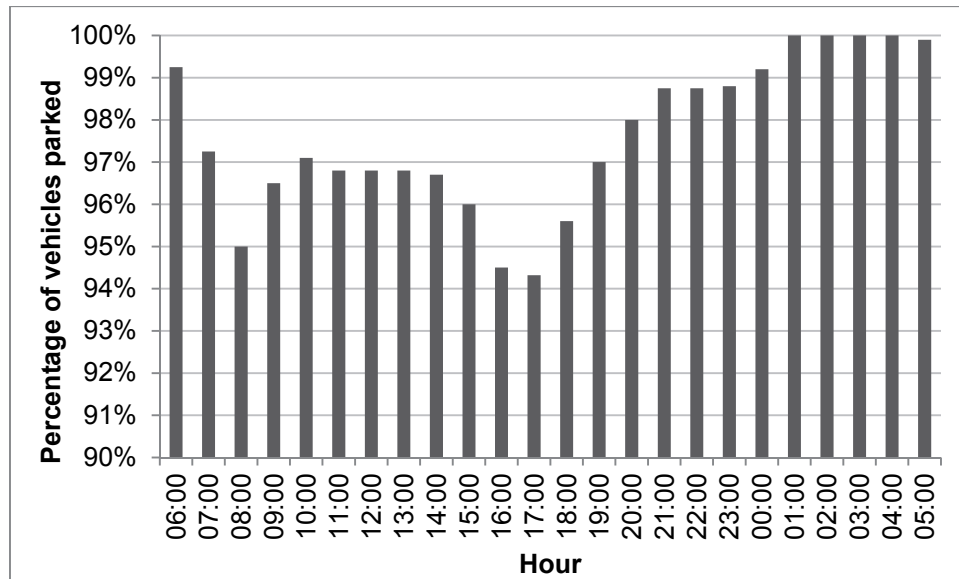


Figure 6.3: Electric vehicle availability for grid services. Adapted from [29] with permission.

For the profit maximization scenario, the data in Figure 6.3 are used to make a separate driving pattern for each of the EVs at node 671 in the 11 node test feeder.

6.3 Daily Power Demand from Charging of the Electric Vehicles

The daily additional power demand from charging the EVs is influenced by the number of EVs and the daily power demand for each EV.

For the purpose of this thesis, it has been assumed that 50 percent of the private vehicles are EVs. In 2013 there were 2 500 265 registered private vehicles in Norway [32]. With a 50% EV adoption, this would lead to 1 250 133 EVs. How many EVs this corresponds to at each node in the 11 node test feeder, depends on the number of houses at each node, how many personal vehicles each household has, and whether or not the EVs are evenly distributed among the nodes.

For the purpose of this thesis, it is assumed that all demand nodes in the 11 node test feeder serves only private households (no industry). In 2009 the average yearly household consumption of electric energy was 16 000 kWh [33], which gives an average consumption of 1.83 kWh per hour. From knowing the average base demand at each node and the average power demand per household, the number of houses connected to each node is calculated, and presented in the third column in Table 6-1.

The average number of personal vehicles per household in 2009 was 1.35 [30]. Assuming that the number of vehicles and EV adoption is evenly distributed among the household in the test case, the number of EVs is calculated and presented in the fourth column in Table 6-1.

Øystein Sagosen concluded in his master thesis “*Analysis of a Large Scale Integration of Electric Vehicles in Nord-Trøndelag*” that whether or not the EVs were evenly distributed in the grid or not have a great influence on the grid impact from charging of the EVs [34].

However, since the focus in this thesis is to compare the different charging strategies with a *given* EV demand, this is not taken into consideration here.

The ratio between energy consumption and traveled distance (kWh/km) depends on the driving speed, road and weather conditions, choice of vehicle model, etc. [18]. These parameters are highly variable and thus an average value (kWh/km) are implemented for EV analysis purposes. For simplicity it is assumed that all vehicles in this study are Nissan Leafs, since this is the most common EV in Norway at the time of writing. Nissan Leaf has a battery capacity of 24 kWh and a range of 199 km. Based on these numbers, the energy consumption is here assumed to be 0.12 kWh/km. Based on this consumption and an average driving distance of 36 km, the average daily demand of each EV is calculated to be 4.32 kWh.

Ricardo analysis based on existing charger technology performed by [20] found a charger efficiency of 90 %. With this, the daily energy demand for charging one EV is calculated to 4.8 kWh. The fifth column in Table 6-1 gives the total daily demand for charging the EVs at each demand node.

Table 6-1 Number of houses and EVs served by each node in the 11 node test case

Node	Average base demand (kW)	Number of houses connected to node	Number of EVs served by node*	Daily demand for charging of the EVs (kWh)
646	230	126	85	408
645	170	93	63	302
632	100	55	37	178
634	400	219	148	710
611	170	93	63	302
671	1255	686	463	2222
675	843	461	311	1493
652	128	70	47	226

*Assuming an average of 1.35 vehicles per household and a 50% EV adoption

6.4 Dumb Charging – A Reference Scenario

The dumb charging scenario assumes that all EVs begin charging immediately when they return from their last journey of the day. This is the most straightforward scenario with no smart control of charging. The dumb charging scenario serves as a reference case when investigating the effectiveness of the algorithms in the profit maximization scenario and power factor control scenario.

When finding the resulting demand pattern at the demand nodes in the 11 node test feeder, it is assumed that the EVs at the nodes follow the pattern of return of the last journey shown in Figure 6.2. Since the return times in Figure 6.2 are given in 30-minute intervals, the resulting demand curve is also given in 30-minute intervals.

For simplicity it is assumed that all EVs have the same energy consumption, and thus the same charging requirement. The average daily charging requirement is calculated in 6.3 to be 4.8 kWh. With a charging rate of 3.3 kW, the resulting demand at all demand nodes are then found by adding a demand of 3.3 kW the two first half hours after demand and 3 kW the third half hour after return.

6.5 Profit Maximization Scenario

In the *profit maximization scenario*, the objective is to maximize the revenue for the overall vehicle fleet. The idea in this scenario is that the EVs charge at low electricity prices and discharge when the electricity prices are high (V2G).

It is assumed that all EVs are connected to a charger, and thus available for grid services, at all times when parked. It is therefore necessary to take the driving pattern into consideration. The driving pattern used for the purpose of this thesis is the one presented in Figure 6.3. Since the driving pattern is given with 15-minute intervals, it is used 15-minute intervals when creating the charging schedules in this scenario.

The algorithm presented here is in fact based on the algorithm in the paper “*Optimal Charging of Electric Vehicles Including Service Provision to the Distribution Network*” by Hexeberg et al., [6] which is given in the appendices. The paper proposes an algorithm for finding the optimal charging schedule under a given set of rules. The problem is formulated as a single-objective linearization problem with several constraints. It is then assumed that *all* EVs adapt to this *exact* same charging schedule. The article is unpublished, and is therefore given in the appendices.

In this thesis the algorithm presented in the paper has been further developed.

6.5.1 Procedure for finding the total demand profile in the profit maximization scenario

To simplify the calculations when finding the resulting demand profiles at all demand nodes in the 11 node test feeder, it is only calculated a new demand profile at node 671, which is the

one with the greatest number of EVs. It is then assumed that the change in demand due to charging of the EVs at this node is representative for the other nodes. The demand pattern at the other demand nodes in 11 node test feeder are thus found by scaling the demand at node 671. There are for example 10.15% less EVs at node 652 than at node 671, so the change in the EV demand at each time step is simply found by reducing the change in EV demand at node 671 with 10.15%.

The procedure for finding the demand pattern at node 671 with 50% EV adoption starts by calculating the charging schedule for one single EV. Then the demand from this EV is added to the base demand. New electricity prices are then calculated by looking at the change in demand due to charging and discharging of this EV. Then the charging/discharging schedule for the next EV is found. The charging/discharging schedule for the first and second EV is not necessarily equal; the driving pattern may not be the same, and the electricity price is somewhat different. After finding the charging/discharging schedule for the second EV, new electricity prices is calculated again, giving a new charging/discharging schedule for the third EV, and so on. A flowchart describing this procedure is presented in Figure 6.5.

6.5.2 Algorithm for finding optimal charging for *one* EV based on electricity prices

The process for finding the optimal charging/discharging schedule for one single EV is illustrated by the sub process to the right in Figure 6.5. This sub process is presented in more detail in 6.5.2.1 and 6.5.2.2.

The procedure for finding the optimal charging/discharging schedule for the EV starts by assuming that the EV is *connected at all times*. It is assumed that if the SOC is below 50%, the EV owner demands that the vehicle is charged to 50% immediately when connecting to the grid, but as soon as a SOC of 50% is reached, the vehicle battery is available for grid services. The algorithm for finding this charging schedule, which assumes a constant availability of the EV, is somewhat similar to the one in the paper in the appendices. Nevertheless, the algorithm is repeated here in 6.5.2.1 for completeness and since there are made some minor changes.

As seen in Figure 6.5, the program calculates a new charging/discharging schedule each time the EV is disconnected from the grid. The reason why this is done, and how, is presented in more detail in 6.5.2.2.

6.5.2.1 Finding optimal charging schedule for one vehicle assuming connected at all times

In this section, the part of the algorithm which is given in the purple box in Figure 6.5 is presented in detail.

The problem is formulated as a single-objective constrained linear programming optimization problem. The decision variables in this case are the values for the 15-minutes charging and discharging of the battery of one EV.

$$\text{Maximize} \quad \sum_{i=1}^{96} ((price_i - e) \cdot d_i) - \sum_{i=1}^{96} (price_i \cdot c_i) \quad e > 0 \quad (9)$$

$$\text{subject to} \quad b_{i-1} + c_i - d_i = b_i \quad i = 1, \dots, 96 \quad (10)$$

$$SOC_{min} \leq b_i \leq SOC_{max} \quad i = 1, \dots, 95 \quad (11)$$

$$0 \leq c_i \leq c_{max} \quad i = 1, \dots, 96 \quad (12)$$

$$0 \leq d_i \leq d_{max} \quad i = 1, \dots, 96 \quad (13)$$

$$b_1 = b_{96} = 85 \quad (14)$$

The objective function (9) maximizes the revenue for the EV owner. Here $price_i$ is the electricity price in time interval i , c_i is the amount of energy bought from the grid in percent of the battery capacity (battery charges) and d_i is the amount of energy sold in percent of the battery capacity (battery discharges). The e in (9) prevents the algorithm to instruct the EV battery to both charge and discharge simultaneously. For the purpose of this thesis the factor e is set to be 2 EUR/MWh. For the algorithm to charge at a given point of time with the plan to sell at another time to get a profit, the price at the point of discharge then have to be at least 2 EUR/MWh greater than at the time of charging.

There are however some restrictions on the decision variables. These restrictions are expressed through a set of constraints (10)-(14).

The algorithm keeps track of the battery's state of charge (SOC) during the whole time period. Each time the battery charges the SOC increases, and each time the battery discharges the SOC decreases. This leads to (10), where b_{i-1} is the battery's SOC at the end of 15-minute period number $i-1$, and b_i is the SOC at the end of 15-minute period number i .

The constraint expressed by (11) makes sure that the battery never exceeds a certain level. In the article in the appendices, [6], this is set to be the maximum capacity of the battery (SOC=100 %). For the purpose of this study, this is reduced to 85%. The constraint expressed by (11) also makes sure that the SOC never falls below a certain minimum value. For the purpose of this thesis, it is chosen to set this value at 50%.

A traditional home charger charges the battery with a charging rate of 3.3 kW [35]. This leads to the constraints expressed by (12) and (13). c_{max} and d_{max} is the maximum amount of energy the battery can charge and discharge during 15 minutes in percent of the battery capacity. With a maximum battery capacity of 24 kWh, c_{max} and d_{max} is calculated to be 3.4375% of the battery capacity.

It is assumed that the EV owner demands that the battery is charged to a SOC of 85% at 6.00 AM each day. Therefore, the schedule starts and ends at 6.00 AM. The restriction expressed by (14) makes sure that the battery SOC is 85% at the beginning and the end of each schedule.

There are a large number of commercial solvers available for solving different optimization models. It is here chosen to use the MATLAB Optimization toolbox.

6.5.2.2 Finding optimal charging schedule for one vehicle by taking into consideration the driving pattern

The optimization algorithm described by equation (9) to (14) does not take into account that the EV can be disconnected from the grid. The way the designed algorithm takes into consideration the driving pattern is presented here.

After finding the optimal charging schedule for the EV assuming that the vehicle is connected to the grid at all times, the algorithm finds out when the vehicle is disconnected from the grid the first time by looking at the predicted driving pattern for this EV. Say the first trip finds place at the 15 minute interval number k . Then the calculated charging schedule for the period until 15 minute interval number k is final, but the charging schedule for the remaining period is deleted. The program then set the charging and discharging to zero for the time period when disconnected and calculates a new charging schedule for the time period from 15 minute k until the end of the studied 24-hour period. The algorithm then finds out if the vehicle is going to be disconnected again during the remaining period. Say the vehicle has a new trip at 15 minute interval number l . then the calculated charging schedule until l is final, but the algorithm calculates a new charging schedule for the period from interval number l and until the end of the studied 24-hour period. The algorithm continues by calculating new charging schedules each time the vehicle is disconnected from the grid. When the program has calculated a new charging schedule for all trips, the calculation of the charging schedule for this EV is considered completed. Please study the sub process in Figure 6.5 for a figurative illustration of this procedure.

It is important to emphasize that it is not in the writer's intension to predict the *actual* charging/discharging schedule for each of the EVs. The calculation of the charging/discharging schedules is only a step in predicting the resulting demand pattern; the total EV demand added to the base demand.

6.5.3 The change in electricity prices due to change in demand

After having completed the calculation of the charging schedule for *one* vehicle, the program calculates new electricity prices based on the change in demand due to charging and discharging of this EV. One of the main conclusions presented in [6], the paper which can be found in appendix C, is that when a large number of EVs were to be charged according to an algorithm similar to the one presented by equation (9) to (14) in this thesis, the relationship between demand and electricity price had to be taken into account. If not there will be a great unwanted peak in demand at the time when the electricity price is at its lowest. This is clearly illustrated in Figure 8 in the paper in appendix B.

One way of taking this into consideration is to calculate the optimal charging schedule for the EVs one by one and to change the electricity prices between the calculations for the EVs. As revealed in the flow chart in Figure 6.5, this is what is done in this thesis.

As mentioned in 2.4, the electricity price is influenced by the supply and demand for electric power. Finding the most realistic relationship between the change in electricity prices and change in demand is not easy and straight forward. The red graph in Figure 6.4 is created by plotting the power demand in Norway during the studied time interval in rising order together with the accompanying electricity prices. The relationship used to find the change in electricity prices in this thesis is a simplification of this curve. This is represented by the black graph in Figure 6.4, which is simply a linearization of the red curve made by taking a visual estimate. As seen in the figure, when the price is below 39.49 EUR/MWh, the slope of the curve is 0.00196 EUR/MW²h, and when the price is above 39.49 EUR/MWh, the slope is 0.01578 EUR/MW²h.

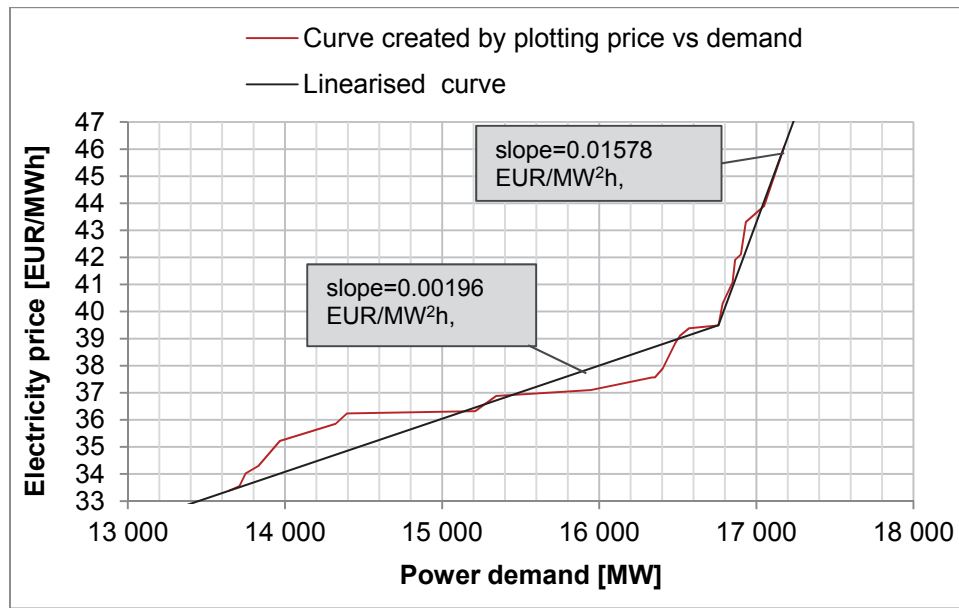


Figure 6.4: Relationship between power demand and electricity prices. This is used to find the change in electricity prices due to change in power demand

When using the slope given by the black graph in Figure 6.4, the new electricity price after adding to the picture the charging and discharging of one EV is given by (15) and (16).

$$p_i^{new} = p_i^{old} + 0.00196 \left[\frac{EUR}{MW^2h} \right] \cdot a \cdot b \cdot 0.001 \cdot \frac{1}{\mu} \cdot (c_i - d_i), \quad p_i^{old} < 39.46 \frac{EUR}{MWh} \quad (15)$$

$$p_i^{new} = p_i^{old} + 0.01578 \left[\frac{EUR}{MW^2h} \right] \cdot a \cdot b \cdot 0.001 \cdot \frac{1}{\mu} \cdot (c_i - d_i), \quad p_i^{old} > 39.46 \frac{EUR}{MWh} \quad (16)$$

The factors a and b can be found by using (17) and (18).

$$a = \frac{(battery\ capacity)}{100 \cdot (duration\ of\ charging)} = \frac{24\ kWh}{100 \cdot 0.25h} = 0.96\ kW \quad (17)$$

$$b = \frac{(number\ of\ EVs\ in\ Norway)}{(number\ of\ EVs\ at\ node\ 671)} = \frac{1\ 250\ 133}{463} = 2700.1 \quad (18)$$

p_i^{old} is the electricity price after adjusting for the change in demand due to charging and discharging of the EV. Since the charge c_i and discharge d_i are given in percentage of maximum battery capacity instead of power (kW), the charge and discharge have to be converted to power (kW) by multiplying with a factor. This factor is represented by the symbol a .

The μ in (15) and (16) is the charger efficiency, which is set to 0.9 in this study. The factor 0.001 is simply to convert kW to MW.

The relationship between electricity prices and demand in Figure 6.4 reflects electricity prices in Norway vs total demand in Norway. It would therefore be wrong to just look at the change in demand from charging and discharging *one* vehicle when changing the electricity price when one vehicle at node 671 charges. This is why the factor b is included in (15) and (16). In 6.3 the number of EVs at node 671 with an EV adoption of 50% was calculated to be 463. Charging of one EV at node 671 is the same as charging $\frac{1}{463} = 0.22\%$ of the EVs at node 671. Then it is assumed that the sample of EVs at node 671 is representative for the rest of the EVs in Norway. In other words, when 0.22% of the EVs at node 671 adapt to the first charging schedule calculated, it is assumed that 0.22% of *all the EVs in Norway* adapt to this exact charging schedule. 0.22% of the EVs in Norway correspond to 2700 EVs, with an EV adoption of 50%.

It is important to emphasize that this is not an attempt to give an accurate prediction of future electricity prices in this thesis. The motivation is rather to find an approximate relationship that satisfies the main characteristics of the electricity price; that there is a high price when the demand is high, and low price when the demand is low. Ideally, when adding the extra power demand due to charging of the EVs according to this charging scheme and with this relationship between demand and electricity prices, both the demand curve and electricity curve smooth out.

It is also important to stress that it is not meant that each EV owner will face different electricity prices; it is only done this way to easily take into consideration the constraints wanted.

6.5.4 Profit maximization scenario with a dynamic time horizon

It is assumed that the EV owners demand that the vehicle should be charged at a certain level each morning. In the simulations it is decided to set the value of SOC to 85% each morning at 06:00. This constraint is taken care of by the part of the algorithm presented in 6.5.2.1 (represented by the purple box in Figure 6.5).

The algorithm here is only suitable for calculating the demand and voltage pattern for a 24 hour period. This algorithm could however easily be adapted to suit for a dynamic time horizon. In that case, the time horizon studied should be consisting of full 24-hour periods. The writer of this thesis suggests finding the final voltage and demanding pattern by first calculating the charging schedules for the first 24 hours. Then the algorithm should take in the predicted driving pattern, demand pattern and electricity prices for the next 24 hours, and calculate the charging schedules for the next day in a similar manner, and so on.

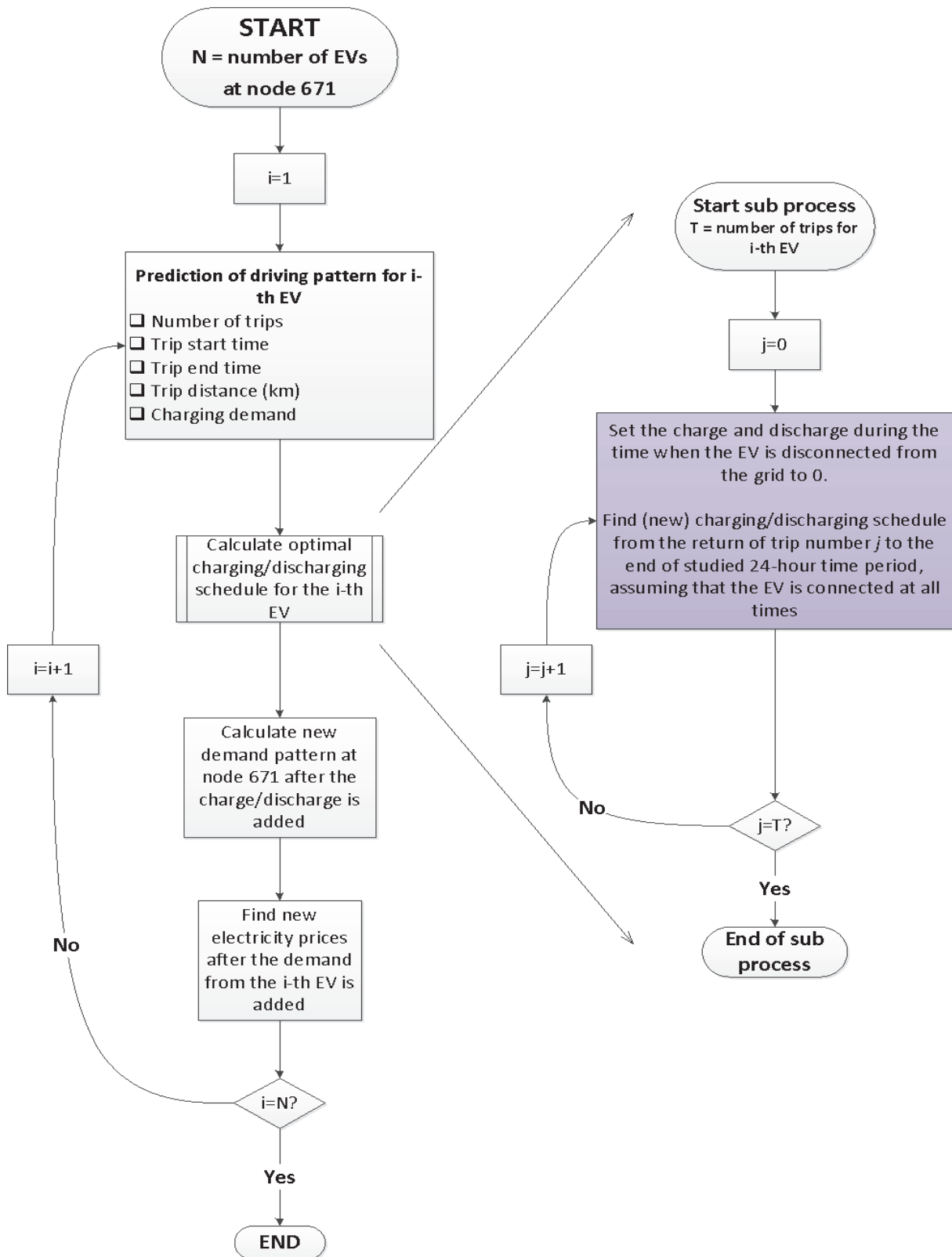


Figure 6.5: Flow chart for finding the final demand at node 671 when the objective is profit maximization of the EV fleet

6.6 Power Factor Regulation Scenario

This section describes the power factor regulation scenario and how the resulting demand curves at the demand nodes in the 11 node test feeder are calculated. The idea in this scenario is to avoid voltages below a determined value by injecting reactive power from the EV battery into the grid. This is done by changing the power factor when charging the EV batteries. A somewhat similar procedure is presented in [36].

The reactive power is to be injected by changing the charging power factor for EVs charging at the time of voltage violation.

As opposed to the other two charging scenarios presented in this thesis, *all* EVs do not charge according to the same charging scheme. (Note that in the profit maximization scenario all EVs charge according to the same algorithm, even though their resulting charging schedule is different). In the power factor regulation scenario the idea is that if the voltage constraints are not violated all EVs charge according to their owner's convenience, with not concern about prices or grid services. It is here assumed that the owners will charge as in the dumb charging scenario presented in 6.4. One can say that the EVs charges according to the *dumb charging mode*. However, when the voltages fall below a certain limit, EVs are instructed to adapt to the *power factor control mode*. For simplicity, it is also assumed in this thesis that when the vehicles start charging according to a charging mode, it continues to charge according to this mode until fully charged. The algorithm cannot in other words instruct an EV to switch from dumb charging mode to power factor control mode in the middle of the charging process.

This control mode is presented in 6.6.1. How the program finds out which EVs that should switch to the *power factor control mode*, and when they should do this, is presented in 6.6.2.

Since the data describing the return of the last journey of the day is given in 30-minute intervals, it is used 30-minute intervals in this scenario.

The procedure here is suitable for input of a dynamic time horizon.

6.6.1 Power factor control mode

It is assumed that the charger capacity is restricted by a maximum apparent power. The relationship between active power (P), reactive power (Q) and maximum apparent power S_{max} is given by the equation below:

$$S_{max} = \sqrt{P^2 + Q^2} \quad (19)$$

Plotting the maximum apparent power for all possible values of P and Q gives the “PQ circle” given in Figure 6.6.

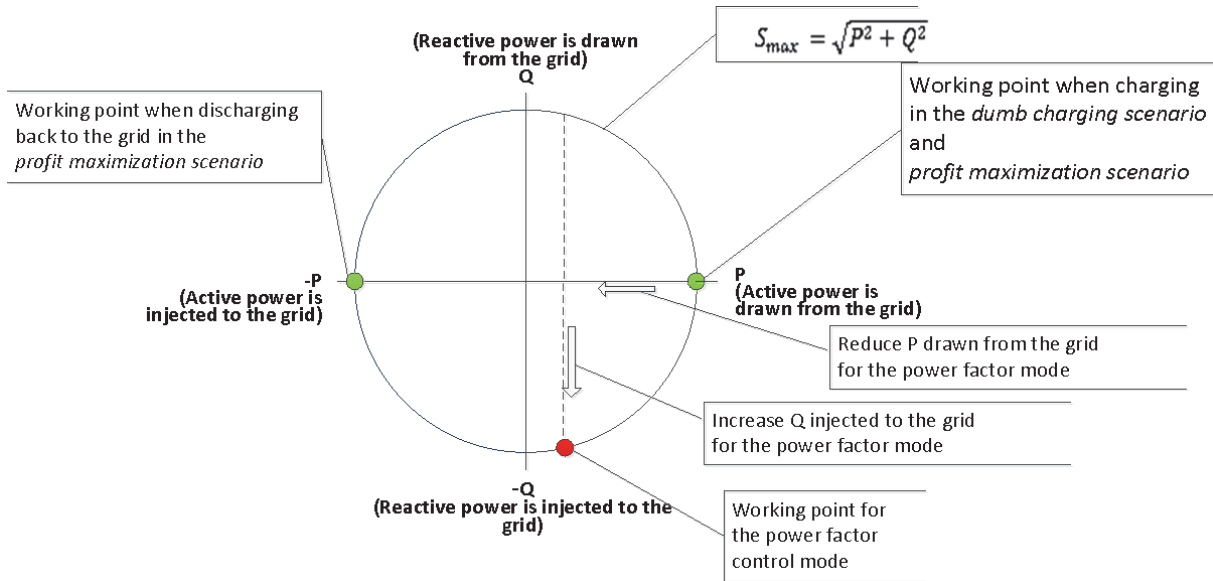


Figure 6.6 PQ circle.

As seen in the figure, when maximum active power is drawn from the grid, the reactive power has to be zero. This is the case when charging in the *dumb charging scenario* and the *profit maximization scenario*. By moving the working point during charging in Figure 6.6 to the left to the red point marked, the active power is decreased and reactive power is injected to the grid.

To allow for reactive power to be injected into the grid, the active power thus have to be reduced, but then the charging time is also increased. The longer the time is set to finish charging, the more reactive power can be injected while charging. It is reasonable to believe that the EV owner demand that the charging should finish by the time for the next trip. It is found no data giving both time for last return *and* time for next trip. It is therefore chosen to assume that the vehicle is connected for the next 8 hours, as it is the *last* trip of the day. In that case, the active power will be as calculated in (20). The available reactive power in this situation is calculated in (21).

$$P = \frac{E_{EVdemand}}{x} = \frac{4.8 \text{ kWh}}{8 \text{ h}} = 0.6 \text{ kW} \quad (20)$$

$$Q = -\sqrt{S_{max}^2 - P^2} = -\sqrt{3.3^2 - 0.6^2} \text{ kVAr} = -3.245 \text{ kVAr} \quad (21)$$

The $E_{EVdemand}$ in (20) is the daily energy demand in kWh for each EV. This is calculated in 6.3 to be 4.8 kWh. The factor x is how long the vehicle is parked before its next trip, and measured in hours. The value for the reactive power injected to the grid, Q , is found by using (21). The reason why the Q is negative here is that reactive power is *injected* into the grid. If the Q is positive, reactive power is drawn from the grid.

6.6.2 Procedure for finding the demand in the power factor control scenario

The procedure for finding out which EVs to charge according to the power factor control mode is illustrated in the flow chart in Figure 6.7.

First the demand and voltage profiles at all demand nodes are calculated assuming that all vehicles charge according to the dumb charging scenario presented in 6.4.

Then the algorithm controls the voltages at the all half hour periods, starting at the first half hour. If the algorithm detects a voltage violation at any of the nodes during a half hour, the algorithm attempts to prevent this violation by instructing an EV at the node of violation to charge according to the power factor control mode instead of the dumb charging mode.

Next, the algorithm checks if there are any EVs having its last return at the time of violation. If there are any EVs returning at this half hour, this EV is set to charge according to the power factor control mode instead of dumb charging mode. If there are no EVs returning at this point of time, the program checks if there are any EVs returning the previous hour. If there is a vehicle returning at this point of time, the program instructs the EV to charge according to the power factor control mode. If not, the program checks if there are any EVs returning the half hour before. The charging time when charging according to the power factor control mode is set to 8 hours. Therefore, if the program has not succeeded to find any available EVs for power factor control during the 8 hours prior to the voltage violation, the program has failed to prevent the voltage violation. Even though the algorithm failed to prevent this voltage violation, the algorithm continues to check if there are any other violations during the rest of the time period.

If the program succeeds in finding an available EV for grid services under these rules, it does not necessarily mean that the voltage violation is avoided. The program therefore has to calculate new voltages and make a new control of the voltages. If there still is a voltage violation, the program keeps on instructing EVs to charge according to power factor control mode until the voltage violation is either cleared or there are no more EVs available for grid services.

Then the program continues to check the other half hours one at a time, to search for voltage violations. If there are found any more voltage violations, the procedure for avoiding the violation is repeated. Please see Figure 6.7 for a figurative illustration of this process.

When choosing the level for the lowest acceptable voltage, it was a wish to choose a voltage that illustrated the effect from the charging scenario in a good way. By looking at the voltages from the dumb charging scenario, the lowest acceptable voltage was set to be 0.935 pu.

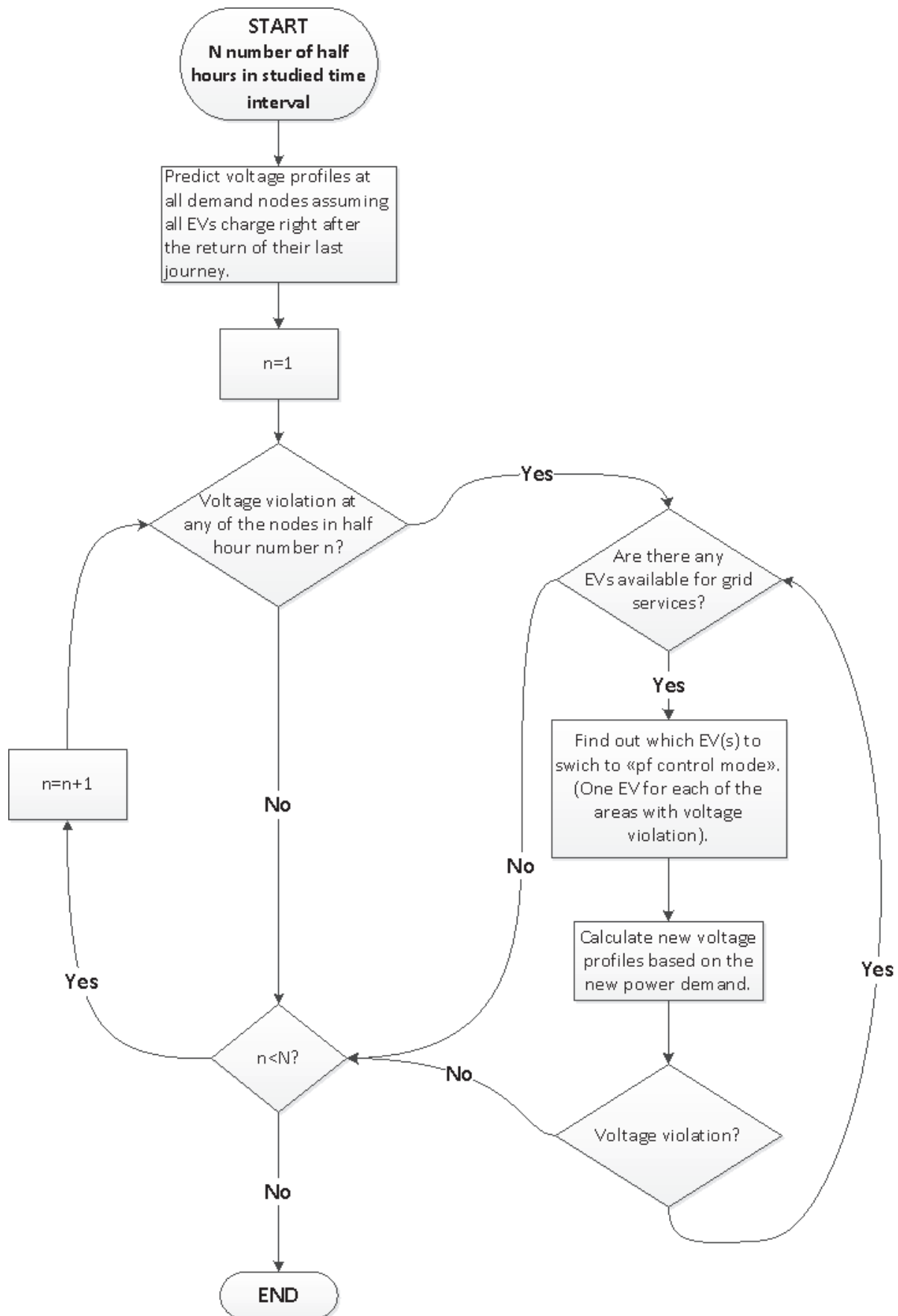


Figure 6.7: Flow chart for finding the voltage and demand pattern for all demand nodes in the reactive power charging control scheme

6.7 Summary of Assumptions

A summary of assumptions for the purpose of the simulations in this thesis is given in Table 6-2. Table 6-3 gives the parameters related to the choice of vehicle model in this thesis.

Table 6-2: Assumptions

DESCRIPTION	SYMBOL	VALUE	SOURCE
Assumptions common for all charging scenarios			
Portion of EVs in Norway's vehicle fleet		50 %	
Availability of charging stations		No restrictions on the availability of charging stations.	
Length of trip		15 minutes	Not based on statistical data. This restriction is made with sole reason to ease calculations.
Charger efficiency	μ	90 %	Ricardo analysis based on existing charger technology performed by [20].
Assumptions for the profit maximization scenario			
SOC in beginning of studied time period	b_1	85 %	Maximum recommended SOC, according to Nissan Leaf user manual.
Max SOC when connected to grid.	SOC_{max}	85 %	Maximum recommended SOC, according to Nissan Leaf user manual.
Min SOC when connected to grid	SOC_{min}	50 %	Not based on statistical data. It is simply assumed by the writer of this thesis that this would be a reasonable demand of capacity.
Max energy charged during time interval of 15 minutes. Given in percentage of battery capacity.	c_{max}	3.4375%	Calculated in 6.5.
Max energy discharged to the grid during time interval of 15 minutes. Given in percentage of battery capacity.	d_{max}	3.4375%	Calculated in 6.5.

Charge rate		3.3 kW	Nissan Leaf's Norwegian home pages [37].
Discharge rate (to the grid in V2G mode)		3.3 kW	Assumed equal the charge rate.
Assumptions for the power factor regulation mode in the power factor regulation scenario			
Charge time	x	8 h	Assumption made by the writer
Charge rate active power	P	0.6 kW	Calculated in (20)
Charge rate reactive power	Q	-2.498 kVAr	Calculated in (21)

Table 6-3: Parameters related to choice of vehicle model

DESCRIPTION	VALUE	SOURCE
Vehicle model	Nissan Leaf	The most common vehicle model at time of writing.
Battery capacity	24 kWh	Nissan Leaf's Norwegian homepages [37]
Battery range	199 km	Nissan Leaf's Norwegian homepages [37]
Vehicle energy requirement	0.12 kWh/km	Based on the battery capacity and range of Nissan Leaf. Influence of the weather conditions, speed, etc. is ignored.

7 RESULTS

This chapter presents the results from the simulations of a 50% EV adoption at the 11 node test feeder. The input for the simulations is based on the actual power demand and electricity prices in Norway during a 24-hour period starting at 06:00 November 5th, 2013.

In all the simulations, the lowest voltage during the studied time period occurred at node 652, making this the most critical node in this context. It is therefore chosen to focus the presentation of the results around this node.

7.1 Impact of Dumb Charging Scenario

The dumb charging scenario assumes that all EVs are plugged in and begin charging, immediately when they return from their last journey of the day. This scenario serves as reference when introducing the designed smart charging strategies. This also illustrates the consequence of introducing significant penetrations of EVs, if no action is taken to meet the challenges and possibilities with this demand.

7.1.1 Demand pattern in the dumb charging scenario

The simulations show that a 50% penetration of EVs, with a dumb charging strategy, would cause an increase in daily peak demand of 46% at all demand nodes at 11 test node feeder. Figure 7.1 shows the impact on the demand at node 652. Due to the assumption of an even distribution of the EVs and equal driving and charging pattern at all the nodes, the demand profile is similar at the other nodes.

As can be seen in Figure 7.1, the demand from charging the EVs is mainly concentrated between 18:00 and 21:00. The increase in demand due to charging of the EVs also coincides somewhat with one of the peaks in the base demand.

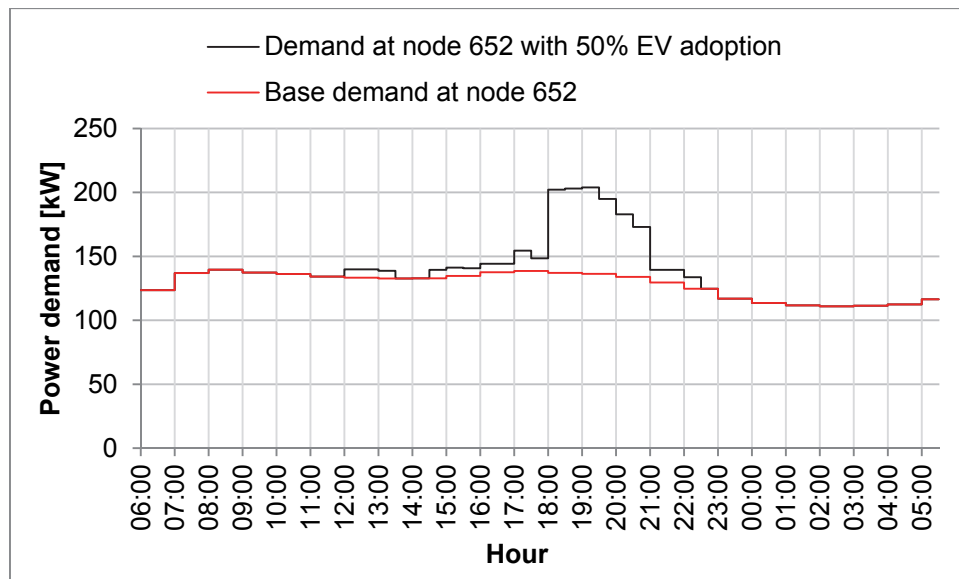


Figure 7.1: Effect of dumb charging scenario on the demand at node 652

7.1.2 Voltage pattern in the dumb charging scenario

The impact of the EV demand on the voltages at node 652, in the case of dumb charging, is shown in Figure 7.2. From the figure, it is clear that the EV demand causes a big drop in the voltages at the time where there is a peak in the demand. The lowest voltage in the base demand is 0.934 pu, and when charging of an EV adoption of 50% is added to the load, the lowest voltage is reduced to 0.915 pu.

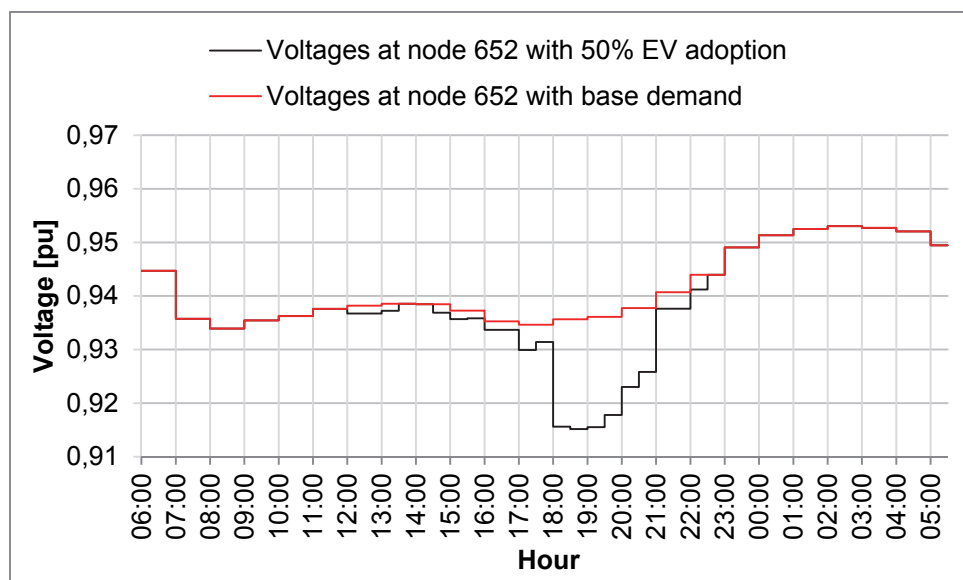


Figure 7.2: Effect of dumb charging scenario on the voltages at node 652

7.2 Impact of Profit Maximization Scenario

In the profit maximization scenario, the designed algorithm calculates the charging schedule for the EVs one by one, changing the electricity prices in between. The objective here is to maximize the overall vehicle fleet profit by charging at low prices and discharge back to the grid at high prices (V2G). This is the only scenario studied in this thesis with the possibility of V2G. The charging schedules for two of the vehicles are included in the presentation of the results for this scenario.

7.2.1 Charging schedule for electric vehicles in the profit maximization scenario

Figure 7.3 and Figure 7.4 give the first and last calculated charging schedule. The electricity prices used to calculate these schedules are included in the figures.

As seen in the figures, the schedules are very different. Note that the last EV does not take part in V2G services. The price curve is too flat to make it profitable, as the price for discharged energy is set to be 2 EUR/MWh lower than the price for charging. In fact, the simulations show that with in this scenario, under the constraints made, only 66% of the EVs discharged back to the grid.

The first vehicle has three trips, each lasting for 15 minutes; one at 5:00, one at 13:00 and one at 17:00. As seen in Figure 7.3, both charge and discharge is set to be zero at those times.

Another thing worth noting from Figure 7.4 is that the EV is instructed to charge only a small amount of energy, over and over again, even though the electricity price pattern seems flat. The reason for interrupting the charge so many times is not due to the driving pattern, as this vehicle returns from its last journey of the day at 15:00. The reason is that there is not included in the code any incentives for charging or discharging for a longer period of time compared to repeatedly switching on and of the charging or discharging. The electricity price pattern from 21:00 to 05:00 are in fact not *completely* flat, the price pattern have actually a variation of 0.02 EUR/MWh, with 37.25 EUR/MWh as minimum and 37.27 EUR/MWh as maximum.

For the single vehicle, it would probably be more attractive to continue charging to finish when started, instead of starting and stopping. (The effect on the battery has not been considered in this thesis). However, the *final* demand pattern should not be very much different. As mentioned in 6.5, the intention by calculating the different charging schedules here are *not* at attempt to predict the actual charging schedules for the EVs. It is only a way of calculating the total demand, by taking both the driving pattern and the change in electricity prices due to change in demand into consideration.

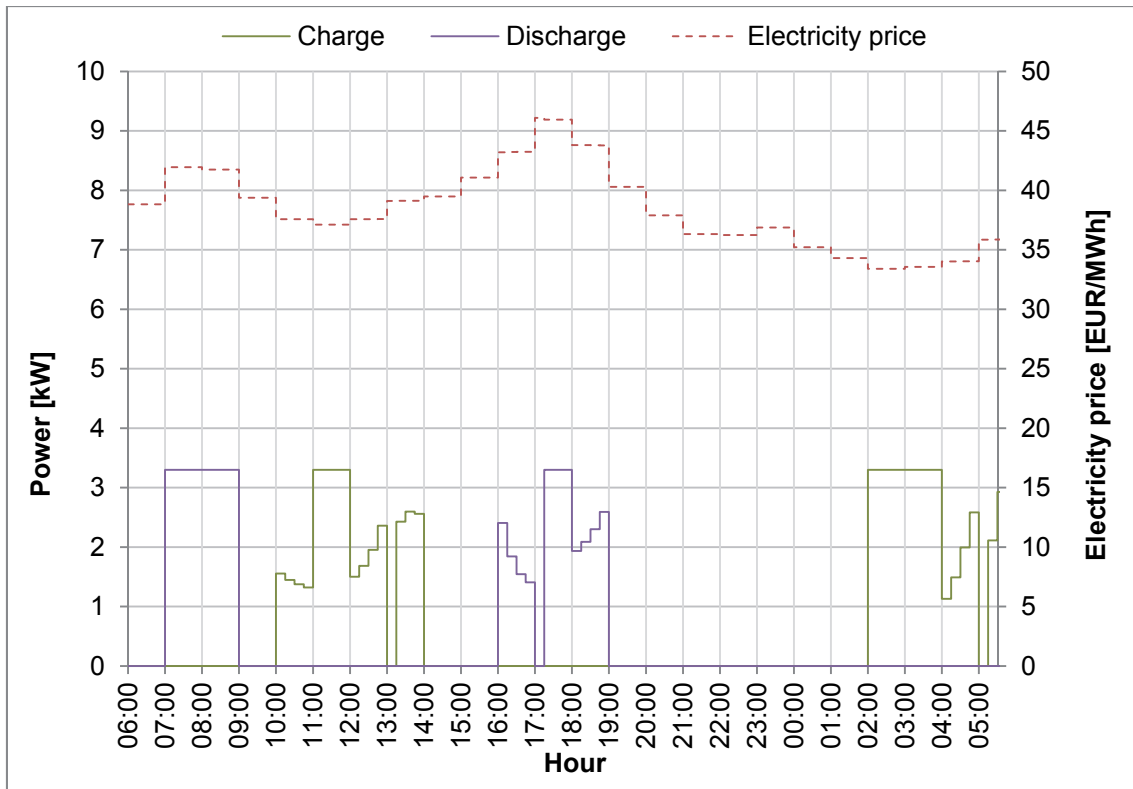


Figure 7.3: Schedule for charging and discharging of the calculated in the profit maximization scenario. This schedule is the first schedule calculated.

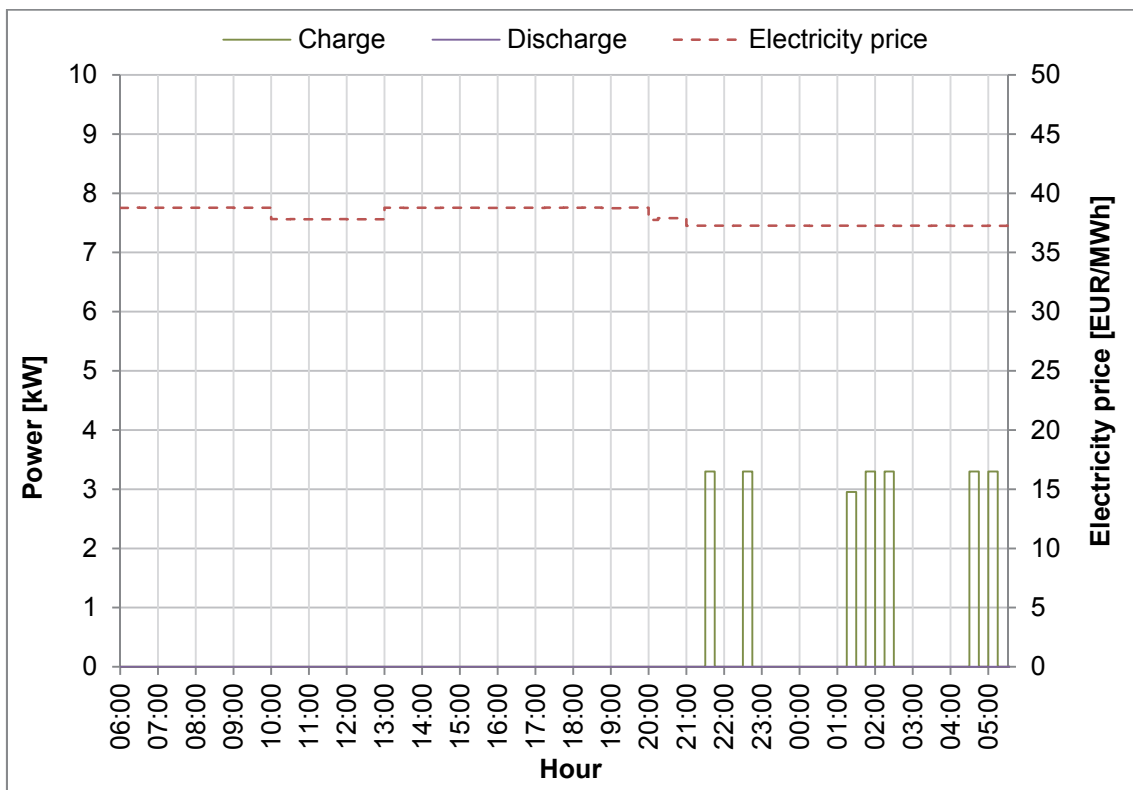


Figure 7.4: Schedule for charging and discharging of the calculated in the profit maximization scenario. This schedule is the last schedule calculated.

7.2.2 Demand pattern in the profit maximization scenario

Figure 7.5 gives the active power demand at node 651 with a 50% EV adoption together with the electricity prices. The red dashed line gives the initial electricity prices; in other words the actual electricity prices during the studied time interval. It is these electricity prices that are used when finding the first charging schedule calculated by the program. The black dashed line is the electricity prices after charging the whole EV fleet.

As seen in Figure 7.5, the base demand and original electricity price follow a similar pattern. The idea behind this scenario is that by changing the electricity price as the vehicles charge, the resulting price pattern and demand pattern would smooth out when there is a sufficiently great enough EV demand.

At a first glance, when looking at Figure 7.5 between 01:00 and 05:00, it seems like the changes in the demand pattern is too high before the price curve flattens out. Remember that all nodes in the 11 node test feeder is assumed to be serving only households, giving it an extra high number of EV compared to the base demand.

The resulting demand in Norway is therefore also calculated and presented in Figure 7.6. The demand pattern here is more smoothen out, but however still not as flat as the electricity price. There was experimented with a variety of different relationships between the price and demand when settling the new electricity prices between the calculations of the charging schedules. The one presented in Figure 6.4 in chapter 6.5 is the relationship found with the most smoothing effect. If perfect it would however have flattened out the demand curve completely.

Note from looking at Figure 7.6 that around 16:00 to 19:00 the electricity prices reduces drastically while the demand curve only increases a bit in comparison. Note also that around 01:00 to 05:00 the electricity price reduces less compared to the increase in demand. This is because the slope of the relationship between electricity price and demand is different for high prices than for low.

In addition to experimenting with the relationship between the electricity price and demand, it was experimented with the effect of changing the difference in price for charging and discharging. The demand and electricity price in Norway when the price for discharge is set to 0.01 EUR/MWh below the price for charging, instead of 2 EUR/MWh, is illustrated in Figure 7.7. As seen in the figure, the electricity price pattern is even more smoothed out than in Figure 7.6, but the resulting demand gets a saw tooth shape from 21:00 to 05:00.

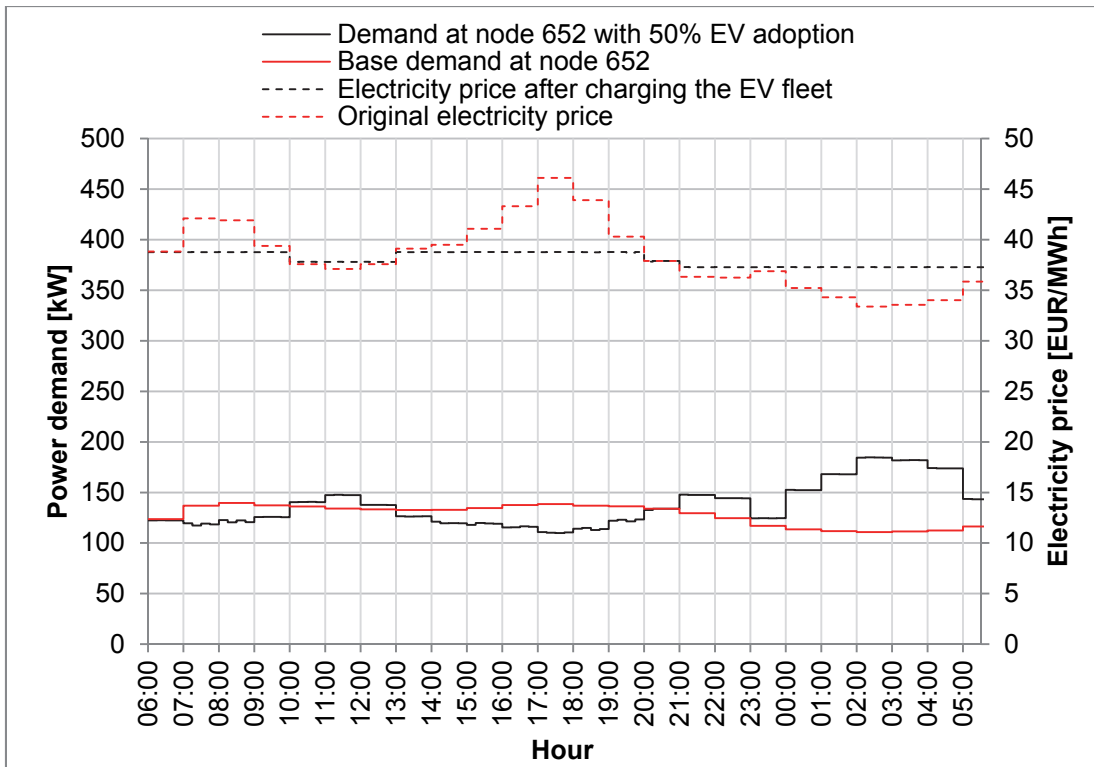


Figure 7.5: Active power demand at node 651 with 50 % EV adoption and all EVs charging according to the profit maximization scenario

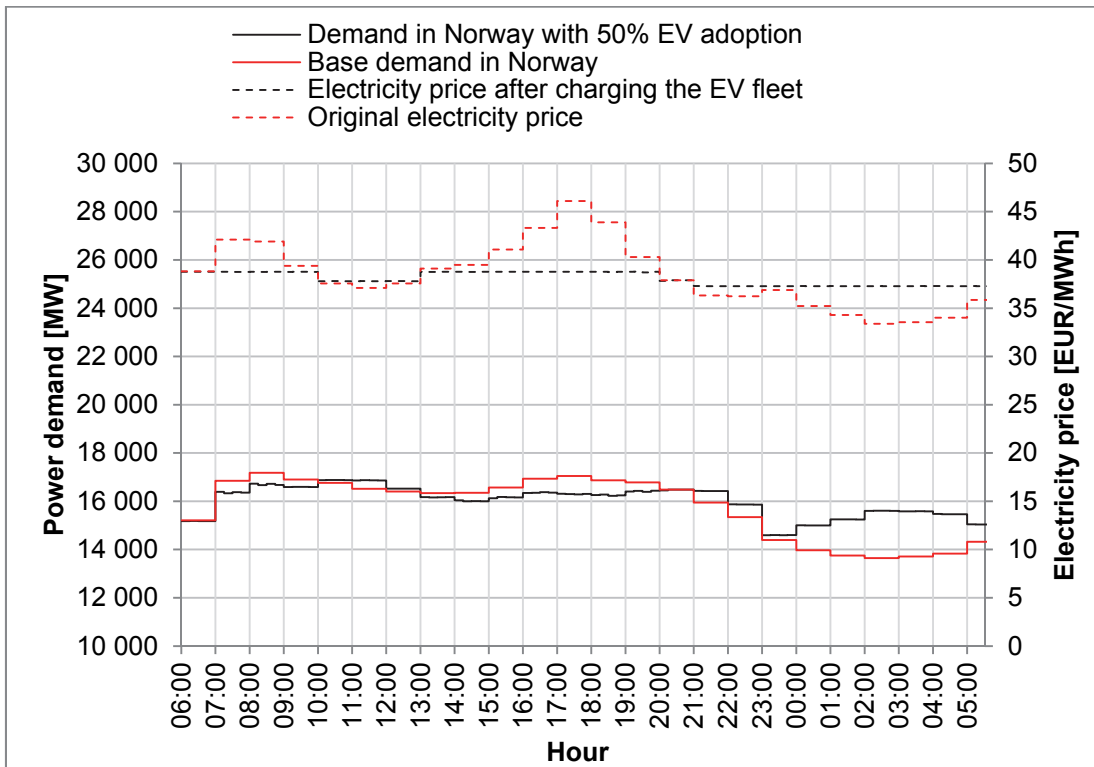


Figure 7.6: Active power demand in Norway with 50% EV adoption and all EVs charging according to the profit maximization scenario

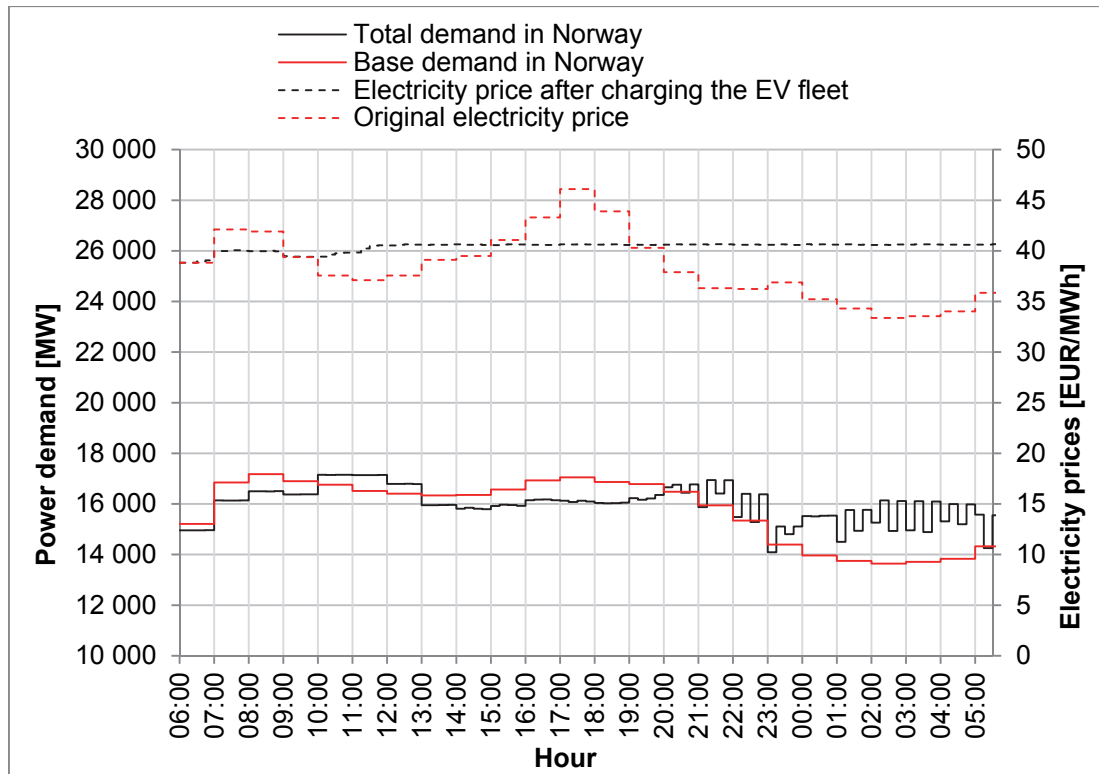


Figure 7.7: Active power demand in Norway with 50 % EV adoption and all EVs charging according to the profit maximization scenario. Price of discharge is set to 0.01 EUR/MWh below the price for charging.

7.2.3 Voltage pattern in the profit maximization scenario

The voltage pattern at node 652 with a 50% EV adoption is presented in Figure 7.8. As seen in the figure, the peak in demand around 02:00 causes a dip in the voltage. The minimum voltage is reduced from 0.934 pu at 08:00 with only the base demand to 0.932 pu at 02:00 with a 50% EV demand.

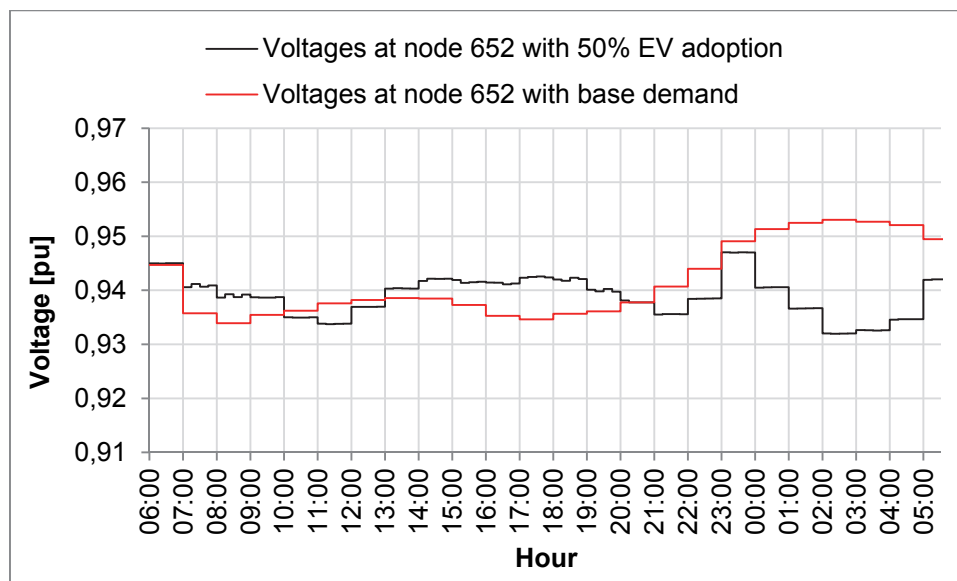


Figure 7.8: Voltages at node 652 with a 50% EV adoption charged in the profit maximization scenario

7.3 Impact of Reactive Power Regulation Scenario

In the reactive power regulation scenario, the idea is to avoid voltages below a certain limit by instructing EVs to charge in power factor control mode instead of dumb charging mode when there is a voltage violation.

When simulating a 50% EV demand at the 11 node test feeder under the rules given in chapter 6, and setting the lower allowable voltage limit to 0.935, it appeared that out of a total of 1217 EVs at the 11 node test feeder, 162 were instructed to charge in the power factor regulation mode. The distribution of the EVs instructed to charge in power factor control mode is given below;

- At node 611 62% of the EVs charge in power factor control mode (39 out of 63)
- At node 671 7% of the EVs charge in power factor control mode (32 out of 463)
- At node 675 16 % of the EVs charge in power factor control mode (49 out of 311)
- At node 652 89 % of the EVs charge in power factor control mode (42 out of 47)
- At the other nodes, all EVs charge as in the dumb charging scenario.

The node with the biggest percentage share of EVs charging in power factor control mode is node 652. This is not very surprising, as this is the node with the lowest voltages.

7.3.1 Demand pattern in the power factor control scenario

The active power demand pattern in the power factor control scenario with a 50% EV adoption is illustrated in Figure 7.9. The demand at node 652 with all vehicles charging like in the dumb charging scenario is included in the figure with the blue dashed line. From comparing the blue dashed line with the black line, one can see that by instructing EVs to

charge in the power factor control mode, the demand is spread out over a longer time period, which in turn reduces the peak in demand significantly.

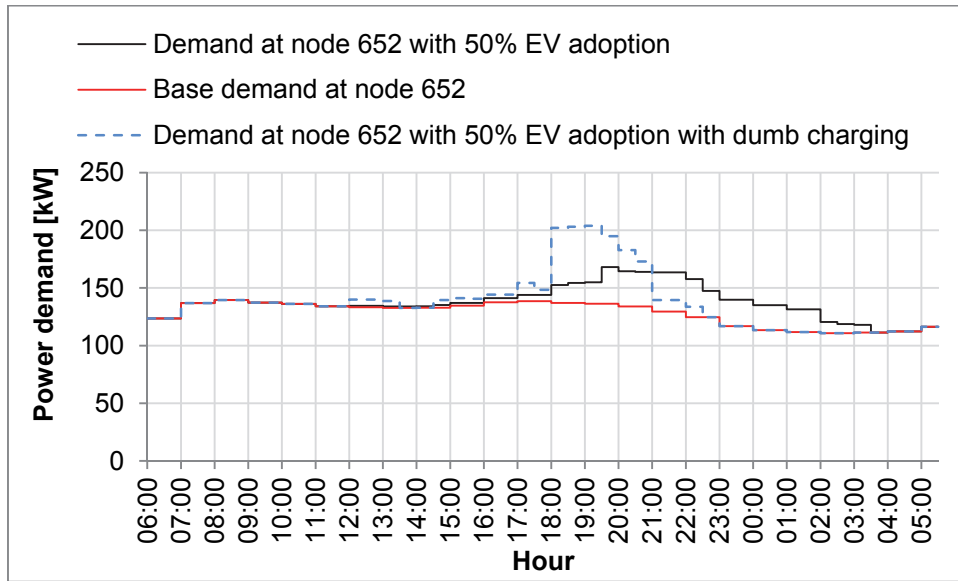


Figure 7.9: Active power demand pattern in the reactive power regulation scenario with 50 % EV adoption

The reactive power demand pattern is presented in Figure 7.10. As seen in the figure, there is a substantial amount of reactive power injected. Between 18:00 and 02:00 the reactive power injected at the node is actually so high that the node acts like a reactive power generator.

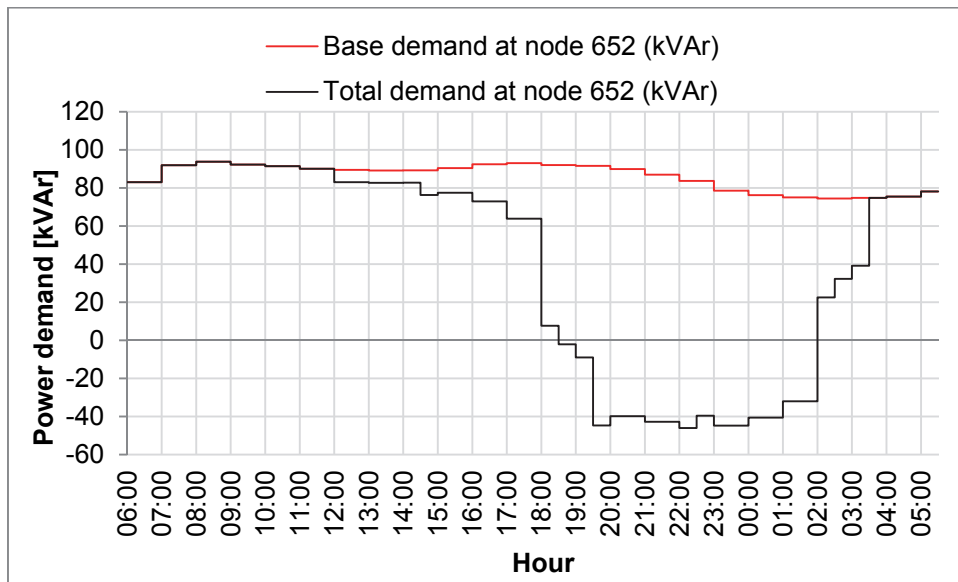


Figure 7.10: Reactive power demand pattern in the reactive power regulation scenario with 50% EV adoption

7.3.2 Voltage pattern in the power factor control scenario

In this scenario all nodes, except node 652, managed to avoid voltages below the minimum allowable value of 0.935 pu by instructing EVs to charge in power factor control mode. At node 652, the voltages are kept over 0.935 pu for much of the time, but not all.

The resulting voltage profile for node 652 is presented in Figure 7.11. At 08:00 and 17:00 the voltage is 0.934, and thus 0.001 pu below the limit. Out of the 47 EVs charging at node 652, there are five vehicles that have not been instructed to switch to power factor control mode. These vehicles return however from their last journey at a later point of time, and are thus not available for grid services at the time of violation, according to the rules set in this scenario. Remember that the vehicles are only assumed to plug in and charge at the time of last return in the power factor control mode, and charge for 8 hours. Outside this time frame, they are not considered available for grid services. The five vehicles that have not been instructed to charge in power factor control mode return from their last journey of the day at 19:30 and 21:00.

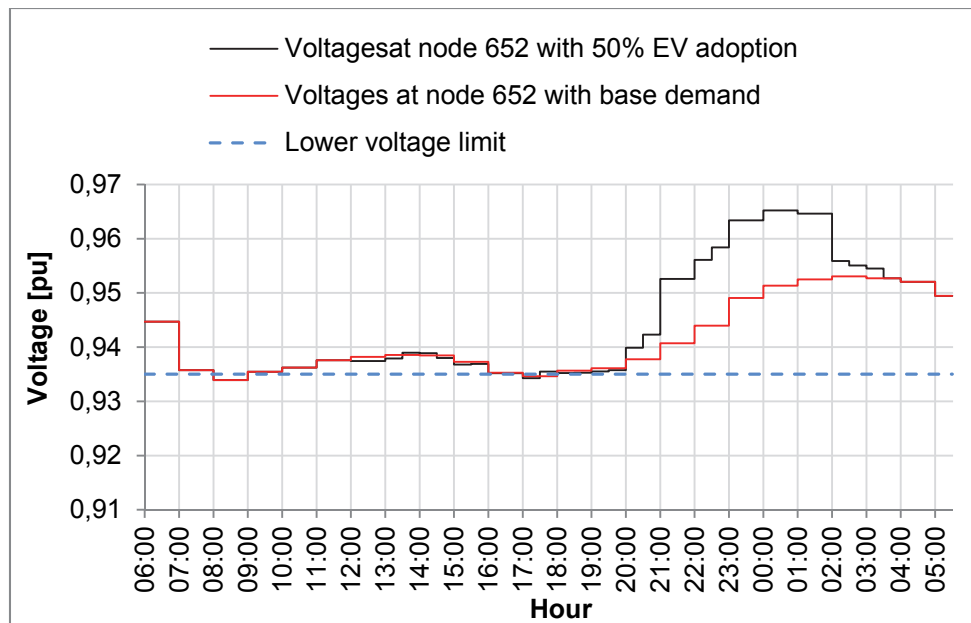


Figure 7.11: Voltage at node 652 in the power factor control scenario

7.4 Summary of Results

In Figure 7.12, the voltage profile at node 652 in the 11 node test feeder is given for an EV adoption of 50%. These curves are the same as the one in Figure 7.2, Figure 7.8 and Figure 7.11. Nevertheless, this figure is included here, as it makes it easy to compare the voltage profile in the three different scenarios. For the same purpose, some of the main findings from the simulations are presented in Table 7-1. In addition to presenting the maximum demand, minimum demand and lowest voltage, Table 7-1 presents the increase in peak demand and variation of demand in percent. The increase in demand, ΔP , is calculated using (22) and the variation in demand, P_{var} , is calculated using (23).

$$\Delta P = \frac{P_{max}^{50} - P_{max}^{base}}{P_{max}^{base}} \quad (22)$$

$$P_{var} = \frac{P_{max}^{50} - P_{min}^{50}}{P_{av}^{50}} \quad (23)$$

Here P_{max}^{50} , P_{min}^{50} and P_{av}^{50} is the peak, minimum and average demand with a 50% EV adoption. P_{max}^{base} is the peak base demand.

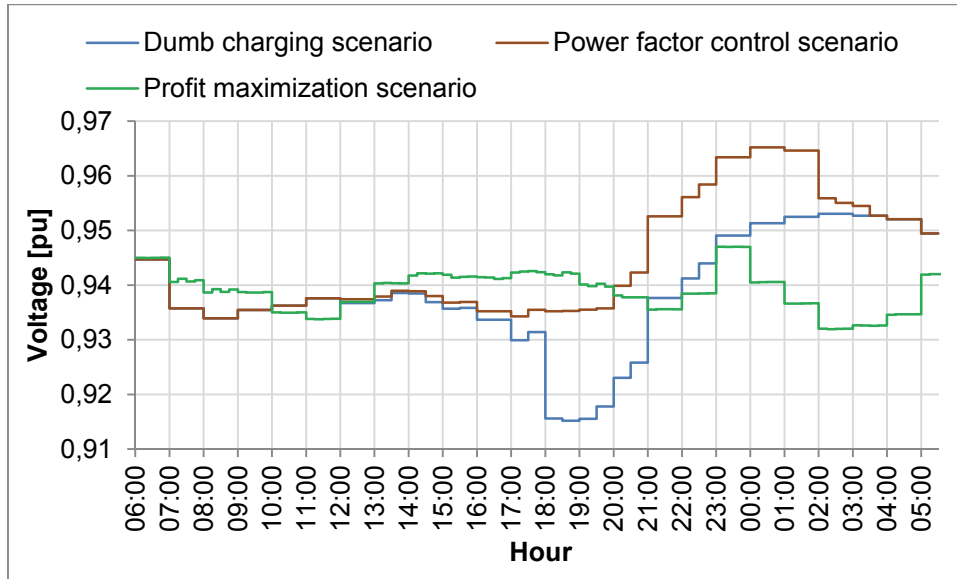


Figure 7.12: Voltage pattern at node 652 at 50% EV adaption

Table 7-1: Results from simulations of a 50% EV demand at 11 node test feeder

	Dumb scenario	Profit maximization scenario	Power factor control scenario
Max demand node 652 (P_{max}^{50})	204 kW	186 kW	168 kW
Min demand node 652 (P_{min}^{50})	111 kW	109 kW	111 kW
Variation in demand (P_{var}) at node 652	68%	56%	41% (The other nodes had a variation between 63%-70%)
Increase in peak demand (ΔP) at node 652	46%	33%	20 % (The other demand nodes had an increase of 42%-48%)
Lowest voltage at node 652	0.915 pu	0.932 pu	0.934 pu

As seen in both the figure and table above, both the voltages and demand pattern improve in the profit maximization scenario and the power factor control scenario compared to the dumb charging scenario.

The value for the lowest voltage was a bit higher in the power factor control scenario than the profit maximization scenario. The profit maximization had also a higher variation in demand for the most critical node, the node 652. For the other nodes in the 11 node test feeder, the variation in demand was however higher in the power factor control scenario.

8 DISCUSSION

The results from the simulations of a 50% EV adoption in the dumb charging scenario, profit maximization scenario and the power factor control scenario are to some extent as expected. The dumb charging scenario led to a peak demand when the majority of the EVs returned from their last journey. When smart charging algorithms were introduced, the power demand pattern changed significantly. From the power flow simulations of the 11 node test feeder, it was seen that when the demand pattern flattened out, the voltage pattern followed.

However, there are some aspects that were not clear after the analysis and need further discussion. There are also some limitations of this study that should be highlighted.

8.1 Simulation Model

For the purpose of this thesis, it was decided to construct a model of the IEEE 13 node test feeder in MATPOWER. When implementing the network in MATPOWER, some simplifications had to be done due to restrictions in MATPOWER. To distinguish the designed simplified network from the original IEEE 13 node test feeder, the designed network is called 11 node test feeder.

One of the main simplifications when designing the 11 node test feeder was to ignore the unbalanced nature of the IEEE 13 node test feeder. This is important to be aware of if wanting to use this model for simulation purposes in other circumstances where the unbalanced nature of the distribution grid cannot be ignored.

Altogether, if willing to ignore the unbalanced nature of the distribution network, the designed 11 node test feeder in MATPOWER is considered as a good option, especially for optimization studies using MATLAB, as MATPOWER is MATLAB based. Simulations can then be done with few intermediate steps, and the simulations can be incorporated in the algorithm. This test feeder has also a potential for further development, by for example introducing the voltage regulator in the IEEE 13 node test feeder.

The results from the model have not been verified by simulations in another simulation program. In the case of a further use and development of this model, this would strengthen the validity of the results obtained from simulations on this model.

8.2 Electric Vehicle Availability for Grid Services

The EV availability for grid services is dependent of several factors, like the driving pattern, charger availability, and the vehicle owners' willingness to adapt to smart charging schedules.

It is not easy finding reliable data for the driving pattern for EVs. The sources for the driving pattern used in this thesis are however considered reliable and sufficient for the purpose of this thesis.

The charger availability has also a very big impact on the electric vehicle availability for grid services. For the dumb charging scenario and reactive power scenario, the charging is assumed to be at the return of the last journey. It can be reasonable to assume that all EVs can access a charger at this point of time, since it would be unrealistic to believe that many people would invest in an EV if they had no chance of charging their vehicle at home.

However for the profit maximization scenario, it is assumed that the EVs are available for grid services at all times when parked, which implies a huge investment in the EV charging infrastructure. It would probably be more realistic to assume that there would be a limited availability for charging stations when not at home.

When it comes to the EV owners' willingness to adapt to smart charging algorithms, it is for the purpose of this thesis assumed that all vehicle owners are willing to commit to the charging strategies. To what extent this is realistic further studies is needed. It could however probably be safe to assume that there at least would be *some* vehicle owners that would like to reserve against a smart charging control.

8.3 Simplifications Made for the Electric Vehicle Battery

In this study, simplifications have been made regarding the EV battery.

One of the assumptions made in this thesis, are that there is a constant ration between energy consumption and traveled distance (kWh/km), while it in reality depends on the driving speed, road and weather conditions, choice of vehicle model, etc., which in fact are highly variable parameters. [18]. The main reason for not taking this into consideration is to reduce the complexity of the study.

The time used for charging the EV battery is assumed to be linear from empty to full charged, while in reality the charging over a certain level goes slower. As it is assumed that the vehicle battery is not charged above an SOC of 85% in this thesis, this simplification is not considered to have a significant influence the results.

In addition to the abovementioned simplifications made concerning the EV battery, it is in this study ignored the battery degradation costs. Of the charging scenarios presented in this thesis, this is most relevant for the profit maximization scenario, as this scenario leads to an substantial amount of energy both charged and discharged from the battery. The price for discharging the energy back to the grid is in this scenario set to 2 EUR/MWh below the price for charging. The main reason for doing this was because simulations showed that the demand pattern got a saw-tooth shape when reducing the difference in price for charging and discharging. Even though it was not the reason for introducing the difference in price between charging and discharging, this difference in price for charging and discharging could make up for the battery degradation costs. However, as the degradation costs have not had any focus in this study, it can't be concluded here if this difference in price for charging and discharging of 2 EUR/MWh is high enough for making up for the degradation costs for the battery for participating in grid services.

8.4 Profit Maximization Scenario

The intention with the profit maximization scenario was that the electricity price would change when there is a change in the demand pattern due to charging of the EVs. When the EVs charge according to a profit maximization objective and a change in electricity prices is taken into account, in theory, both the demand, voltage and electricity profile should smooth out.

The results showed that with the profit maximization algorithm and parameters set as in this study, the demand profile did not smooth out completely to satisfaction. The demand and voltage profile did however improve compared to the dumb charging scenario. While the lowest voltage in the dumb charging scenario was 0.915 pu, the lowest voltage in the profit maximization scenario was 0.932 pu. The experience from changing the relationship between the electricity price and demand however showed that this had a major impact on the results. The writer of this thesis believes that a better relationship between the change in demand and electricity prices would improve the results for the simulations of this scenario.

Another observation from the results from this scenario is that when looking at the total demand in Norway, both the peak demand and variation in demand is *reduced* when the EV demand is added to the base demand. However when looking at the demand pattern for the nodes at the 11 node test feeder, both peak demand and variation in demand *increases* when adding the EV demand to the base demand. The reason is that the EV demand at the 11 node test feeder is a greater part of the total demand at the 11 node test feeder, than the part the total EV demand in Norway is compared to the total demand in Norway. This observation can be used in other circumstances than for only EVs. It is not only the load of the EVs that can be allocated according to the electricity prices. This observation should therefore be taken into consideration when allocating other loads according to the electricity prices.

Altogether, the procedure for finding the resulting demand profile in this scenario is still considered good, but the writer suggest a thorough study of the relationship between the change in demand and electricity prices.

8.5 Power Factor Control Scenario

In the power factor control scenario, the EVs are assumed to charge as in the dumb charging scenario as long as there are no voltage violations at any of the demand nodes. In the case of a voltage violation, EVs at the violated nodes are instructed to charge according to the power factor control mode. In that case the charging starts at the same time as for the dumb charge scenario, but with a reduced power factor, facilitating for reactive power injection to the grid.

Results from simulations of the power factor control scenario presented in this thesis, show that the voltages in the grid are improved compared to the dumb charging scheme. The lowest voltage when simulating a 50% EV adoption charging according to this scenario was 0.934 pu. The algorithm was however not able to avoid voltages below the lowest allowable voltage set in this thesis, which was 0.935 pu.

Another alternative is to let the EVs charge according to dumb charging, but to let them be available for voltage regulation when finished charging. However, by doing this there would still be a high active power load when the EV is parked.

8.6 Combination of Different Charging Scenarios

This study assumes that all EVs charges according to the same strategy. This assumption also applies for the power factor control scenario, even though not all vehicles charges in the same smart charging mode. –The power factor control scenario still assumes that all vehicle owners are willing to charge according to the power factor control mode if necessary. In reality, there would probably be a combination of different charging scenarios.

9 CONCLUSION AND FURTHER WORK

9.1 Conclusion

Regardless of which type of charging scheme used, the EVs constitute a new load for the grid. When EV charging remains completely uncontrolled, the profile of the charging demand is highly dependent on the time of return from the last journey of the day. According to the statistical data used in this thesis, the majority of the vehicles return from the last journey between 17:00 and 20:00. With no smart control of the charging, this leads to a high peak in demand around that time. As the base demand pattern also is rather high at that time, the EV demand can easily be synchronized with the peak in the base demand.

Two smart charging scenarios are studied in this thesis; the *profit maximization* scenario and the *power factor control* scenario. This study does not conclude in which of the two charging strategies that would be the best choice, this was not the aim of doing this study either. The motivation was more to investigate the impact different charging scenarios could have on the demand and voltage. For both designed smart charging strategies, the maximum demands at all demand nodes in the test feeder were reduced. This is mainly because the dumb charging scenario constitutes significant proportions of vehicles to charge in a short timeframe, while the other charging strategies allow the charging to be spread over a longer timeframe.

When analyzing the different charging schedules calculated in the profit maximization scenario, it became clear that the part of the algorithm that calculated the charging schedule for a single EV worked in the sense that the vehicle charged when the price was low and discharged back to the grid when the price was higher. The demand pattern, when adding the load of a 50% EV adoption on the base demand, did not become as smoothed out as anticipated. The resulting demand pattern did however become much better than the one presented in the paper in the appendices, where the change in electricity prices due to change in demand was ignored. From this it can be concluded that when calculating the final demand pattern for a large scale adoption of electric vehicles, it is crucial to take into account the change in electricity prices when there is a change in demand. This study further concludes that finding this relationship between change in demand and electricity prices is not straightforward. The writer of this thesis claim that the main reason the demand pattern did not flat out as much as anticipated is due to the chosen relationship between change in demand and electricity prices.

The study of the profit maximization scenario, also showed that although the total demand in Norway flattens somewhat out when moving the flexible EV demand to times of the day where the electricity price is low, and discharge back to the grid when the electricity price is high, it does not mean that the demand pattern is smoothed out at all nodes. In a network where the EV demand is a greater part of the total demand at that network compared to the part the total EV fleet is of the total demand in Norway, the resulting demand pattern can actually have both a higher peak demand and variations. This is an important fact to be aware of, not only for EVs, but also for other flexible loads. At nodes where the flexible load is at a

certain part of the total demand, it should be considered to limit the amount charging according to the electricity prices.

In the power factor control scenario, the aim was to avoid voltages below a certain level. The minimum value for the voltages set for the purpose of the simulations in this thesis was 0.935 pu. One of the nodes in the test feeder experienced voltages below this value during simulations in this scenario. The lowest voltage for this node was 0.934 pu. This is however above the lowest voltage found in both the dumb charging scenario and the profit maximization scenario. In the dumb charging scenario the lowest voltage was 0.915, and in the profit maximization scenario, the lowest voltage was 0.932 pu.

9.2 Further work

If the profit maximization scenario presented in this thesis were to be studied further, the writer of this thesis strongly suggests a detailed study on how the change in demand effects the change in electricity prices. This is because experiences from simulations done with different parameters describing this relationship resulted in very different demand and voltage patterns. A further study on this relationship would therefore strengthen this analysis and the reliability of the results.

A further study of the profit maximization scenario should also take into consideration that there might be a limited availability of charging stations, especially during daytime when the vehicles are not parked at home. A study of the battery degradation costs could also strengthen the analysis of the profit maximization scenario.

In the simulations for the profit maximization scenario, the price for discharging was set to 2 EUR/MWh below the price for charging. When reducing the price difference for discharge and charge to 0.01 EUR/MWh, the resulting demand pattern got a saw-tooth shape. The reason why this happened was not discovered. Further study and analysis should therefore be carried out to find the reason for this phenomenon.

If the power factor control scenario presented in this thesis were to be studied further, it could be considered letting the EVs being available for reactive power services at all times when parked at places where there is an available charger, instead of only the eight first hours after the return from the last journey of the day.

A study of the vehicle owners' willingness to participate in grid services would strengthen the analysis of both of the two smart charging strategies presented in this thesis. During such a study, the focus should not only be on whether or not they would participate in any grid services at all, but also if there are any grid services they would be more likely to participate in than others. Would it for example be easier to make the vehicle owners to participate in the power factor regulation scenario than the profit maximization scenario?

The simulations of the scenarios used in this study are for a specific 24-hour period. A further study of any of the two smart charging strategies in this thesis could also compare the effect of the strategy for different days during the year, as there are some changes in both daily and

seasonal changes in the demand pattern. The simulation period could also be done over more than one day.

REFERENCES

- [1] M. Holm, J. Randers, E. Andresen, S. Bysveen, K. Høyland, T. Wigdahl, *et al.*, "Action Plan for Electrification of Road Transport," Ministry of Transport and Communications, Oslo2009.
- [2] E. Figenbaum and M. Kolbenstvedt, "Electromobility in Norway - experiences and opportunities with Electric vehicles," Institute of Transport Economics. Norwegian Centre for Transport Research, Oslo2013.
- [3] O. H. Hannisdahl. (2012, January 21, 2014). *Eventyrlig elbilsalg i 2011* [Adventurous electric vehicle sales in 2011]. Available: <http://www.gronnbil.no/nyheter/eventyrlig-elbilsalg-i-2011-article218-239.html>
- [4] (2014, June 5, 2014). *Ladbare biler i Norge mai, 2014* [EVs in Norway in May, 2014]. Available: <http://www.gronnbil.no/statistikk/>
- [5] A. Aabrandt, P. B. Andersen, A. B. Pedersen, Y. Shi, B. Poulsen, N. O'Connell, *et al.*, "Prediction and optimization methods for electric vehicle charging schedules in the EDISON project," in *Innovative Smart Grid Technologies (ISGT), 2012 IEEE PES, 2012*, pp. 1-7.
- [6] L. F. Hexeberg, O. B. Fosso, and M. Molinas, "Optimal Charging of Electric Vehicles Including Service Provision to the Distribution Network," p. 8, December 2013 Unpublished.
- [7] "Topic Paper #20. Vehicle to Grid (V2G)," The National Petroleum Council (NPC)August 1 2012.
- [8] L. Freris and D. Infield, *Renewable energy in power systems*. Chichester: Wiley, 2008.
- [9] "ReGrid: Frequency and voltage generation in electrical grids," Renewables Academy (RENAC) AG, BerlinJune 2013.
- [10] M. C. Kisacikoglu, "Vehicle-to-grid (V2G) Reactive Power Operation Analysis of the EV/PHEV Bidirectional Battery Charger.," PhD diss, University of Tennessee, Knoxville, 2013.
- [11] (2014, April 1, 2014). *NordpoolSpot*. Available: <http://www.nordpoolspot.com/>
- [12] J. O. Tande, "Impact of integrating wind power in the Norwegian power system," SINTEF Energy ResearchApril 18 2006.
- [13] I. Shandurkova, B. Bremdal, R. Bacher, S. Ottesen, and A. Nilsen, "A Prosumer Oriented Energy Market. Developments and future outlooks for Smart Grid oriented energy markets.," NCE Smart Energy Markets, Halden2012.
- [14] (2013, June 1). *ICT and climate*. Available: <http://www.regjeringen.no/en/dep/fad/documents/government-propositions-and-reports-/reports-to-the-storting-white-papers/2012-2013/meld-st-23-20122013-2/7.html?id=729060>
- [15] (February 2, 2014). *Types of Electric Vehicles*. Available: http://www.tva.gov/environment/technology/car_vehicles.htm
- [16] J. Lowry and J. Larminie, *Electric vehicle technology explained*. Hoboken, N.J.: Wiley, 2012.
- [17] D. Doerffel and S. A. Sharkh, "A critical review of using the Peukert equation for determining the remaining capacity of lead-acid and lithium-ion batteries," *Journal of Power Sources*, vol. 155, pp. 395-400, 4/21/ 2006.
- [18] R. Garcia-Valle and J. A. Peças Lopes, *Electric Vehicle Integration into Modern Power Networks*. New York, NY: Springer New York, 2013.
- [19] "2012 NISSAN leaf owner's manual," USAApril 2012.
- [20] N. Downing and M. Ferdowsi, "Mobile Energy Resources in Grids of Electricity," BerlinMay 11 2010.
- [21] E. Sortomme and M. A. El-Sharkawi, "Optimal Scheduling of Vehicle-to-Grid Energy and Ancillary Services," *Smart Grid, IEEE Transactions on*, vol. 3, pp. 351-359, 2012.
- [22] K. Turitsyn, P. Sulc, S. Backhaus, and M. Chertkov, "Local Control of Reactive Power by Distributed Photovoltaic Generators," in *Smart Grid Communications (SmartGridComm), 2010 First IEEE International Conference on*, 2010, pp. 79-84.

- [23] M. Ehsani, M. Falahi, and S. Lotfifard, "Vehicle to Grid Services: Potential and Applications," *Energies*, vol. 5, pp. 4076-4090, 2012.
- [24] R. A. Verzijlbergh, Z. Lukszo, and M. D. Ilic, "Comparing different EV charging strategies in liberalized power systems," in *European Energy Market (EEM), 2012 9th International Conference on the*, 2012, pp. 1-8.
- [25] W. H. Kersting, "Radial distribution test feeders," in *Power Engineering Society Winter Meeting, 2001. IEEE*, 2001, pp. 908-912 vol.2.
- [26] R. D. Zimmerman and C. E. Murillo-Sánchez, "MATPOWER 4.1 User's Manual," December 14 ed: Power Systems Engineering Research Center (PSERC), 2011.
- [27] R. D. Zimmerman, S. Murillo, x, C. E. nchez, and R. J. Thomas, "MATPOWER: Steady-State Operations, Planning, and Analysis Tools for Power Systems Research and Education," *Power Systems, IEEE Transactions on*, vol. 26, pp. 12-19, 2011.
- [28] R. A. M. Van Amerongen, "A general-purpose version of the fast decoupled load flow," *Power Systems, IEEE Transactions on*, vol. 4, pp. 760-770, 1989.
- [29] W. Qiuwei, A. H. Nielsen, x00D, J. stergaard, C. Seung Tae, F. Marra, *et al.*, "Driving Pattern Analysis for Electric Vehicle (EV) Grid Integration Study," in *Innovative Smart Grid Technologies Conference Europe (ISGT Europe), 2010 IEEE PES*, 2010.
- [30] L. Vågane, I. Brechan, and Hjorthol, "Den nasjonale reisevaneundersøkelsen 2009 - nøkkelrapport," Institute of Transport Economics, Oslo, 2009 Norwegian Travel Survey - key results January 01 2011.
- [31] (2013, April 14, 2014). *Road traffic volumes, 2012*. Available: <https://www.ssb.no/en/transport-og-reiseliv/statistikker/klreg/aar/2013-05-14>
- [32] (2014, May 3, 2014). *Registered vehicles, 2013*. Available: <http://www.ssb.no/en/transport-og-reiseliv/statistikker/bilreg>
- [33] (2011, May 2, 2014). *Energy consumption in households, 2009*. Available: <http://www.ssb.no/en/energi-og-industri/statistikker/husenergi>
- [34] Ø. Søgosen, "Analysis of Large Scale Integration of Electric Vehicles in Nord-Trøndelag," Master of Energy and Environmental Engineering Master thesis, Department of Electric Power Engineering, Norwegian University of Science and Technology (NTNU), Trondheim, 2013.
- [35] www.nissan.no. Available: http://www.nissan.no/etc/medialib/nissaneu/ NO no/ Other pdf/ spec sheets.Par.67627.File.dat/LEAF_Teknisk_spesifikasjon_23-09-13_0374.pdf
- [36] Y. Mitsurkuri, R. Hara, H. Kita, E. Kamiya, S. Taki, and E. Kogure, "Study on Voltage Regulation in a Distribution System Using Electric Vehicles - Optimal Real and Reactive Power Dispatch by Centralized Control -," *Journal of International Council on Electrical Engineering*, vol. 3, p. 7, 2013.
- [37] (2014, June 1, 2014). *Hvordan lader du Nissan Leaf?* [How do your charge the Nissan Leaf?]. Available: <http://www.nissan.no/NO/no/vehicle/electric-vehicles/leaf/charging-and-battery/charging-nissan-leaf-and-battery.html>

APPENDICES

APPENDIX A

Calculation of Line Phase Impedances and Total Line Charging Susceptance for the 11 Node Test Feeder.

MATPOWER uses the standard pi one-line equivalent of a three phase transmission line, where all lines are modeled with a series impedance $z_s = r_s + jx_s$ and a total line charging susceptance b [1].

The IEEE 13 node test feeder, which the test feeder in this thesis is based on, consists of single-phase, two-phase and three-phase distribution lines. These lines are described by six different configurations.

This appendix presents the calculation done for finding the phase impedances from the given phase impedance matrices. The line susceptance is found in using the same procedure. When doing this calculation some simplifications had to be done, due to the unbalanced nature of the 13 node test feeder. To give a better understanding of the simplifications made and the consequences by doing this, it is crucial to have some knowledge of transposed and untransposed power lines. Therefore some theory concerning this is presented in A.1, before the calculated impedances and susceptances are presented in A.2.

A.1 Theoretic background for the calculations of line impedance and susceptance

Single-phase representation of three-phase transposed lines

High voltage transmission lines are usually three-phase and assumed to be transposed, meaning that each phase occupies the same physical position on the structure for one-third of the length of the line [2].

For transposed three-phase lines the phase impedance is equal the positive-sequence impedance of the line. For more information of sequence impedances, the reader is referred to [2].

The positive sequence impedance of a three phase-line can be found from the phase impedance matrix. The notation used here for the phase impedance matrix is shown in (1) ;

$$[z_{abc}] = \begin{bmatrix} z_{aa} & z_{ab} & z_{ac} \\ z_{ba} & z_{bb} & z_{bc} \\ z_{ca} & z_{cb} & z_{cc} \end{bmatrix} \Omega/mile \quad (1)$$

z_{aa} , z_{bb} and z_{cc} are the self-impedances, and z_{ab} , z_{ac} , z_{ba} , z_{bc} , z_{ca} and z_{cb} are the mutual impedances.

For a transposed line $z_{aa} = z_{bb} = z_{cc}$ and $z_{ab} = z_{bc} = z_{ca}$. In addition, the matrix will be symmetric [3]. This gives:

$$[z_{abc}] = \begin{bmatrix} z_s & z_m & z_m \\ z_m & z_s & z_m \\ z_m & z_m & z_s \end{bmatrix} \Omega/mile \quad (2)$$

Here z_s is the self-impedance and z_m is the mutual impedance.

The symmetrical component matrix is given by:

$$[z_{sym}] = [A][z_{abc}][A^{-1}] \quad (3)$$

When the off-diagonal terms of the phase impedance matrix is equal, the off-diagonal terms of the sequence impedance matrix will be zero, and the symmetrical component matrix turns out to be:

$$[z_{sym}] = \begin{bmatrix} z_s + 2z_m & 0 & 0 \\ 0 & z_s - z_m & 0 \\ 0 & 0 & z_s - z_m \end{bmatrix} ohm/mile \quad (4)$$

In the symmetrical component matrix, the diagonal terms are the zero-, positive-, and negative-sequence impedance of the line. Note that the off-diagonal terms are zero which indicates that there is no coupling between the zero-, positive-, and negative-sequence

networks for the transposed line [3]. The zero-, positive-, and negative sequence components of the impedances are z_0 , z_1 and z_2 .

$$z_0 = z_s + 2z_m \quad (5)$$

$$z_1 = z_s - z_m \quad (6)$$

$$z_2 = z_s - z_m \quad (7)$$

When dealing with transposed lines, the phase impedance needed for modelling in MATPOWER is in other words found by subtracting one of the off diagonal terms from one of the diagonal terms.

The line susceptance is found in the same way when modelling the 11 node test feeder.

Single-phase representation of three-phase untransposed lines

The single-phase representation of an untransposed line also uses the positive sequence impedance.

As distribution lines are rarely, if ever, transposed, neither the diagonal terms nor the off-diagonal terms in (2) are equal to each other [4]. The matrix will however usually be symmetrical. To find the positive sequence impedance of the three-phase untransposed lines, the phase impedance matrix therefore has to be modified so the three diagonal terms in (2) are equal and all of the off-diagonal terms in (2) are equal. The usual procedure is to set the three diagonal terms of the phase impedance matrix equal to the average of the diagonal terms and the off-diagonal terms equal to the average of the off-diagonal terms of equation (1) [2, 5]. When this is done, the self and mutual impedances are defined as:

$$z_s = \frac{1}{3} \cdot (z_{aa} + z_{bb} + z_{cc}) \Omega/mile \quad (8)$$

$$z_m = \frac{1}{6} \cdot (z_{ab} + z_{ac} + z_{ba} + z_{bc} + z_{ca} + z_{cb}) \Omega/mile \quad (9)$$

By doing this, the impedance matrix will be as in (10).

$$[z_{abc}] = \begin{bmatrix} z_s & z_m & z_m \\ z_m & z_s & z_m \\ z_m & z_m & z_s \end{bmatrix} \Omega/mile \quad (10)$$

Note that (10) is exactly the same as (2). The next steps of the procedure for finding the zero-, positive-, and negative-sequence impedances will therefore be the same as for the transposed line, and equation (6) can be used to find the positive sequence component.

Single phase representation of two-phase and single-phase lines

Two-phase lines have two out of three phases. When finding the phase-impedance for the single-phase representation of the two phase lines it is in this thesis chosen to use a similar approach as for the three-phase untransposed lines. While it may seem odd to look at the positive-sequence impedance of a two-phase line, the analysis approach described above is useful. (In reality there are obviously no such thing as zero-, positive-, and negative sequence

for a two-phase line.) This approach can be used if adding fictitious conductors for the missing phases to model the lines as an equivalent three-phase line. (No current actually flows in these fictitious phases) [5].

When calculating the z_s in (2) for the two-phase lines, the z_s is set to be the average of the diagonal terms for the two phases and the z_m is set equal the average of the off-diagonal terms of the two phases.

$$z_s = \frac{1}{2} \cdot (z_{aa} + z_{bb} + z_{cc}) \Omega/mile \quad (11)$$

$$z_m = \frac{1}{2} \cdot (z_{ab} + z_{ac} + z_{ba} + z_{bc} + z_{ca} + z_{cb}) \Omega/mile \quad (12)$$

For the single phase lines, the single phase impedance is simply the impedance given for the existing phase.

Line susceptance

Susceptance is the imaginary part of admittance, and the admittance is the inverse of the impedance.

$$Y = \frac{1}{Z} = G + jB \quad (13)$$

Y is the admittance, Z is the impedance, G is conductance and B is the susceptance. The admittance, conductance and susceptance are all measured in Siemens (S).

Making a single phase representation of distribution lines is not easy and straight-forward. When modeling the total charging susceptance for the 11 node test feeder, it is here assumed that it can be modeled by using the same procedure as presented for the impedance.

A.2 Calculated line impedances and susceptances for the six line configurations in IEEE 13 node test feeder

The lines in the IEEE 13 node test feeder are described by six different configurations. This section presents the given impedance matrices and the calculated phase impedances, z_1 and phase capacitance b for the different configurations.

Configuration 601

Lines of this configuration are untransposed overhead three-phase lines.

$$[z_{abc}] = \begin{bmatrix} 0.3465 + j1.0179 & 0.1560 + j0.5017 & 0.1580 + j0.4236 \\ 0.1560 + j0.5017 & 0.3375 + j1.0478 & 0.1535 + j0.3849 \\ 0.1580 + j0.4236 & 0.1535 + j0.3849 & 0.3414 + j1.0348 \end{bmatrix} \Omega/mile$$

$$B = \begin{bmatrix} 6.2998 & -1.9958 & -1.2595 \\ -1.9958 & 5.9597 & -0.7417 \\ -1.9958 & -0.7417 & 5.6386 \end{bmatrix}$$

The positive sequence impedance and total line charging susceptance is found by using (8), (9) and (6).

$$z_1 = 0.1860 + j0.5968 \Omega/mile$$

$$b = 7.298 \mu S/mile$$

Configuration 602

Lines of this configuration are untransposed overhead three-phase lines.

$$[z_{abc}] = \begin{bmatrix} 0.7526 + j1.1814 & 0.1580 + j0.4236 & 0.1560 + j0.5017 \\ 0.1580 + j0.4236 & 0.7475 + j1.1983 & 0.1535 + j0.3849 \\ 0.1560 + j0.5017 & 0.1535 + j0.3849 & 0.7436 + j1.2112 \end{bmatrix} \Omega/mile$$

$$B = \begin{bmatrix} 5.6990 & -1.0817 & -1.6905 \\ -1.0817 & 5.1795 & -0.6588 \\ -1.6905 & -0.6588 & 5.4246 \end{bmatrix}$$

The positive sequence impedance total line charging susceptance is found by using (8), (9) and (6).

$$z_1 = 0.5921 + j0.7602 \Omega/mile$$

$$b = 6.5780 \mu S/mile$$

Configuration 603

Lines of this configuration are untransposed overhead two-phase lines consisting of only phase b and c.

$$[z_{abc}] = \begin{bmatrix} 0.0000 + j0.0000 & 0.0000 + j0.0000 & 0.0000 + j0.0000 \\ 0.0000 + j0.0000 & 1.3294 + j1.3471 & 0.2066 + j0.4591 \\ 0.0000 + j0.0000 & 0.2066 + j0.4591 & 1.3238 + j1.3569 \end{bmatrix} \Omega/mile$$

$$B = \begin{bmatrix} 0.0000 & 0.0000 & 0.0000 \\ 0.0000 & 4.7097 & -0.8999 \\ 0.0000 & -0.8999 & 4.6658 \end{bmatrix}$$

The “positive sequence impedance” total line charging susceptance is found by using (11) and (12).

$$z_1 = 1.1200 + j0.8429 \Omega/mile$$

$$b = 5.5876 \mu S/mile$$

Configuration 604

Lines of this configuration are untransposed overhead two-phase lines consisting of only phase a and c.

$$[z_{abc}] = \begin{bmatrix} 1.3238 + j1.3569 & 0.0000 + j0.0000 & 0.2066 + j0.4591 \\ 0.0000 + j0.0000 & 0.0000 + j0.0000 & 0.0000 + j0.0000 \\ 0.2066 + j0.4591 & 0.0000 + j0.0000 & 1.3294 + j1.3471 \end{bmatrix} \Omega/mile$$

$$B = \begin{bmatrix} 4.6658 & 0.0000 & -0.8999 \\ 0.0000 & 0.0000 & 0.0000 \\ -0.8999 & 0.0000 & 4.7097 \end{bmatrix}$$

The “positive sequence impedance” total line charging susceptance is found by using (11) and (12).

$$z_1 = 1.1200 + j0.8929 \text{ ohm}/mile$$

$$b = 5.5876 \mu S/mile$$

Configuration 605

Lines of this configuration are overhead single-phase lines consisting of only phase c.

$$[z_{abc}] = \begin{bmatrix} 0.0000 + j0.0000 & 0.0000 + j0.0000 & 0.0000 + j0.0000 \\ 0.0000 + j0.0000 & 0.0000 + j0.0000 & 0.0000 + j0.0000 \\ 0.0000 + j0.0000 & 0.0000 + j0.0000 & 1.3292 + j1.3475 \end{bmatrix} \Omega/mile$$

$$B = \begin{bmatrix} 0.0000 & 0.0000 & 0.0000 \\ 0.0000 & 0.0000 & 0.0000 \\ 0.0000 & 0.0000 & 4.5193 \end{bmatrix}$$

The phase impedance and total line charging susceptance used when modelling these lines is simply the line impedance and susceptance of the single phase line.

$$z_1 = 1.3292 + j1.3475 \Omega/mile$$

$$b = 4.5193 \mu S/mile$$

Configuration 606

Lines of this configuration are untransposed underground three-phase lines.

$$[z_{abc}] = \begin{bmatrix} 0.7982 + j0.4463 & 0.3192 + j0.0328 & 0.2849 - j0.0143 \\ 0.3192 + j0.0328 & 0.7891 + j0.4041 & 0.3192 + j0.0328 \\ 0.2849 - j0.0143 & 0.3192 + j0.0328 & 0.7982 + j0.4463 \end{bmatrix} \Omega/mile$$

$$B = \begin{bmatrix} 96.8897 & 0.0000 & 0.0000 \\ 0.0000 & 96.8897 & 0.0000 \\ 0.0000 & 0.0000 & 96.8897 \end{bmatrix}$$

The positive sequence impedance and total line charging susceptance are found by using (8), (9) and (6).

$$z_1 = 0.4874 + j0.4151 \Omega/mile$$

$$b = 96.8897 \mu S/mile$$

Configuration 607

Lines of this configuration are underground single-phase lines consisting of only phase a.

$$[z_{abc}] = \begin{bmatrix} 1.3425 + j0.5124 & 0.0000 + j0.0000 & 0.0000 + j0.0000 \\ 0.0000 + j0.0000 & 0.0000 + j0.0000 & 0.0000 + j0.0000 \\ 0.0000 + j0.0000 & 0.0000 + j0.0000 & 0.0000 + j0.0000 \end{bmatrix} \Omega/mile$$

$$B = \begin{bmatrix} 88.9912 & 0.0000 & 0.0000 \\ 0.0000 & 0.0000 & 0.0000 \\ 0.0000 & 0.0000 & 0.0000 \end{bmatrix}$$

The phase impedance and total line charging susceptance used when modelling these lines is simply the line impedance and susceptance of the single phase line.

$$z_1 = 1.3425 + j0.5124 \Omega/mile$$

$$b = 88.9912 \mu S/mile$$

Line impedances and susceptances in pu

The base values chosen for the purpose of this thesis are presented in Table 1.

Table 1: Base values

Unit	Base
P_{base}	100 MW
V_{base}	4.16 kV
Z_{base}	0.173 Ω
B_{base}	$\frac{1}{0.173}$ S

Table 2 presents the calculated line impedances and susceptances in pu. As seen in the table, and explained in the thesis, the line between node 671 and 692 and the line between node 633 and node 634 is removed.

Table 2: Line impedances and susceptances for modelling the 11 node test feeder

Node A	Node B	Length (ft)	Configuration	Z (Ω /mile)	b (μ S/mile)	Z (Ω)	b (μ S)	Z (pu)	b $\cdot 10^{-7}$ (pu)
632	645	500	603	1.1200+j0.8429	5.5876	0.1061+j0.0798	0.5291	0.6131+j0.4614	0.9154
632	634	500	602	0.5921+j0.7602	6.5780	0.0561+j0.0720	0.6229	0.3241+j0.4161	1.0777
645	646	300	603	1.1200+j0.8429	5.5876	0.0636+j0.0479	0.3175	0.3678+j0.2768	0.5492
650	632	2000	601	0.1860+j0.5968	7.2984	0.0704+j0.2260	2.7645	0.4072+j1.3066	4.7826
684	652	800	607	1.3425+j0.5124	88.9912	0.2034+j0.0776	13.484	1.1758+j0.4488	23.326
632	671	2000	601	0.1860+j0.5968	7.2984	0.0704+j0.2260	2.7645	0.4072+j1.3066	4.7826
671	684	300	604	1.1200+j0.8929	5.5876	0.0636+j0.0507	0.3175	0.3678+j0.2933	0.5492
671	680	1000	601	0.1860+j0.5968	7.2984	0.0352+j0.1130	1.3823	0.2036+j0.6533	2.3913
684	611	300	605	1.3293+j1.3475	4.5193	0.0755+j0.0766	0.2568	0.4366+j0.4426	0.4442
671	675	500	606	0.4874+j0.4151	96.8897	0.0462+j0.0393	9.1752	0.2668+j0.2272	15.873

References

- [1] R. D. Zimmerman and C. E. Murillo-Sánchez, "MATPOWER 4.1 User's Manual," December 14 ed: Power Systems Engineering Research Center (PSERC), 2011.
- [2] W. H. Kersting, *Distribution system modeling and analysis*. Boca Raton, Fla.: CRC Press, 2007.
- [3] S. E. Zocholl, "Symmetrical components: line transposition," Schweitzer Engineering Laboratories, Inc., Pullman, WA, USA1999.
- [4] L. L. Grigsby, *Electric power generation, transmission, and distribution*. Boca Raton, Fla.: CRC Press, 2012.
- [5] T. A. Short, *Electric power distribution equipment and systems*. Boca Raton, Fla.: Taylor & Francis, 2006.

APPENDIX B

This appendix gives the MATLAB code used for the simulations.

11 Node Test Feeder

This script is used in all three charging scenarios.

Contents

- ----- Power Flow Data -----
- ----- OPF Data -----
- Warnings from original ieeee 13 node test feeder (<http://ewh.ieee.org/soc/pes/dsacom/testfeeders/>) conversion:

```
function mpc = case11
```

The 11 node test feeder is constructed from the data describing the IEEE 13 node test feeder, but the regulator, capacitor, switch and distribution lines with zero length have been neglected.

The IEEE 13 node test feeder can be found at:
<http://ewh.ieee.org/soc/pes/dsacom/testfeeders/>

MATPOWER Case Format : Version 1.0

```
mpc.version = '2';
```

----- Power Flow Data -----

system MVA base

```
mpc.baseMVA = 100;
```

bus data

bus *i* type Pd Qd Gs Bs area Vm Va baseKV zone Vmax Vmin

```
mpc.bus = [
    650  3    0    0    0  0  1  1.000  0    4.16  1  1.1  0.9;
    646  1  0.230  0.132  0  0  1  1.022 -2.045  4.16  1  1.1  0.9;
    645  1  0.170  0.125  0  0  1  1.024 -2.043  4.16  1  1.1  0.9;
    632  1  0.100  0.058  0  0  1  1.027 -2.124  4.16  1  1.1  0.9;
    634  1  0.400  0.290  0  0  1  1.004 -2.699  4.16  1  1.1  0.9;
    611  1  0.170  0.080  0  0.1  1  0.978 -4.069  4.16  1  1.1  0.9;
    684  1  0    0    0  0  1  0.866 14.3723  4.16  1  1.1  0.9;
    671  1  1.255  0.718  0  0  1  1.007 -3.841  4.16  1  1.1  0.9;
    675  1  0.843  0.462  0  0.6  1  1.004 -3.981  4.16  1  1.1  0.9;
    652  1  0.128  0.086  0  0  1  0.983 -5.250  4.16  1  1.1  0.9;
    680  1  0    0    0  0  1  1.007 -3.841  4.16  1  1.1  0.9;
];
```

generator data

bus Pg Qg Qmax Qmin Vg mBase status Pmax Pmin Pc1 Pc2 Qc1min Qc1max Qc2min Qc2max ramp_agc ramp_10 ramp_30 ramp_q apf

```
mpc.gen = [
    650  1.2  0.575  40  0  1.0 100  1  20  0  0  0  0  0  0  0  0
    0    0    0    0;
];
```

branch data

```
%      fbustbusr  x      b      rateA  rateB  rateC  ratio      angle  status  angmin
angmax
```

```
mpc.branch = [
    650    632    0.4072  1.3066  4.7826*(10^-7)  0.2333  0      0      0      0      1      -360
360;
    646    645    0.3678  0.2768  0.5492*(10^-7)  0.2333  0      0      0      0      1      -360
360;
    645    632    0.6131  0.4614  0.9154*(10^-7)  0.2333  0      0      0      0      1
-360 360;
    632    634    0.3241  0.4161  1.0777*(10^-7)  0.2333  0      0      0      0      1      -360
360;
    632    671    0.4072  1.3066  4.7826*(10^-7)  0.2333  0      0      0      0      1      -360
360;
    671    684    0.3678  0.2933  0.5492*(10^-7)  0.2333  0      0      0      0      1
-360 360;
    684    611    0.4366  0.4442  2.57*(10^-7)  0.2333  0      0      0      0      1      -360
360;
    684    652    1.1758  0.4488  23.326*(10^-7)  0.2333  0      0      0      0      1
-360 360;
    671  680    0.2036  0.6533  2.3913*(10^-7)  0.2333  0      0      0      0      1      -360 360;
    671    675    0.2668  0.2272  15.873*(10^-7)  0.2333  0      0      0      0      1
-360 360;
];
```

----- OPF Data -----

generator cost data

1 startup shutdown n x1 y1 ... xn yn

2 startup shutdown n c(n-1) ... c0

```
mpc.gencost = [
    2      0      0      3      0      0      0;
    2      0      0      3      0      0      0;
];
```

Warnings from original ieee 13 node test feeder (<http://ewh.ieee.org/soc/pes/dsacom/testfeeders/>) conversion:

*** Primary CT Rating =700 kVA. This value is used to find the MVA limit of all branches. MVA limit is set to (700/3)kVA = 0.2333 kVA.

*** Gencost not given.

*** Qmax and Qmin not given for the generator. Qmax is set to 10MVA and Qmin is set to 0 MVA.

*** The generator cost data are not given in the available data. The generator costs are set to zero, which in practice means that the objective in OPF becomes minimizing losses (that is, minimizing generation).

Data Needed in the Algorithms

This script is used in all three algorithms.

Data needed for the algorithms

This script is used in all three charging scenarios. In this script, the matrices and arrays giving the electricity prices, base power demand and driving pattern needed in the algorithms is created

Contents

- Electricity prices
- Baseline power demand
- Driving Pattern

Electricity prices

The array *elPrice* gives the actual hourly electricity prices in Norway from 06:00 November 5 to 06:00 November 6. These data are needed in the profit maximization charging scenario. In this scenario, it is used intervals of 15 minutes. The array *elPriceQuarter* is therefore created, giving the same electricity prices as *elPrice* but in 15 minute intervals.

```
elPrice=[38.83 42.11 41.91 39.38 37.57 37.1 37.57 39.11 39.49 41.08 43.31 46.1 43.9 40.3 37.9
36.32 36.24 36.88 35.22 34.3 33.38 33.55 34.02 35.85];

elPriceQuarter=zeros(1,96);
count=1;
for i=1:24
    elPriceQuarter(count)=elPrice(i);
    count=count+1;
    elPriceQuarter(count)=elPrice(i);
    count=count+1;
    elPriceQuarter(count)=elPrice(i);
    count=count+1;
    elPriceQuarter(count)=elPrice(i);
    count=count+1;
end
```

Baseline power demand

The 24x8 matrices *basePd* and *baseQd* are extracted from tables in Microsoft Excel. *basePd* and *baseQd* gives the hourly active and reactive base power demand for each of the 8 demand nodes in each of the 24 hours of the studied time period.

- The 1st column gives the base demand for node 646
- The 2nd column gives the base demand for node 645
- The 3rd column gives the base demand for node 632
- The 4th column gives the base demand for node 634
- The 5th column gives the base demand for node 611
- The 6th column gives the base demand for node 671
- The 7th column gives the base demand for node 675
- The 8th column gives the base demand for node 652

```
basePd=xlsread('demand.xlsx',1,'D3:K26');
baseQd=xlsread('demand.xlsx',1,'O3:V26');
```

basePdHalf and *baseQdHalf* gives the base demand in intervals of 30 minutes. This is used in the dumb charging scenario and power factor control scenario.

```
basePdHalf=zeros(48,8);
```



```

baseQdHalf=zeros(48,8);
for i=1:24
    for j=1:8
        basePdHalf(i*2-1,j)=basePd(i,j);
        basePdHalf(i*2,j)=basePd(i,j);
        baseQdHalf(i*2-1,j)=baseQd(i,j);
        baseQdHalf(i*2,j)=baseQd(i,j);
    end
end
end

```

basePdQuarter and *baseQdQuarter* gives the active power base demand in intervals of 15 minutes. This is used in the profit maximization scenario.

```

basePdQuarter=zeros(96,8);
baseQdQuarter=zeros(96,8);
for i=1:48
    for j=1:8
        basePdQuarter(i*2-1,j)=basePdHalf(i,j);
        basePdQuarter(i*2,j)=basePdHalf(i,j);
        baseQdQuarter(i*2-1,j)=baseQdHalf(i,j);
        baseQdQuarter(i*2,j)=baseQdHalf(i,j);
    end
end
end

```

Driving Pattern

lastReturn is a 8x48 matrix extracted from a table in an Microsoft Excel work sheet. *lastReturn* gives the number of EVs having their last return in each of the 48 half-hours in the studied time interval for each of the 8 demand nodes.

```
lastReturn=xlsread('lastReturn.xlsx',1,'B4:I51');
```

drivingPattern is a 463x4 matrix extracted from a table in an Microsoft Excel work sheet. This matrix gives information about the driving pattern at node 671. With a 50% EV adoption there are 463 EVs at node 671. Each row in *drivingPattern* represents one EV. The first column indicate how long the EV is parked from the beginning of the 24 hour time period, and until the first trip (measured in 15 minute periods). The second column indicate how long the EV is parked between the first and second trip, and so on. It is assumed that each trip lasts for 15 minutes.

```
drivingPattern=xlsread('drivingPattern.xlsx',1,'B3:E465');
```

Find Node Voltages

This script is used in all three charging scenarios.

```
function [ voltage ] = findNodeVoltages( pd, qd )
```

This function is used in all scenarios to find the voltages at all the 11 nodes in the 11 node test feeder. The function takes the $m \times 8$ matrices pd and qd as input. pd and qd contain the active and reactive power demand at each of the 8 demand nodes at the m studied half hours. Then the function calculates the node voltages with this demand and returns the voltages in the 48×12 matrix $voltage$.

The 12th column in the return vector $voltage$ gives information of the convergence of the power flow.

```
define_constants;
mpc=loadcase(case11v2);

[m n]=size(pd);
voltage=zeros(m,12);

for i=1:m
    mpc.bus(2,PD)=pd(i,1)/1000; %Node 2 in case11hex is node 646
    mpc.bus(2,QD)=qd(i,1)/1000;
    mpc.bus(3,PD)=pd(i,2)/1000; %Node 3 in case11hex is node 645
    mpc.bus(3,QD)=qd(i,2)/1000;
    mpc.bus(4,PD)=pd(i,3)/1000; %Node 4 in case11hex is node 632
    mpc.bus(4,QD)=qd(i,3)/1000;
    mpc.bus(5,PD)=pd(i,4)/1000; %Node 5 in case11hex is node 634
    mpc.bus(5,QD)=qd(i,4)/1000;
    mpc.bus(6,PD)=pd(i,5)/1000; %Node 6 in case11hex is node 611
    mpc.bus(6,QD)=qd(i,5)/1000;
    mpc.bus(8,PD)=pd(i,6)/1000; %Node 8 in case11hex is node 671
    mpc.bus(8,QD)=qd(i,6)/1000;
    mpc.bus(9,PD)=pd(i,7)/1000; %Node 9 in case11hex is node 675
    mpc.bus(9,QD)=qd(i,7)/1000;
    mpc.bus(10,PD)=pd(i,8)/1000; %Node 10 in case11hex is node 652
    mpc.bus(10,QD)=qd(i,8)/1000;

    opt=mpoption('PF_ALG', 2);
    results=runpf(mpc, opt);

    voltage(i,1)=results.bus(1,VM);
    voltage(i,2)=results.bus(2,VM);
    voltage(i,3)=results.bus(3,VM);
    voltage(i,4)=results.bus(4,VM);
    voltage(i,5)=results.bus(5,VM);
    voltage(i,6)=results.bus(6,VM);
    voltage(i,7)=results.bus(7,VM);
    voltage(i,8)=results.bus(8,VM);
    voltage(i,9)=results.bus(9,VM);
    voltage(i,10)=results.bus(10,VM);
    voltage(i,11)=results.bus(11,VM);
    voltage(i,12)=results.success; % If results.success==1: the power flow converged
end
```

```
end
```

Dumb Charging Scenario – Main Script

This script is used in the dumb charging scenario and power factor control scenario.

Dumb charging scenario - main script

This script calculates the active power demand at the 8 demand nodes in the 11 node test feeder by adding to the base demand the extra power demand from charging the EVs. It is assumed that all EVs charge right after the return of their last journey of the day.

```
clear
data; % By calling the script "data", all vectors and matrices in "data" become available.
```

The daily extra charging demand per vehicle is calculated in chapter 6.3 to be 4.8 kWh.

Charge rate is 3.3 kWh/h so the charging has to be divided between the three first half hours after the return.

```
dumbPd=basePdHalf; % Initially the demand pattern is equal the base demand.
                    %Then the demand from charging of the EVs is added.

for i=1:48 % For each half hour of the studied time interval...
    for j=1:8 % For each of the 8 demand nodes...
        if lastReturn(i,j)>0 % If there are any EVs returning at demand node j at half
                               % hour number "i"...
            dumbPd(i,j)=dumbPd(i,j)+lastReturn(i,j)*3.3;
            dumbPd(i+1,j)=dumbPd(i+1,j)+lastReturn(i,j)*3.3;
            dumbPd(i+2,j)=dumbPd(i+2,j)+lastReturn(i,j)*3;
        end
    end
end
```

Published with MATLAB® R2014a

Profit Maximization Scenario – Main Script

This script is used in the profit maximization scenario only.

Profit maximization scenario - main script

This script calculates the active power demand at the 8 demand nodes in the 11 node test feeder by adding to the base demand the extra power demand from charging the EVs with profit maximization as objective.

The charging of the EVs at each demand node is assumed to constitute of the same percentage of the total demand at each node (e.g. the EVs are evenly distributed). It is therefore sufficient to only calculate the total demand at one of the nodes. It is here chosen to calculate the demand at node 671. Then the results are used to calculate the demand at the other demand nodes

```
clear
data; % By calling the script "data", all vectors and matrices in "data" become available.
charge=zeros(1,96); % The vector charge will be filled with the optimal charge for each of
    % the 15-minute periods.
discharge=zeros(1,96); % The vector discharge will be filled with the optimal discharge
    % for each of the 15-minute periods.
SOC=zeros(1,96); % The vector SOC will be filled with the SOC for each of the 15-minute
    % periods.

profMaxPd=basePdQuarter; % at the end of the script, profMaxPd will contain the total
    % active power demand for the 8 demand nodes.
breakNumber=sum(drivingPattern,2); % breakNumber contains the number of times each of the
    % 463 EVs at node 671 are parked during the studied time interval.
```

Find optimal charging schedule for the i-th EV.

```
for i=1:463 % The optimal charging scheme have to be found for all 463 EVs served by node 671.
```

Set/reset values for parameters for the i-th EV

```
initSOC=85; % The initial SOC (in the start of the time period) is 85%.

inputElPrice=elPriceQuarter; % "inputElPrice" is to be used as input for the function
    % "optimization()".
tripNmb=96-breakNumber(i); % "tripNmb" is the number of trips during the studied 24 hour
    % period for the i-th EV.

tripCount=0;
breakCount=0;
```

The optimal charging schedule is found by calling the function *optimization()* with the initial SOC and electricity prices for the time interval of interest as input values. The function *optimization()* assumes that the EV is connected at all times. It is therefore necessary to do a new optimization each time the EV is disconnected from the grid.

```
for j=1:tripNmb+1 % It has to be done the same number of optimizations as number of
    % trips+1 (=tripNmb+1).
tripCount=tripCount+1;
breakCount=breakCount+drivingPattern(i,j);
if initSOC>=50 % The EV is only available for grid services when the SOC>50
    solution=optimization(inputElPrice,initSOC); % The function "optimization()"
        % returns a vector containing information
        % about optimal charge, discharge and SOC.
        % Note that the charge and discharge are
        % not given in power or energy, but in
        % percentage of battery capacity.

    count=0;
else % If SOC<50, charging is forced until SOC reaches 50%.
count=1;
```

```

while initSOC<50
    charge(1,breakCount-drivingPattern(i,j)+count)=3.4375;
    discharge(1,breakCount-drivingPattern(i,j)+count+1)=0;
    SOC(1,breakCount-drivingPattern(i,j)+count+2)=initSOC+3.4375;
    initSOC=initSOC+3.4375;
    inputElPrice(1)=[];
    count=count+1;
end
solution=optimization(inputElPrice,initSOC); %When the SOC reaches 50,
        % optimization() is called to find the optimal
        % charging schedule for the rest of the time period.
end
solution(length(solution)+1)=85;

for k=(0+count):(drivingPattern(i,j)-1); % The charge, discharge and SOC for the
        % time period until the next time the EV is
        % disconnected from the grid is saved into the
        % vectors "charge", "discharge" and "SOC".
    charge(breakCount-drivingPattern(i,j)+k+tripCount)=solution((k-count)*3+1);
        % Every third cell, starting at the
        % first in "solution" gives the charge.
    discharge(breakCount-drivingPattern(i,j)+k+tripCount)=solution((k-count)*3+2);
        % Every third cell, starting at the
        % second in "solution" gives the
        % discharge.
    SOC(breakCount-drivingPattern(i,j)+k+tripCount)=solution((k-count)*3+3);
        % Every third cell, starting at the
        % third, in "solution" gives the SOC.
end

charge(breakCount+tripCount)=0; % The charge and discharge during the period
discharge(breakCount+tripCount)=0; % when the EV is driving are set to zero.

if breakCount==0;
    SOC(breakCount+tripCount)=85-7.9; % SOC is reduced by 7.9% when driving 15 min.
else
    if tripCount<=tripNmb
        SOC(breakCount+tripCount)=SOC(breakCount+tripCount-1)-7.9; % SOC is
            % reduced by 7.9% when driving 15 min.
    end
end
if tripCount<=tripNmb % If the EV is going to be disconnected from the grid
    % any more times during the rest of the time period...
    for k=(1+count):(drivingPattern(i,j)+1)
        inputElPrice(1)=[]; % ...delete the cells in inputElPrice that we have
            % found charging schedule for (the time until
            % the next trip).
        initSOC=SOC(breakCount+tripCount); % The initial SOC for the next
            % optimization is the same as the
            % SOC right before the EV is
            % disconnected from the grid.
    end
end
end
end

```

At this point the final charging schedule for the i -th EV is found. Now the changes in electricity price due to charging/discharging of the i -th EV is predicted.

For detailed information of how the change in electricity prices is calculated, please see chapter 6.5.3.

```

for j=1:96
    if elPriceQuarter(j)<39.49
        elPriceQuarter(j)=elPriceQuarter(j)+2700.1*0.002*0.96*(1/0.9)*(charge(j)-

```



```

discharge(j))/1000;
    else
        elPriceQuarter(j)=elPriceQuarter(j)+2700.1*0.016*0.96*(1/0.9)*(charge(j)-
discharge(j))/1000;
    end
end
end

```

Now the charge/discharge (kW) of the i-th EV at node 671 is added to the demand curve at node 671.

```

for j=1:96
    profMaxPd(j,6)=profMaxPd(j,6)+charge(j)*(1/0.9)*(4*0.24)-discharge(j)*(1/0.9)*(4*0.24);
end
utladning(i,1)=sum(discharge);

```

```

end

```

Now the demand at the other 7 demand nodes is found by scaling the calculated demand at node 671.

```

for i=1:96
    for j=1:8
        profMaxPd(i,j)=basePdQuarter(i,j)*profMaxPd(i,6)/basePdQuarter(i,6);
    end
end
end

```

Optimization

This script is used in the profit maximization scenario only.

optimization()

This function is used to find the optimal charging schedule for *one* EV, with profit maximization as objective. The function assumes that the EV is connected to the grid and available for grid services at all times.

Contents

- [Objective function \(1\)](#)
- [Inequality matrix \(2\)](#)
- [Equality matrix \(3\)](#)
- [Lower and upper bounds \(4\)](#)
- [Calling linprog.m](#)

```
function [ x ] = optimization( elPrice,initSOC )
```

This function has two inputs:

- *elPrice*
- *initSOC*

The vector *elPrice* contains electricity prices in 15-minute intervals. The scalar *initSOC* gives the initial SOC.

The return vector *x* gives the optimal values for the charging, discharging and SOC for all the 15-minute intervals in the studied time period. Note that the length of the vector *elPrice* gives the length of the studied time interval.

To do the optimization, the function *linprog.m* in the MATLAB Optimization toolbox is used. *Linprog.m* is designed to solve minimization problems on the form described by the four equations below.

1. $f^T x \rightarrow \min$
2. $Ax \leq b$
3. $A_{eq}x = b_{eq}$
4. $lb \leq ub$

Objective function (1)

Since *linprog.m* attempt to minimize the objective function and the problem adressed in this thesis is a maximization problem, the objective function in *linprog.m*, $f^T x$, is defined as

$$f^T x = -g^T x$$

where $g^T x$ is the objective function in this thesis.

```
f=zeros(length(elPrice)*3-1,1);
count=1;
for i=1:length(elPrice)
    f(count)=elPrice(i); % Cell 1, 4, 7, 10 (...) in "f" give the price for charging.
    f(count+1)=-(elPrice(i)-2); % Cell 2, 5, 8, 11 (...) in "f" gives the price for
                                % discharge, set to 2 EUR/MWh below the charge price
    count=count+3;
end
```

Inequality matrix (2)

There are no inequality constraints

```
A=zeros(1,length(e1Price)*3-1);
b=zeros(1,1);
```

Equality matrix (3)

```
Aeq=zeros(length(e1Price),length(e1Price)*3-1);
beq=zeros(length(e1Price),1);
if length(e1Price)>1
    count=1;
    Aeq(1,[1,2,3])=[1,-1,-1];
    for i=2:(length(e1Price)-1)
        Aeq(i,[count*3,count*3+1,count*3+2,count*3+3])=[1,1,-1,-1];
        count=count+1;
    end
    Aeq(length(e1Price),[count*3,count*3+1,count*3+2])=[1,1,-1];
    beq(1)=-initSOC;
    beq(length(e1Price))=85; %SOC at end of charging schedule is 85
else
    f(1,1)=(85-initSOC);
end
```

Lower and upper bounds (4)

```
lb=zeros(length(e1Price)*3-1,1);
for i=1:(length(e1Price)-1)
    lb(i*3)=50; %The SOC should never be below 50
end
ub=Inf(length(e1Price)*3-1,1);
ub(1)=3.4375; %15 minute charging can not exceed 3.4375% of the battery's capacity
ub(2)=3.4375; %15 minute discharging can not exceed 3.4375% of the battery's capacity
for i=1:(length(e1Price)-1)
    ub(i*3)=85; %The SOC can never exceed 85%.
    ub(i*3+1)=3.4375; %15 min charging can not exceed 3.4375% of the battery's capacity
    ub(i*3+2)=3.4375; %15 min discharging can not exceed 3.4375% of the battery's capacity
end
```

Calling linprog.m

linprog.m is called, and the optimal values for the variables in vector x are returned

```
[x]=linprog(f,A,b,Aeq,beq,lb,ub);
```

```
end
```

Power Factor Control Scenario – Main Script

This script is used in the power factor control scenario only.

Power factor control scenario - main script

This script calculates the active and reactive power demand at all demand nodes at the 11 node test feeder for the power factor control scenario.

Initially it is assumed that all EVs charge as in the *dumb charging scenario*. Then this script starts controlling the voltages, one half-hour at the time. If there is a voltage violation (e.g. the voltage falls below 0.935 pu) at any of the nodes, EVs at the relevant nodes is instructed to charge according to the "power factor control charging mode". Please see chapter 6.6 for detailed information about this charging scenario.

Contents

- Find demand node voltages for the dumb charging scenario
- Find which EVs to switch to power factor control
- Find final node voltages for the power factor control scenario

```
clear
```

Find demand node voltages for the dumb charging scenario

```
dumbScenario; % By running the script "dumbScenario", the matrix "lastReturn" and
               % "dumbPd" become available

pfPd=dumbPd;      % "pfPd" and "pfQd" is the active and reactive power demand at all
pfQd=baseQdHalf; % demand nodes.

pfVoltages=findDemandNodeVoltages(pfPd, pfQd); % "pfVoltages" is filled with demand node
                                                % voltages from the dumb charging scenario

[minVoltage, timeOfMinVoltage]=min(pfVoltages); % "minVoltage" is filled with the lowest
                                                % voltages at each demand node
```

Find which EVs to switch to power factor control

```
available=1;

while min(minVoltage)<0.935 && available==1

    available=0;

    for i=1:8

        if minVoltage(i)<0.935 % If the lowest voltage at node j is below 0.935 pu...

            lastReturnOfEV=findEV(i, timeOfMinVoltage(i), lastReturn); %Finds which EV to
                                % change to power factor control mode, and
                                % returns the time for the last journey of the
                                % day for this EV

            if lastReturnOfEV==0 % In this case, there were no available EVs to avoid the
                                % low voltage found. Checking if there are any other
                                % violations that can be avoided.

                tempVolt=pfVoltages;

                while lastReturnOfEV==0 && minVoltage(i)<0.935

                    tempVolt(timeOfMinVoltage(i),i)=10;
```

```

        [minVoltage, timeOfMinVoltage]=min(tempVolt);

        if minVoltage(i)<0.935

            lastReturnOfEV=findEV(i, timeOfMinVoltage(i), lastReturn);

        end
    end
end

if lastReturnOfEV~=0 % In this case, there is an available EV for grid
    % services

    available=1; % We will then take another round in the while loop

    lastReturn(lastReturnOfEV,i)=lastReturn(lastReturnOfEV,i)-1; % Delete the
        % EV that has swithced to power factor
        % control from the matrix "lastReturn"

    pfPd(lastReturnOfEV,i)=pfPd(lastReturnOfEV,i)-3.3; % Remove the dumb
    pfPd(lastReturnOfEV+1,i)=pfPd(lastReturnOfEV+1,i)-3.3; % charging from
    pfPd(lastReturnOfEV+2,i)=pfPd(lastReturnOfEV+2,i)-3; % this EV

    for j=1:16
        pfPd(lastReturnOfEV+j-1,i)=pfPd(lastReturnOfEV+j-1,i)+0.6; % The next
            % 16 half-hours after the last return, the
            % EV charges with a rate of
            % P=0.6kW and Q=-3.245 kVAr
        pfQd(lastReturnOfEV+j-1,i)=pfQd(lastReturnOfEV+j-1,i)-3.245;

    end
end

pfVoltages=findDemandNodeVoltages(pfPd, pfQd);
[minVoltage, timeOfMinVoltage]=min(pfVoltages); % minVoltage is filled with
    % the lowest voltages at each node

end
end
end

```

Find final node voltages for the power factor control scenario

```

finalVoltages=findNodeVoltages(pfPd, pfQd);

```

Find Demand Node Voltages

This script is used in the power factor control scenario only.


```
function [ voltage ] = findDemandNodeVoltages( pd, qd )
```

This function is used in the power factor control scenario to find the voltages at the demand nodes. The function takes the $m \times 8$ matrices pd and qd as input. pd and qd contains the active and reactive power demand at each of the 8 demand nodes at for m studied half hours. Then the function calculates the node voltages with this demand and returns the voltages in the 48×8 matrix $voltage$.

Note that the only difference between this function and the function `findDemandNodeVoltages()` is that this function only returns the voltages at the *demand* nodes.

```
define_constants;
mpc=loadcase(case11);

[m n]=size(pd);

voltage=zeros(48,8);

for i=1:m
    mpc.bus(2,PD)=pd(i,1)/1000; %node 2 in case11 is node 646
    mpc.bus(2,QD)=qd(i,1)/1000;
    mpc.bus(3,PD)=pd(i,2)/1000; %node 3 in case11 is node 645
    mpc.bus(3,QD)=qd(i,2)/1000;
    mpc.bus(4,PD)=pd(i,3)/1000; %node 4 in case11 is node 632
    mpc.bus(4,QD)=qd(i,3)/1000;
    mpc.bus(5,PD)=pd(i,4)/1000; %node 5 in case11 is node 634
    mpc.bus(5,QD)=qd(i,4)/1000;
    mpc.bus(6,PD)=pd(i,5)/1000; %node 6 in case11 is node 611
    mpc.bus(6,QD)=qd(i,5)/1000;
    mpc.bus(8,PD)=pd(i,6)/1000; %node 8 in case11 is node 671
    mpc.bus(8,QD)=qd(i,6)/1000;
    mpc.bus(9,PD)=pd(i,7)/1000; %node 9 in case11 is node 675
    mpc.bus(9,QD)=qd(i,7)/1000;
    mpc.bus(10,PD)=pd(i,8)/1000; %node 10 in case11 is node 652
    mpc.bus(10,QD)=qd(i,8)/1000;

    opt=mpoption('PF_ALG', 2);
    results=runpf(mpc, opt);

    voltage(i,1)=results.bus(2,VM);
    voltage(i,2)=results.bus(3,VM);
    voltage(i,3)=results.bus(4,VM);
    voltage(i,4)=results.bus(5,VM);
    voltage(i,5)=results.bus(6,VM);
    voltage(i,6)=results.bus(8,VM);
    voltage(i,7)=results.bus(9,VM);
    voltage(i,8)=results.bus(10,VM);
end
```

```
end
```

Find EV

This script is used in the power factor control scenario only.

```
function [ timeOfReturn ] = findEV( node, timeOfViolation, lastReturn )
```

This function has three inputs:

- *node*
- *timeOfViolation*
- *lastReturn*

The scalar *node* is the node where the violation occurs and the scalar *timeOfViolation* is simply the time of the violation (e.g. the number of half hours into the studied time period). *lastReturn* is a matrix giving the number of EVs having their last return at each half hour at each node.

The objective for the function is to find which EV to charge according the power factor control mode. The function returns the time of return from the last journey of the day for this EV.

If the function returns the number 0, the function failed in finding an available vehicle for grid services.

```
timeOfReturn=0;
```

First the while loop tries to find an EV having its last return the half hour of violation. If there are no available EVs for grid services returning at this half-hour, the program take another turn in the while loop in an attempt to find an EV having its last return the half-hour before. If there are no EVs having its last return this half hour either, then the program takes a new turn in the while loop in an attempt of finding one having its last return the half-hour before, and so on. If there are no EVs having its last return in any of the 16 half hours before the voltage violation, the function returns the value 0, meaning that there are no EVs available for grid services.

```
count=0;
while count<15

    if (timeOfViolation-count)<1
        break;
    end

    if lastReturn(timeOfViolation-count,node)>0; % In this case the program finds an available EV
        timeOfReturn=timeOfViolation-count; % "timeOfReturn" is set to half-hour
                                            % number ("timeOfViolation"-count)
        count=16; %...and then the program jump out of the while loop
    else
        count=count+1;
    end
end
```


APPENDIX C

Paper presenting the results from the specialization project, fall 2013.

Optimal Charging of Electric Vehicles Including Service Provision to the Distribution Network

Line Fiskum Hexeberg Marta Molinas Olav B. Fosso

Department of Electric Power Engineering

Norwegian University of Science and Technology

Trondheim, Norway

linefi@stud.ntnu.no,

marta.molinas@ntnu.no,

olav.fosso@ntnu.no

Abstract—This paper presents an algorithm for a smart charging procedure of electric vehicles where the storage capability of the batteries can be used to provide network services under a given set of rules. The smart charging follows an optimization routine where the battery operates in analogous way to a pumped storage hydro power. To illustrate the concept, the designed algorithm is applied to a number of electrical vehicles corresponding to a 50 percent adoption of electric vehicles in Norway. The algorithm effectiveness is rated according to its capability to smoothen out the demand curve and to avoid low voltages on some feeders during the charging process, by using charging control and coordination as well as active power injection.

Keywords— *Smart Charging, Network Services, Optimization Algorithm, Price Curve, Battery Storage, V2G*

I. INTRODUCTION

As of December 2012, there were over 180,000 highway-capable plug-in electric passenger vehicles and utility vans worldwide, including all-electrics and plug-in hybrids, representing 0.02% of the stock of total registered passenger vehicles [1]. Market penetration and electric vehicles (EV) sales vary significantly among countries. Norway is currently the country with the largest EV ownership per capita in the world, with Oslo recognized as the EV capital of the world [2]. The Norwegian *Action Plan for Electrification of Road Transport* states that a percentage of 50 percent EVs will give a reduction in greenhouse gas emissions of 36 percent in comparison with a fleet of cars efficiently powered only by fossil fuels [3].

As the number of EVs running purely on batteries will continue to increase, measures must be taken to control and coordinate the charging profiles in the distribution network to avoid hampering effects such as unacceptable low voltages during the charging process. Without a dedicated charging procedure, a typical pattern may be to plug the EVs into the charger after work until batteries are fully charged. Lack of smart control and coordination will probably result in a large number of cars being unnecessarily charged at the same time when the load in the system will be high. An obvious solution is to postpone the charging until the network load is reduced but the peak load could still remain quite high. One proposed way to aid in addressing these challenges is vehicle-to-grid (V2G). With V2G, the storage capability of the batteries could provide services such as regulation and ancillary services.

Through V2G, EV owners can also potentially generate revenue by charging their vehicles when the electricity price is low and discharge when the price is high.

This paper focus on the V2G charging scheme and presents an algorithm for a smart charging and discharging procedure of EVs adapting to the following principles and rules:

1. The battery should be fully charged every morning at 06.00 AM.
2. The battery connected to a charger will never discharge if the battery is below 50 percent of its capacity.
3. When the battery is above 50 percent of its capacity, the charging and discharging will follow a schedule forecasted for the remaining period where the aim is to maximize the revenue for the EV owner.
4. Charging could be stopped at any time for using the vehicle and when connecting again it will adapt to the strategy for the remaining period.

The algorithm's capability to smoothen out the power demand curve is rated by investigating two different scenarios; a *dumb charging* scenario, and a *V2G* scenario. In both scenarios the power demand pattern is created by adding an extra load due to charging of a number of EVs corresponding to a 50 percent adoption of EVs to a particular base load. The base load for the purpose of this investigation is the actual 24-hour demand profile in Norway from 06:00 PM 11.05.13 to 06:00 PM 11.06.13. In the dumb charging scenario, it is assumed that all EVs start charging at 5:00 PM, and continue to charge until the battery is fully charged. In the V2G scenario, the demand pattern is created by adding to the base load the charging and discharging found by the designed algorithm. For simplicity, it is assumed that all the EVs in the model are Nissan Leaf as it is currently the most common EV in Norway.

One way to investigate the effectiveness of the algorithm is through its ability to avoid low voltages on some sensitive feeders in a given network. It is demonstrated by using MATPOWER how a simulation tool could be used to do this.

The various sections in this paper are organized as follows. Section II briefly presents the key features of the

electricity price in Norway and section III summarizes the different charging schemes for EVs. The designed optimization algorithm for the V2G charging scheme is presented in section IV. The scenarios and assumptions considered for the simulations are given in section V. Section VI and VII presents the results and conclusions.

II. ELECTRICITY PRICE IN NORWAY

The Nordic countries deregulated their power markets in the early 1990s, and their individual markets were brought into a common Nordic market. Estonia and Lithuania deregulated their power markets in the late 2000s, integrating the Nordic and Baltic power markets. The market place, which is called Nord Pool Spot, is own by the Nordic and Baltic transmission system operators and runs the leading power market in Europe.

In the deregulated power market, the electricity price is mainly determined by the balance between generation and supply of electric power [4]. The higher the demand gets, more expensive units have to produce power, and the higher the price gets. Due to transmission restrictions, the prices in different areas are however somewhat different. The Norwegian electricity market is for instance divided into five price areas.

The hourly electricity prices for the different Nordic and Baltic countries can be found at Nord Pool Spot’s webpages [4]. It is clear that there is a smaller variation in the electricity prices in Norway compared to the other Nordic and Baltic countries. This is due to the fact that most of the Norwegian power production comes from hydroelectric power plants, which has excellent regulation ability compared to most other types of power plants. Norway’s potential for wind power is however excellent and wind power is predicted to constitute a significant part of the Norwegian electricity supply in the future [5]. Wind power is known to have large variations in production, which in turn will give more variation in the electricity prices. There is also a transition from reliance on fossil fuels towards utilizing renewables-based energy with more fluctuations in production in other countries in the northern part of Europe. This is also likely to influence the Norwegian energy prices since the national energy markets are integrated.

Currently most Norwegian consumers do not face any incentive to respond to price changes as their meters account for accumulated consumption only and the hourly prices remain invisible due to lack of enabling technology and respective pricing methods [6]. Norwegian Government has however decided that the implementation of advanced metering system should be completed before January 1, 2019 [7]. The smart meters will make it possible to give a more accurate billing, and thereby making it more attractive to shift some of the load from periods of the day when the price is high at its highest, to periods when the electricity price is lower.

III. CHARGING SCHEMES FOR ELECTRIC VEHICLES

The impact the EVs will have on the power grid will depend on the number of EVs and the charging scheme used. Three different charging schemes are described in this section.

1. Dumb Charging

The most conventional charging scheme is to plug in the vehicle and get it charged like any other regular load. This is often called *dumb charging* [8].

2. Smart charging

Smart charging is when the vehicle is charged when the grid allows or needs it to, shifting the load from peak to off-peak periods. To make this charging scheme possible, there have to be communications between the grid and the vehicle. The smart grid concept with advanced metering infrastructure facilitates this application [8].

3. Vehicle-to-Grid

Vehicle-to-grid (V2G) is the most complicated charging scheme and can be considered as an extension of the smart charging. In addition to the functions for the smart charging, it also allows the energy stored in the EV batteries to be delivered back to the grid for grid support .V2G can be accomplished by discharging energy through bidirectional power flow [8].

The algorithm presented in section IV in this paper is based on the vehicle-to-grid charging scheme.

IV. OPTIMIZATION OF CHARGING ALGORITHM

The optimal charging schedule is influenced by a set of parameters. Some of them are connected with the choice of vehicle model. For simplicity it is assumed that all vehicles in this study are Nissan Leafs, since this is the most common EV in Norway at the time of writing. Nissan Leaf has a battery capacity of 24 kWh and a range of 199 km [9]. The driving distance varies somewhat during the different days of the week, and in the different parts of the country. The average daily driving distance in Norway is however 35 km [10]. For the purpose of this paper it is therefore assumed that each vehicle drives 35 km during the studied 24-hour time period. The parameters presented here are summarized in Table 1.

TABLE 1. PARAMETERS RELATED TO CHOICE OF VEHICLE MODEL AND DRIVING DISTANCE

Vehicle model	Battery capacity	Battery range	Daily driving distance
Nissan Leaf	24 kWh	199 km	35 km

A. The designed optimization algorithm

This section present the designed optimization algorithm for the V2G charging scheme. The problem is formulated as a single-objective constrained linear programming optimization problem. The decision variables in this case are the values for the hourly charging and discharging of the battery of one EV. Initially it is assumed that the vehicle is connected to the grid at all times.

$$\text{Max.} \quad \sum_{i=1}^{24} (\text{price}_i \cdot d_i) - \sum_{i=1}^{24} (\text{price}_i \cdot c_i) \quad (1)$$

$$\text{s.t.} \quad b_{i-1} + c_i - d_i = b_i \quad i = 1, \dots, 24 \quad (2)$$

$$SOC_{min} \leq b_i \leq SOC_{max} \quad i = 1, \dots, 23 \quad (3)$$

$$0 \leq c_i \leq c_{max} \quad i = 1, \dots, 24 \quad (4)$$

$$0 \leq d_i \leq d_{max} \quad i = 1, \dots, 24 \quad (5)$$

$$b_0 = b_{24} = 100 \quad (6)$$

The objective function (1) maximizes the revenue for the EV owner. Here price_i is the electricity price in time interval i , c_i is the amount of energy bought from the grid in percent of the battery capacity (battery charges) and d_i is the amount of energy sold in percent of the battery capacity (battery discharges).

There are however some restrictions on the decision variables. These restrictions are expressed through a set of constraints (2)-(6).

The program keeps track of the battery's state of charge (SOC) during the whole time period. Each time the battery charges, the SOC increases, and each time the battery discharges, the SOC decreases. This leads to (2), where b_{i-1} is the battery's SOC at the end of hour $i-1$, and b_i is the SOC at the end of hour i .

The constraint expressed by (3) makes sure that the battery never exceeds its maximum capacity. This constraint also makes sure that the SOC never falls below a certain minimum value. For the purpose of this paper, it is chosen to set this value at 50 percent.

A traditional home charger charges the battery with a charging rate of 3.3 kWh/h [9]. Next generation home charger could however potentially have a charging rate of 12 kWh/h [11]. The higher the charging rate is, the more the battery could charge at the hour with the lowest prices and the more the battery could discharge at the highest prices. For the purpose of this paper, it is however assumed a charging/discharging rate of 3.3 kWh/h. This leads to the constraints expressed by (4) and (5). c_{max} and d_{max} is the

maximum amount of energy the battery can charge and discharge during one hour in percent of the battery capacity. With a maximum battery capacity of 24 kWh, c_{max} and d_{max} is calculated to be 13.75 percent of the battery capacity.

It is assumed that the EV owner demands that the battery is fully charged at 6.00 AM each day. Therefore, the schedule starts and ends at 6.00 AM. The restriction expressed by (6) makes sure that the battery is fully charged at the beginning and the end of each schedule.

The values for c_{max} , d_{max} , SOC_{min} and SOC_{max} chosen for the purpose of this paper are given in Table 2.

TABLE 2. CONSTANTS USED IN THE CHARGING ALGORITHM.

SOC_{min}	SOC_{max}	c_{max}	d_{max}
50 percent	100 percent	13,75 %*	13,75 %*

* Given in percentage of total battery capacity

B. Solving the problem with MATLAB Optimization Toolbox

There are a large number of commercial solvers available for solving different optimization models. It is here chosen to use the MATLAB Optimization toolbox. The MATLAB Optimization toolbox includes a function called `linprog.m`, which is suitable for minimization problems on a linear form. Since the problem addressed in this paper is a maximization problem, a function $g(x)$ is defined, so that

$$f(x) = -g(x) \quad (7)$$

Here $f(x)$ is the objective function to be maximized, and it is found by minimizing $g(x)$ in MATLAB.

The optimization algorithm described by (1) to (6) does not take into account that the EV can be disconnected from the grid. To allow for this, a MATLAB script is created.

When deciding if the battery should charge or discharge, it is not taken into consideration when the vehicle is going to be in use the next time. The script therefore starts by finding the optimal values for all the variables by calling `linprog.m`, assuming that the vehicle is connected to the grid at all times. The function `linprog.m` has two input values; the battery's initial SOC and the electricity prices during the time period. After calling `linprog.m`, the variables associated to the hours before the first time the vehicle is disconnected from the grid is saved. The charging and discharging to the grid for the hour the EV is disconnected is set to zero. Next, the program calculates a new optimization by calling `linprog.m` again. The input values in `linprog.m` this time is the SOC at the end of the hour the EV is disconnected for the first time, and the electricity prices for the remaining period. With this, the `linprog.m` only determines the values for the variables associated to the hours after the car were in use for the first time. Then the proposed charging and discharging for the hours before the vehicle is used the next time are saved. The program continues to call `linprog.m` to do new optimizations until the last time the EV is disconnected from the grid. This procedure is illustrated in Fig 1.

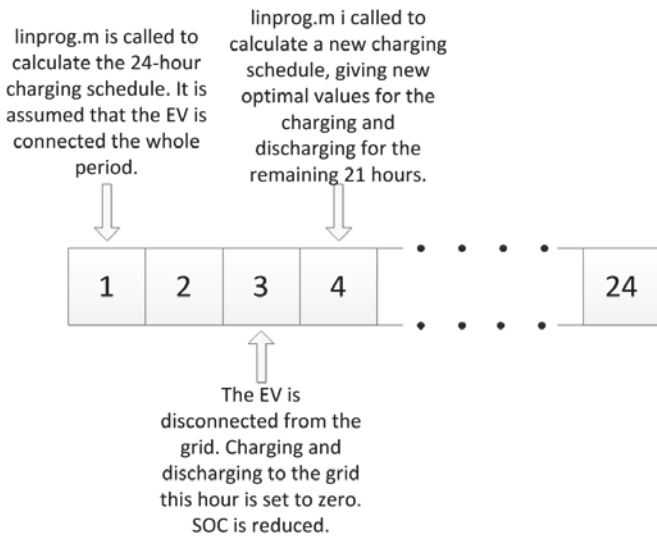


Figure 1. Finding optimal charging schedule by calling linprog.m each time the vehicle is disconnected from the grid.

The program keeps track of the battery's SOC during the whole 24-hour period. Each time the battery charges from the grid, the SOC increases and each time the battery discharges to the grid, the SOC decreases. To account for the reduction in SOC when the vehicle is in use, the SOC also have to be reduced when the vehicle is disconnected from the grid. According to Table 1, the chosen vehicle model has a battery capacity of 24 kWh and a range of 199 km. With these chosen parameters and a driving distance of 35 km, it can be calculated that the EV discharges 4.22 kWh during the studied 24-hour period due to driving.

For the purpose of this study, it is assumed that the vehicle will be used twice during the 24-hour period; the first time during the second hour (7:00 – 8:00 AM), and the second time during the eleventh hour (4:00-5:00 PM). It is also assumed that the SOC will be reduced the same amount each time the EV is in use. With a daily discharge of 4.22 kWh during driving and a battery capacity of 24 kWh, it can be calculated that the SOC is reduced by 8.79 percent each of the two times the EV is disconnected from the grid.

V. CASE STUDY

MATPOWER is used as simulation tool when investigating the effectiveness of the designed charging algorithm. MATPOWER is a package of MATLAB files for solving power flow and optimal power flow problems. It is intended for researchers and educators and is easy to use and modify [12]. MATPOWER works in the workspace of MATLAB, and therefore the calculated results from the optimization can be used with few intermediate steps.

A. Network description

As test case it is chosen the case 9 in MATPOWER. Case 9 is illustrated in Fig 2. For detailed information about the network parameters, the reader is referred to [12].

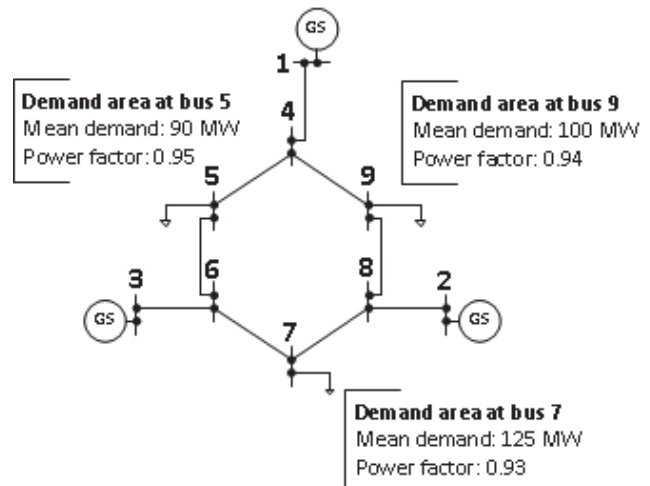


Figure 2. MATPOWER case 9. The given values for the mean demand and power factor are for the base load, i.e. before the large scale adoption of EVs.

As illustrated in Fig 2, there are nine buses in case 9, where bus 5, 7 and 9 are load buses. For the purpose of this study, each load is considered to be a distribution network in Norway. It is performed optimal power flow simulations on these loads, assuming a vehicle fleet with a 50 percent EV adoption. For the optimal power flow, the bus voltages are modelled with a lower bound of 0.9 pu and an upper bound of 1.1 pu.

B. Power demand with no electric vehicles

As basis for all the simulations in this paper, it is chosen to look at the actual demand in Norway from 6:00 AM November 5 to 06:00 AM November 6, 2013. The chosen data gives a typical demand profile in Norway with two demand peaks; one in the morning and one in the afternoon. The mean demand for this time period is 15 785 MW. When doing the simulations in MATPOWER, the hourly demand at bus 5 is found by multiplying the hourly demand in Norway with $\frac{15\ 785}{90}$. With that, the resulting demand curve at bus 5 gets the same shape as the total demand curve in Norway, but with a mean demand of 90 MW. Similar is done for the demand at bus 7 and 9, but at these buses the mean demand is 100 MW and 125 MW. In the situation where there are no EVs, the power factor is kept constant at the values given in Fig 2 for the whole time period.

The designed charging algorithm uses the electricity prices to find the optimal charging scheme. As mentioned in II, the Norwegian electricity market is divided into five areas, and the prices in these areas are often somewhat different due to transmission restrictions. For the purpose of this study it is chosen to use the electricity prices in Mid-Norway. The electricity prices of Mid-Norway for the studied time period is illustrated Fig 3 together with the calculated power demand at bus 5. As expected, the price pattern resembles the demand pattern.

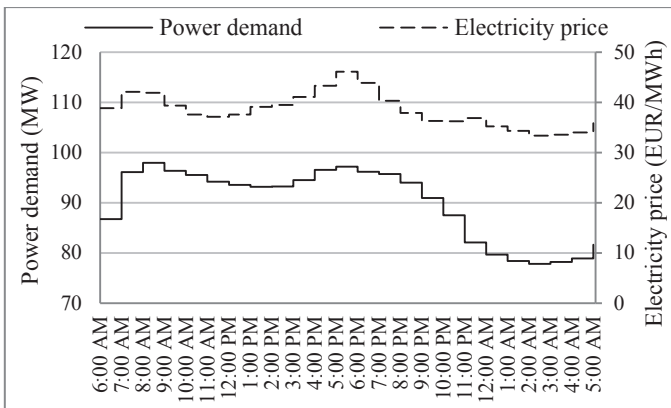


Figure 3. Electricity prices and power demand pattern at bus 5 with a 0% EV adoption

Since there are rather small variations in the hourly power demand in Norway, it is also chosen to scale the demand curves. This is to illustrate the effect of the charging algorithm in countries with greater hourly variations in the demand. To scale the demand, (7) is used.

$$d_{2,i} = d_{average} + a \cdot (d_{1,i} - d_{average}) \quad i = 1, \dots, 24 \quad (7)$$

Here $d_{2,i}$ is the demand of hour i in the scaled scenario, $d_{1,i}$ is the demand of hour i in the unscaled scenario and $d_{average}$ is the average demand for the studied time period. If $a < 1$, the curve smoothens out and if $a > 1$, the variations in demand (difference between maximum and minimum demand) increases. The variation in demand during the studied time period was 22 percent. For the purpose of this paper, it is chosen to use $a=2.233$ when scaling the demand curves, which gives a variation in demand of 50 percent. Fig 4 illustrates the demand curves at bus 5 for both the original and scaled scenario.

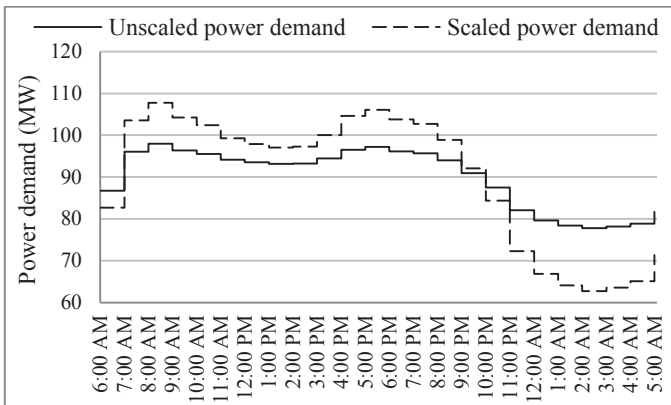


Figure 4. Demand pattern for bus 5 with no electric vehicles.

Adding to the demand curve the extra load due to a 50 percent electric vehicle adoption

The extra load due to a 50 percent EV adoption is added to the base load at bus 5, 7 and 9 in the MATPOWER case 9. IT is assumed that the extra load due to the EVs has a unity power factor. The number of EVs in each area is found by (8).

$$x_j = 0.50 \cdot x_{tot} \cdot \frac{\sum_{i=1}^{24} P_{d,i}}{\sum_{i=1}^{24} P_{d,tot}} \quad (8)$$

Here x_j is the number of EVs in area j , x_{tot} is the total number of EVs in Norway, $P_{d,i}$ is the power demand in area j in hour i , and $P_{d,tot}$ is the power demand in Norway in hour i . In 2012 there were 2 442 968 passenger cars in Norway, so x_{tot} is set to 2 442 968. With a 50 percent adoption of EVs, this equation gives a number of 6978 EVs at bus 5, 7753 EVs at bus 7 and 9692 EVs at bus 9.

The extra load is added according to both the dumb charging scheme and by using the designed V2G charging algorithm. For both scenarios it is assumed that each EV consumes 4.2 kWh daily, giving a total extra demand of 29.3 MWh at bus 5, 32.56 MWh at bus 7 and 40.71 at bus 9.

For the scenario with the dumb charging scheme, it is assumed that all EVs will start charging at 5:00 PM, and continue to charge until the batteries are fully charged. It is probably not realistic that all the EV owners will charge their vehicles at the exact same time, which argues for a lower extra demand at this hour. But on the other hand, there will probably be days where the driving distance is significantly higher, which argues for an even higher extra load in the chosen hour.

As for the dumb charging approach, it is assumed that each EV consumes 4.2 kWh daily, but now the charging algorithm presented in section IV is used. In this study it is not taken into consideration that the electricity price most probably will change as a consequence of a large scale adoption of EVs. It is also assumed that all EVs charges and discharges at the same time and at the same rate.

VI. RESULTS

A. Vehicle-to-grid charging schedule

The hourly charge and discharge rate set by the designed charging algorithm is presented in Fig 5 and Fig 6. The electricity price is plotted in the same figures. As intended, the battery charges when the price is low and discharges when the price is high. The EV is in use the third and twelfth hour, which is why the battery does not discharge these hours, even though the electricity price is relatively high.

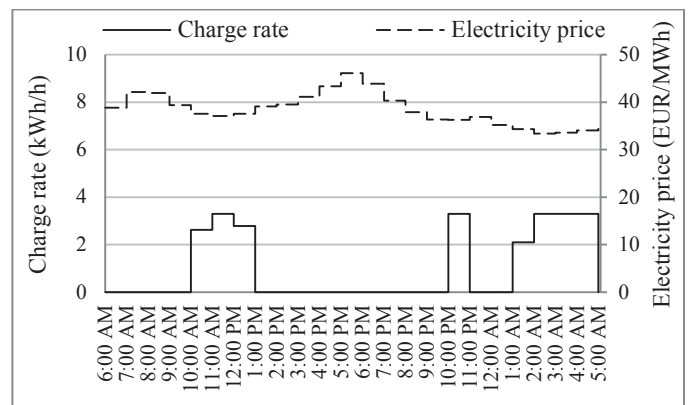


Figure 5. Charge rate with the designed V2G charging algorithm

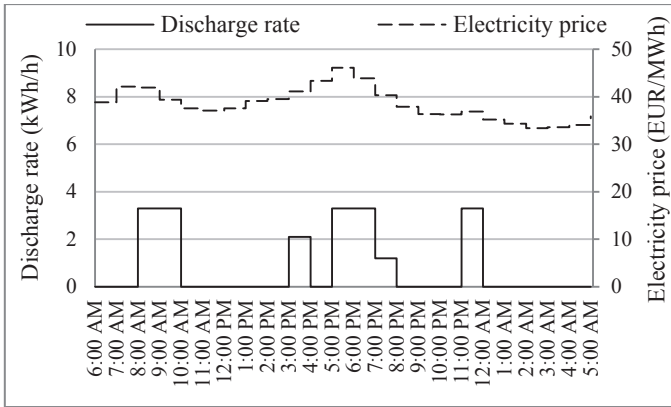


Figure 6. Discharge rate with the designed V2G charging algorithm

B. Power demand with a 50 percent electric vehicle adoption

1) Unscaled scenario

As mentioned in V, the variation in the actual demand in Norway was 22 percent of the average demand during the studied time period. The dashed line in Fig 7 and Fig 8 illustrates the hourly power demand at bus 5 when the variation in demand is 22 percent. The solid line in these figures illustrates the resulting power demand at bus 5 when the extra power demand due to charging of the EVs is added.

In Fig 7 the EVs are charged according to the dumb charging scheme. The extra load due to the charging results in a high peak at 5:00 PM, i.e. when the EVs are plugged in. The figure also reveals that the charging occurs when there already is a peak in the base demand.

In Fig 8, the designed algorithm is used when charging the EVs. Ideally, the algorithm would smoothen out the curve. It is however clear that the variation in demand in the resulting demand curve are much higher than for the situation with no EVs. One reason is that it is not taken into consideration that the shift in load might change the electricity prices and that all EVs charges at the same time. The variations in demand would not be as big if the vehicles were charged at different times, or if the EV penetration had been significantly lower. The maximum load is not as high as with the dumb charging, but it is quite high compared to the highest peak in the base load.

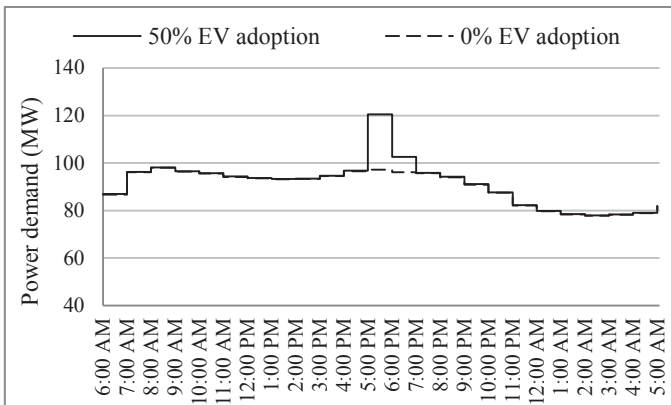


Figure 7. Power demand at bus 5 when the dumb charging scheme is used.

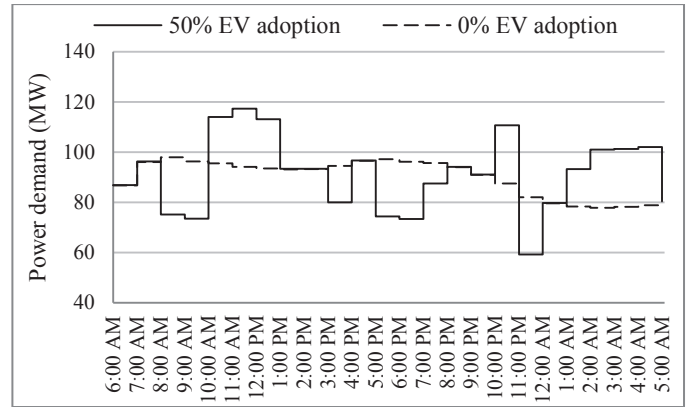


Figure 8 Power demand at bus 5 when the designed charging algorithm is used

2) Scaled scenario

The dashed line in Fig 9 illustrates the power demand when the demand is scaled to a 50 percent variation in demand, and there are no electric vehicles. Comparing Fig 9 with Fig 8, it is evident that the designed smart charging algorithm has a somewhat more valley filling effect when the base load is scaled. The demand pattern is however still not improved compared to the situation with no EVs.

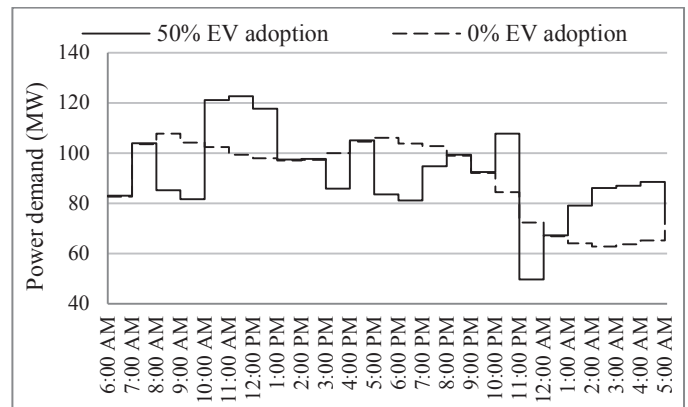


Figure 9. Power demand at bus 5 when the designed charging algorithm is used. Scaled scenario.

C. The effect of a 50 percent electric vehicle adoption on the voltages

Table 3 gives the minimum and maximum voltages at the load buses for the unscaled scenario. Contrary to expectations, the voltages appear not to be very much influenced by the extra demand due to charging of a vehicle fleet with a 50 percent share of EVs.

TABLE 3. MINIMUM AND MAXIMUM VOLTAGES AT LOAD BUSES IN CASE 9, DURING THE STUDIED 24-HOUR PERIOD, GIVEN IN PER UNIT.

	Bus 5		Bus 7		Bus 9	
	U _{min}	U _{max}	U _{min}	U _{max}	U _{min}	U _{max}
No EVs	1.081	1.088	1.088	1.093	1.072	1.080
50% EVs Dumb charging	1.076	1.088	1.086	1.093	1.066	1.080
50% EVs V2G charging	1.078	1.090	1.088	1.093	1.069	1.083

The parameters in case 9 describe a high voltage network with a base voltage of 345 kV and a low R/X ratio. In the distribution grid, the lines are however predominantly resistive. Based on this, the results listed here from simulating in MATPOWER should not be emphasized.

VII. CONCLUSIONS

In section IV of this paper, an algorithmic procedure for deciding the optimal charging and discharging of one EV, utilizing V2G technology is proposed. The hourly charging and discharging of the EV is set by the electricity price. The objective is to maximize the profit for the EV owner, i.e. the vehicle charges when the electricity price is low, and discharges when the electricity price is high.

The resulting demand pattern is studied when a vehicle fleet consisting of 50 percent EVs are charging and discharging according to this schedule. When applying the algorithm on this large number of EVs, it is evident that the power curve is not improved if all the EVs charges at the same time.

The electricity prices are based on the actual base load, i.e. in a situation where no EVs are charging according to the proposed schedule. With a large scale adoption of EVs, charging according to the schedule, price signals will however most probably be sent real time and thereby changing the electricity prices. If the electricity prices were to be changed real time, it would lead to a dissipation of the total charging and discharging of the EVs. Measures should be taken to take this into consideration. This study is an ongoing work, and improvements on the charging schedule for a large scale adoption of EVs is under construction.

One way of investigating the effectiveness of the algorithm is to assess the voltages at some sensitive feeders. The voltages should stay within a certain range, e.g. between 0.9 and 1.1 pu. This can be assessed by running simulations on a defined grid for all the demands found by the algorithm. It is demonstrated in this paper how case 9 in MATPOWER could be used for this purpose. The authors of this paper does however not recommend using this exact test case as it describes a high voltage network with a R/X relationship that differs quite from a distribution grid. The results presented in this paper from this simulation should therefore not be emphasized. If MATPOWER is to be used, it is recommended to change the parameters in the case to better suit a distribution network, or to create a new test case.

REFERENCES

- [1] International Energy Agency, Clean Energy Ministerial and Electric Vehicles Initiative, "Global EV Outlook 2013 - Understanding the Electric Vehicle Landscape to 2020," International Energy Agency, Paris, 2013.
- [2] The European Association for Battery, Hybrid and Fuel Cell Electric Vehicles. (2013, oct 15). *Norwegian Parliament extends electric car initiatives until 2018*. Available: <http://www.aveve.org/>
- [3] Ressursgruppen EBL, "Handlingsplan for elektrifisering av veitransport [Action Plan for Electrification of Road Transport]," Samferdselsdepartementet, Oslo, 2013.
- [4] Nord Pool Spot. (2013, oct 20). *Nord Pool Spot*. Available: <http://www.nordpoolspot.com/>
- [5] Energi Norge. (2013, sept 19). *Impact of integrating wind power in the Norwegian power system*. Available: <http://www.energinorge.no/>
- [6] Iliana Shandurkova, Bernt A. Bremdal, Rainer Bacher, Stig Ottesen, Andreas Nilsen, "A Prosumer Oriented Energy Market. Developments and future outlooks for Smart Grid oriented energy markets." IMPROSUME Publication Series, Halden, 2012.
- [7] Ministry of Government administration, Reform and Church Affairs 2013, *Digital Agenda for Norway – ICT for Growth and Value Creation: Meld.St23 (2012-2013) Report to the Storting (white paper)* Available: http://www.regjeringen.no/pages/38354256/PDFS/ST_M201220130023000EN_PDFS.pdf
- [8] R. Garcia-Valle and J. A. Peças Lopes, *Electric Vehicle Integration into Modern Power Networks*. New York, NY: Springer New York, 2013.
- [9] Nissan, (2013, nov 20). *Nissan Leaf*. Available: <http://www.nissan.no/>
- [10] Statistics Norway, (2013, aug 31). *Road traffic volumes 2012*. Available: <http://www.ssb.no/en/klreg/>
- [11] Transnova, (2013, oct 19). *Ladefart [Charge rate]*. Available: <http://www.transnova.no/skal-du-etablere-ladepunkt/ladefart/>
- [12] R. D. Zimmerman, S. Murillo, and R. J. Thomas, "MATPOWER: Steady-State Operations, Planning, and Analysis Tools for Power Systems Research and Education," *Power Systems, IEEE Transactions on*, vol. 26, pp. 12-19, 2011